Theses and Dissertations

3-23-2017

The Impacts of Climate Change and Anthropogenic Processes on Permafrost Soils and USAF Infrastructure within Northern Tier Bases

Alexander J. Graboski

Follow this and additional works at: https://scholar.afit.edu/etd

Part of the Construction Engineering and Management Commons

THE IMPACTS OF CLIMATE CHANGE AND ANTHROPOGENIC PROCESSES ON PERMAFROST SOILS AND USAF INFRASTRUCTURE WITHIN NORTHERN TIER BASES

THESIS

Alexander J. Graboski, Captain, USAF

AFIT-ENV-MS-17-M-189

DEPARTMENT OF THE AIR FORCE
AIR UNIVERSITY

AIR FORCE INSTITUTE OF TECHNOLOGY

Wright-Patterson Air Force Base, Ohio

AFIT-ENV-MS-17-M-189

THE IMPACTS OF CLIMATE CHANGE AND ANTHROPOGENIC PROCESSES ON PERMAFROST SOILS AND USAF INFRASTRUCTURE WITHIN NORTHERN TIER BASES

THESIS

Presented to the Faculty

Department of Systems Engineering and Management

Graduate School of Engineering and Management

Air Force Institute of Technology

Air University

Air Education and Training Command

In Partial Fulfillment of the Requirements for the

Degree of Master of Science in Engineering Management

Alexander J. Graboski, B.S.

Captain, USAF

March 2017

AFIT-ENV-MS-17-M-189

THE IMPACTS OF CLIMATE CHANGE AND ANTHROPOGENIC PROCESSES ON PERMAFROST SOILS AND USAF INFRASTRUCTURE WITHIN NORTHERN TIER BASES

Alexander J. Graboski, BS
Captain, USAF

Committee Membership:

Lt Col Kevin S. Bartlett, PhD
Chair

Dr. Diedrich V. Prigge
Member

Lt Col Vhance V. Valencia, PhD
Member

AFIT-ENV-MS-17-M-189

Abstract

The Department of Defense is planning over $552M in military construction on Eielson Air Force Base within the next three fiscal years. Although many studies have been conducted on permafrost and climate change, the future of our climate as well as any impacts on permafrost soils, remains unclear. This research focused on future climate predictions to determine likely scenarios for the United States Air Force's Strategic Planners to consider. The most recent 2013 International Panel on Climate Change report predicts a 2.2ºC to 7.8ºC temperature rise in Arctic regions by the end of the 21st Century in the Representative Concentration Pathways, (RCP4.5) emissions scenario. This study provides an explanation as to the impacts of this temperature rise on permafrost soils and Arctic infrastructure.

This study developed regression models to analyze historical data related to degree-days, temperature, and seasonal lengths. Initial analysis using regression/forecast techniques show a 1.17ºC temperature increase in the Arctic by the end of the 21st Century. Additionally, UAF's GIPL 2.1 model was used to calculate active layer thicknesses and permafrost thickness changes from 1947 to 2100. Results show that the active layer is thinning with some permafrost degradation. This research focused on Central Alaska while further research is recommended on the Alaskan North Slope and Greenland to determine additional impacts on Department of Defense infrastructure.

To God and my family.

Acknowledgments

Table of Contents

List of Figures

List of Tables

THE IMPACTS OF CLIMATE CHANGE ON PERMAFROST SOILS WITHIN
UNITED STATES AIR FORCE'S NORTHERN TIER BASES

I. Introduction

Background

Climate change is a highly debated topic with some scientists proposing extreme temperature rises, and others claiming no changes are taking place. Despite the ongoing political debate, researchers from across the globe have been tracking air and ground temperature data and are currently discovering varying trends based on regions. In artic regions, these changing temperatures have an effect on different aspects of the ecosystem. In Alaska, permafrost is highly susceptible to these temperature changes and is mirroring much of the upward warming trends (Solomon, Qin, Manning, Chen, Marquis, Averyt, Tignor, & Miller, 2007).

Although different definitions exist around the world (V. Romanovsky, personal communication, 13 May 2016), the generally accepted definition for permafrost in North America is, "a thickness of soil or other superficial deposit or even of bedrock, at a variable depth beneath the surface of the earth which a temperature of 0°C has existed continually for a long time (≥2 years)" (Washburn, 1979). Permafrost is also categorized by the amount of moisture and ice that exists in it. Soil with high amounts of ice is identified as ice-rich permafrost. The University of Alaska (UAF) in Fairbank's Permafrost Laboratory, as well as permafrost scientists around the globe are currently predicting a large loss of permafrost by the year 2100 across much of Alaska where some predictions say the majority of the loss will be seen in Central Alaska versus the North

Slope (Pastick, Jorgenson, & Wylie, 2015). Models created show that nearly 40% of boreal and arctic permafrost will be reduced by more than 15% by the end of 2100 (Brewer & Jin, 2008; IPCC, 2013; Survey, 2015).

The University of Alaska in Fairbanks (UAF) is one of the leading research organizations exploring permafrost and is performing ongoing research on the changes taking place in permafrost soils in Alaska and Russia. Various organizations have placed numerous boreholes around the world, which are being monitored by the Permafrost Laboratory at UAF. Based on the data gathered, the UAF laboratory concluded that permafrost is degrading at an alarming rate (Osterkamp & Jorgenson, 2009). The United States Army Corps of Engineers' Cold Regions Research and Engineering Laboratory (CRREL) also has been monitoring permafrost conditions at a Permafrost Experiment Station in Fairbanks, Alaska, as well as at their Permafrost Tunnel in Fox, Alaska. Their research has focused on how infrastructure and changing climate is affecting permafrost and how permafrost is affecting arctic infrastructure. Both of these research organizations have found that clearing vegetation and manmade infrastructure play a major role in the degradation of permafrost (K. Bjella, personal communication, May 10, 2016).

Due to a lack of understanding of the climate-permafrost relationship, the 1990 International Panels on Climate Change (IPCC) encouraged scientists to begin researching the effects of temperature variations, seasonal snow cover, surficial sediments, and bedrock types on permafrost conditions (IPCC, 1990a; Riseborough, Shiklomanov, Etzelmuller, Gruber, & Marchenko, 2008). From this research, various methods were created to model active layer changes and permafrost degradation. Some of these methods include Stefan's Formula, Neuman's Theory, and Kudryavtsev's

Equations (Anisimov, Shiklomanov, & Nelson, 1997; Jumikis, 1966; Kudryavtsev,

Garagulya, Kondrat yeva, & Melamed, 1977). Most recently, UAF's Geophysical

Institute Permafrost Lab (GIPL) used these abovementioned methods to create a

permafrost modeling tool, the GIPL 2.1 model, which calculates active layer thickness,

soil temperatures at various soil layers, liquid water content fields, as well as permafrost

maps ("GIPL 2.0," 2010; Romanovsky & Marchenko, 2009).

The soils on Eielson Air Force Base, Alaska are made up of a thin layer of

alluvial deposits, which range around 10 feet in thickness. Below this layer is a much

thicker layer of gravels (Foreman, Rajek, & Bliss, 2016). Even though frozen gravels

have strong bearing capacities in both the frozen and thawed states, there are concerns

with the strength of the gravels during seismic activity (K. Bjella, personal

communication, April 12, 2016).

Ice-rich permafrost poses the biggest threat to manmade infrastructure. On

Eielson AFB, discontinuous, syngenetic permafrost exists on parts of the base. Although

much of the base's soil has already undergone thawing, certain sites are of particular

concern, such as a proposed F-35 (USAF Joint Strike Fighter) hangar and other facilities.

These facilities will be constructed on thawed soils as well as frozen permafrost. The

disparity between the capabilities of these two soil conditions will need to be taken into

account when designing the facility.

Problem Statement

The IPCC claims extreme temperature changes by the year 2100, with an increase

around 1-3.7°C globally and 2.2-5°C in the Arctic. However, their projections and

models have changed and evolved over time, which has allowed much speculation regarding the future of the world's climate. Their projections and the accuracy of recorded historical data have been a subject of much debate throughout scientific communities due to the political drive behind the science (Hamilton, 2011).

Roughly $552M in Military Construction (MILCON) is being programmed for Eielson Air Force Base (AFB) in Alaska in the next three years. Currently, little is known about the potential impacts of climate change to Air Force infrastructure in arctic regions. However, many researchers are claiming climate change is affecting the soils' capacity to support structural foundations (A. Instanes & Anisimov, 2008). The United States Air Force (USAF) needs to know the potential risks of climate change and how a change in surface temperatures will affect permafrost soils on northern-tier bases.

In order to adequately plan these MILCON projects and corresponding construction standards that should be used, the strength and deformation characteristics of the frozen soil need to be determined. In order determine these soil properties, active layer thicknesses (maximum thaw depth) and permafrost temperatures need to be determined (A. Instanes & Anisimov, 2008). To-date the USAF does not fully understand permafrost soils or have a method to accurately perform these calculations.

Research Objectives/Questions/Hypotheses

The researcher sought to adequately model permafrost conditions on Eielson AFB historically and into the future with as little variability and error as possible. The data around this research included USAF surface observations, geotechnical reports, and Scenarios Network for Alaska and Arctic Planning (SNAP) Data from UAF's

International Arctic Research Center, which can be fed into various models to predict

permafrost conditions at various locations around Alaska. According to the literature,

theories from Kudryavtsev's Equations and Stefan Formula could be used to accurately

model permafrost characteristics over time ("GIPL 2.0," 2010; Panda, Marchenko, &

Romanovsky, 2014; Romanovsky & Marchenko, 2009). By performing this analysis, the

study focused on answering the following questions:

       1.   *What is a likely climate scenario for Central Alaska into the year 2100?*

The first question seeks to understand the different IPCC emissions scenarios and

determine which one most closely correlates with observed temperature trends at Eielson

Air Force Base.

       2.   *Will climate change have a negative impact on USAF infrastructure assets on northern tier bases?*

This question takes a qualitative look at the potential impacts of permafrost

degradation on Arctic infrastructure, as well as the potential mitigation techniques

available in construction.

       3.   *Will climate change lead to permafrost degradation at specific construction sites on Eielson AFB?*

This question seeks to understand how the climate is impacting permafrost soils at

two construction sites on Eielson Air Force Base using two modeling techniques. The

first is an analytical method, known as the Stefan Formula, and the other a more robust

numerical model, UAF's GIPL 2.1 Permafrost Model.

Scope and Methodology

This research was conducted in a series of steps. The first major section of the research focused on analyzing historical USAF weather data. This data collected by U.S. Weather Service and the USAF over the last 60-70 years. To perform the analysis, simple linear regression modeling was used to plot mean annual air temperature (MAAT), mean annual dew points, degree-days, and seasonal lengths against the various years to determine a trend over the given number of years (1947-2015). The entire dataset encompassed 1944-2016 but data was carefully scrubbed for errors, such as long periods of missing data which can skew the regression model. Due to erroneous data, some years were removed while performing the analysis.

The next major section used weather data, geotechnical data, and snow cover data to model permafrost conditions in the past and into the future. Both the Stefan's Formula and Kudryavtsev's Approach provide theoretical modeling of active layer thickness but are required to make a number of unrealistic assumptions. Some of these limitations include: ignoring seasonal variations in the ground surface temperatures, changes in snow cover, and temperature dependent thermal properties of soils. However, there are two ways to overcome these limitations. For one, approximate analytical models can make simplifying assumptions of these conditions. Another possibility is to use a numerical technique to solve more complex problems (Riseborough, Shiklomanov, Etzelmuller, Gruber, & Marchenko, 2008).

UAF attempted to fill this gap and more realistically model soil temperatures by creating the GIPL 1.0, and most recently the GIPL 2.1 permafrost modeling tool ("GIPL 2.0," 2010; Romanovsky & Marchenko, 2009). This model was used in two ways: to

model active soil layer changes from 1947 to 2015, and predict active soil layer changes

and permafrost temperatures from 2016 to 2100 using multiple data sets.

In order to model the past roughly 70 years, daily temperatures and snow cover

data, along with soil characteristics were used. All of this data were used as inputs for the

GIPL 2.1 model to create cross sectional views of the soil layers with respect to time. The

model has the capability of creating matrices of soil temperatures and liquid water

content fields at various depths, as well as permafrost maps through the use of ArcGIS

("GIPL 2.0," 2010).

The next step calculated model projections for 2016 to 2100 on two separate

construction sites on Eielson AFB. In order to perform this analysis, projected average

monthly temperatures and snow cover, along with thermal soil characteristics were

plugged into the GIPL 2.1 model.

In order to gather the necessary temperature data for the GIPL model, projected

temperature data was acquired from UAF's International Arctic Research Center SNAP

database. This database was created in 2007 by Dr. Scott Rupp and uses various IPCC

emissions scenarios to predict the Alaskan climate until 2100 (Rupp, 2007). Soil data was

gathered from geotechnical reports provided by United States Army Corps of Engineers

(USACE). The snow data was acquired from the 14th Weather Squadron located in

Asheville, North Carolina.

Significance

The degradation of permafrost has major ecological and engineering implications,

which can range from local changes in hydrology and vegetation to possible increases in

global greenhouse gases (Davis, 2001; Panda, 2011). Although research has been accomplished on climate change and the climate-permafrost relationship across the arctic, no climate modeling or active-layer modeling has been accomplished on any northern-tier USAF bases. This research will provide pertinent information to Air Force Civil Engineer Center (AFCEC) strategic planners when overseeing arctic construction projects. Specifically, it will provide planners with the ability to plan foundation designs and mitigation techniques for changing soil characteristics.

II. Literature Review

Chapter Overview

A large amount of research has been accomplished regarding climate change, with the International Panel on Climate Change (IPCC) being the main focal point of this movement. Some research supports climate warming, while research is more critical and concludes other possibilities. Despite the unknown direction of the temperature shift, the U.S. Government, in particular the Department of Defense (DoD), is greatly concerned with climate change's impact on its operations (GAO, 2014). This chapter focuses predominately on climate change and permafrost soils and their interactions, as well as impacts on arctic infrastructure. The chapter also addresses permafrost and active layer modeling techniques along with the statistical methods utilized.

Climate Change

The Earth's climate is controlled by a number of factors. These include: the amount and direction of solar energy arriving at the top of the atmosphere, absorption of incoming radiation by the atmosphere and the ground, reflection of incoming solar radiation from clouds, snow, soil, and water surfaces (the Earth's albedo), the distribution of continents and oceans, and topography (Davis, 2001, pp. 253-254).

The main theory behind climate change rests in the theory of increasing concentrations of greenhouse gases. As the Sun's radiant heat passes through the Earth's atmosphere it warms the surface. Traditionally, longwave radiation is radiated back out of the atmosphere and back into space. However, increasing greenhouse gasses are absorbing

9

the outgoing heat and projecting them in all directions. This prevents the heat from fully escaping the Earth's atmosphere and warms the atmosphere (IPCC, 1990b).

According to meteorological experts around the globe, our climate is changing (IPCC, 2013). The IPCC began tracking these changes and producing their own predictions beginning in 1990. Following the earliest panel in 1990, the First Assessment Report was published and made available to the public. In this report, the board predicted a global mean surface air temperature increase of 1.5°C to 4.5°C by the year 2100 (IPCC, 1990b). As more knowledge became available, along with changes in the political environment, the IPCCs altered their predictions throughout the years. Additional IPCCs met in 1995, 2001, 2007, and most recently in 2013. Each IPCC utilized emissions scenarios and Representative Concentration Pathway (RCP) models to predict possible changes in the climate.

The most recent IPCC published the Fifth Assessment Report (2013). In this piece, the experts projected an increase in global mean annual air temperature of 1.5°C to 7.8°C by the year 2100 in their RCP4.5 emissions scenario. The RCP 4.5 emissions scenario projects growing emissions until 2040, where it will peak and begin to decline. Additionally, this report claimed an increase of global mean annual air temperature increase of 1°C per decade since 1900, with most of the warming occurring prior to 1930 in Table 14.1 (IPCC, 2013).

Much like the global mean annual air temperature change, the Arctic will experience its fair share of temperature warming. Some experts predict this warming will be much higher than the global average (IPCC, 2007). However, there is some speculation as an overall cooling trend was observed in Alaska up until 1980, at which

point a small warming trend started and continued through 2005 (Brewer & Jin, 2008). In

contradiction to the claim of cooling, Leiserowitz (2005) observed a 2°C warming in

Alaska since the 1950s, and a 4°C rise in the interior during the winter months. This

warming has resulted in a 30% increase in precipitation between 1968 and 1990, as well

as a retreat and thinning of sea ice by 14% and 60% respectively since the 1960s and

1970s around the state of Alaska (Leiserowitz, 2005). Furthermore, Osterkamp (2005)

stated that most weather stations in Central Alaska have reported mean air temperatures

1°C to 2°C warmer than the three previous decades after 1977. He also concluded that the

models point to a 2°C to 5°C rise in the arctic air temperature in the next half century or

by 2050 (Osterkamp, 2005).

Figure 1 shows IPCC prediction changes from 1990 to 2013. These predictions

are indicative of the predicted increase in mean annual air temperatures by the years

2090-2099 relative to 1980 to 1999. For example, in 2007 the IPCC predicted that the

global mean annual temperature would increase by 4.0°C in their extreme prediction

scenario (A1F1 emissions scenario) and 1.8°C in their moderate (B1 emission) scenario

(Solomon et al., 2007). Some of the factors behind these changes could be due to

increased analysis techniques and technology, changing political environments, or

availability in data. Figure 2 also shows IPCC projections specific to Arctic Regions.
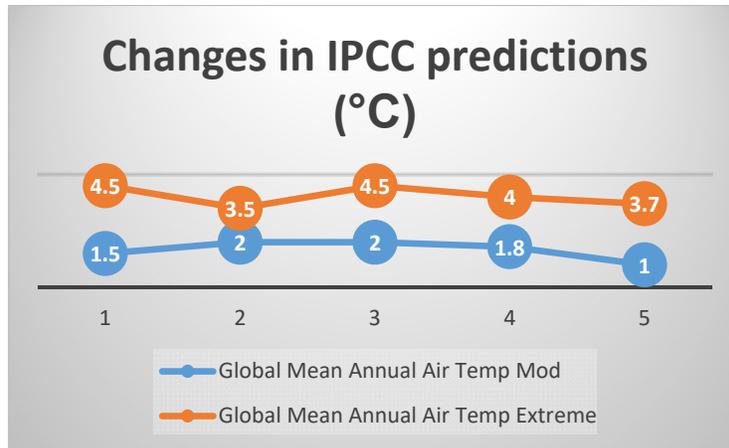
Figure 1: Global IPCC Projections
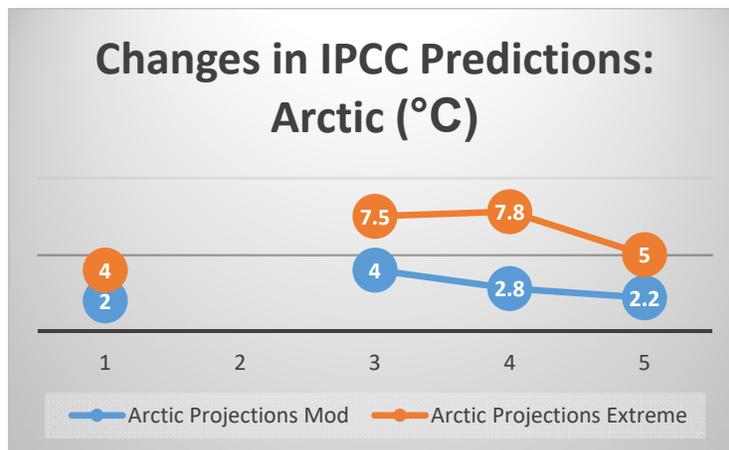
Figure 2: Arctic IPCC Projections

UAF's SNAP data has been used to graphically display the changes expected in Alaska based on multiple IPCC scenarios. Figure 3 shows the expected changes across Alaska in accordance with IPCC's A1B emissions scenario. This map shows a change of from the -4.4°C to 2.2°C range to 0.1°C to 2.3°C range (Alaska, 2016). A change of this magnitude would be detrimental to permafrost soils as the mean annual air temperature increases above freezing (0°C).
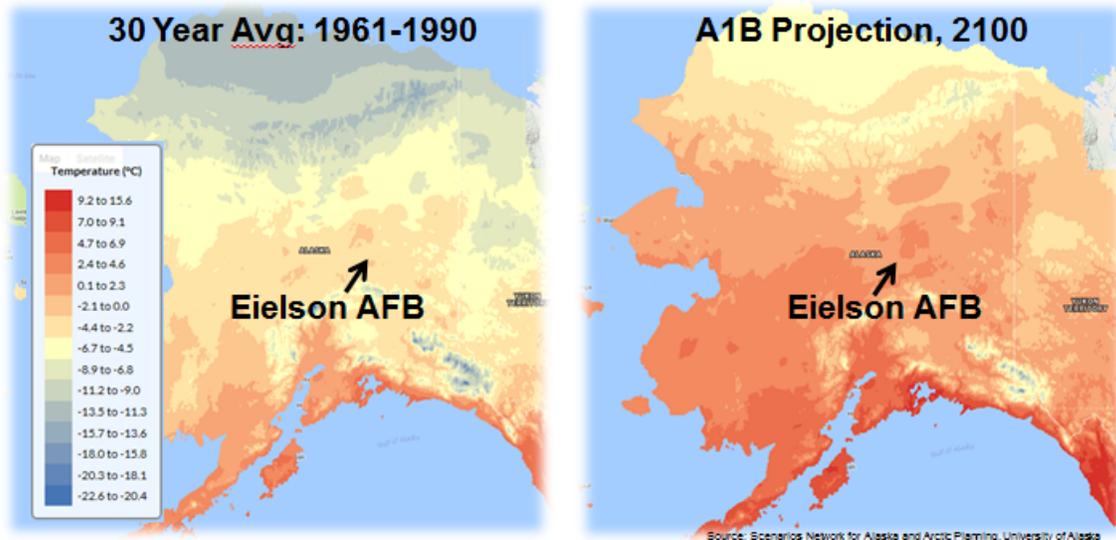
Figure 3: IPCC Projections A1B

Around any contentious issue, such as climate change, there is often much disagreement. A number of studies have been conducted to refute climate change. Reports and investigations have also been performed to try and prove the erroneous methodology in the climate change calculations and data. On occasion, the investigations have found traces of falsified documents and altered quantitative data, which increased the amount of uncertainty into the validity of the IPCC reports (Alexander, 2012). These observed changes in atmospheric air temperatures have had direct effects on ecosystems around the world (Christensen et al., 2013; IPCC, 2013). In northern regions, this was most commonly observed in permafrost soils.

Climate Change and the Department of Defense

Climate change is a topic that is concerning to any nation's government. In the United States of America (U.S.), various organizations have been studying and planning for climate change at all levels. This planning has ranged from strategic to tactical levels, and includes mission, infrastructure, and budget impacts (GAO, 2013, 2014, 2016). In the

latter part of the 20th Century, the Government Accountability Office (GAO) began looking at potential hazards to U.S. Government infrastructure, such as roads, bridges, facilities, etc. Their findings, along with results published by the several IPCC reports, have forced various initiatives across the government to incorporate climate change in its planning efforts.

From 2006 to 2016, extreme weather cost the federal government roughly $320B in repairs to infrastructure. According to the President's 2017 budget request, these costs may continue to rise if the climate continues to change (GAO, 2016). A GAO report in 2013 concluded that decision makers have systematically failed to consider climate change impacts on infrastructure. To help combat this the report recommended four actions for local decision makers: having information on local weather-related crises that resulted in repairs, understanding how to use the information available, knowing who to talk to in the local area, and considering how climate impacts have been used in past planning processes. The findings also concluded that all federal entities should utilize the best available climate-related information in their infrastructure planning. They found that infrastructure are vulnerable to changes in the climate from variations in precipitation, sea levels, and increased frequency and intensity of weather events (GAO, 2013).

In 2009, President Barak Obama published Executive Order 13514. This Order required all Federal Departments and Agencies to assess climate change risks, along with the vulnerabilities to the agencies. Responding to this Order, the Secretary of Defense published the Quadrennial Defense Review (QDR) in 2010, which expressed how the national defense strategy changes in order to prepare the military for challenges and

opportunities in the 21st Century and beyond (DoD, 2014). In response to this review, along with Executive Orders 13514 and 13653, the DoD published its first Climate Change Adaptation Roadmap in Fiscal Year (FY) 2012 and again in FY 2014. In this roadmap, they identified that rising temperatures and sea levels were threatening its infrastructure (GAO, 2014). Due to the unique mission of the DoD, a failure to incorporate climate change in planning will result in threats to the U.S.' national security. To accentuate the risk, the report referred climate change as a "threat multiplier."

In order to combat climate change, the Department established three adaptation goals that focused on identifying the effects of climate change, integrating climate change across the Department's processes, managing the risks, and working with internal and external stakeholders on climate change challenges. Four lines of effort were then outlined to support these goals: plans and operations, training and testing, built and natural infrastructure, and acquisition and supply chain (DoD, 2014).

Of particular importance to USAF Civil Engineering (CE) is the third line of effort, built and natural infrastructure. The roadmap highlights the importance of DoD infrastructure to mission preparedness and readiness, as it is the staging platform for defense and humanitarian mission areas (DoD, 2014). It is imperative that USAF CE planners account for these risks in planning objectives to prevent the negative consequences of climate change.

AF Construction on Eielson AFB

The Air Force is currently planning roughly $552M in military construction (MILCON) on Eielson AFB. These facilities are being built to house and support the new F-35, Joint Strike Fighter mission scheduled for FY2020.

Eielson AFB is located between the Tanana-Kuskokwim lowland and the Yukon-Tanana Upland areas of the Northern Plateaus. The base sits along the Chana River and is 20 miles southeast of Fairbanks in the Tanana River basin. Throughout the Pleistocene and Holocene periods, deposition and erosion were caused by glacial advance and recession. These cycles left fluvial and glaciofluvial alluvial deposits of gravel, sand, and silt. Eielson AFB has an alluvial mantel that extends roughly 10 feet below the surface. Below this mantel are layers of gravels that range anywhere from 20-30 feet or more (Foreman et al., 2016).

Some of the proposed facilities at Eielson AFB will be constructed on permafrost soils. Golder Associates (2016) states in their design report,

> If permafrost soils are encountered, two of the 50-foot-deep boreholes located under the building footprint will be completed with sealed 1-inch diameter Schedule 120 PVC to allow for subsurface ground temperature measurement. Subsurface ground temperature readings will be collected at intervals of 5 feet or less at each of the monitoring pipes at the end of the field investigation, after sufficient time has passed for the soil to freeze back and ground temperatures to stabilize. (Inc, 2016a, p. 4)

Boreholes drilled in 1987 showed evidence of discontinuous permafrost around the construction area, with the highest probability of occurrence today in the wooded areas. It

is less likely to be found in areas of existing development or areas of removed vegetation (Inc, 2016, p. 4). The hills around Eielson AFB likely contain permafrost soils similar to the CRREL permafrost tunnel in Fox, Alaska (K. Bjella, personal communication, 19 April 2016).

At least two of the proposed construction locations were found to have permafrost soils. Multiple small, heated facilities will be built on the north end of the base. Two of the borehole samples were found to have traces of massive-ice permafrost soils (Inc, 2016b). The other location is on the interior of the South Loop where the large, heated facility will be located. This location showed areas of frozen soils on the perimeter and surrounding area of the proposed construction site.

Due to the presence of permafrost soils, multiple methods were recommended by USACE. For the F-35A Flight Simulator Facility, (shallow-foundation) perimeter spread footings and strip footings were recommended (Foreman et al., 2016). These types of foundations are widely used across the arctic and on Eielson AFB. Pile foundations are also used in arctic infrastructure but are not common on Eielson AFB (K. Bjella, personal communication, 17 April 2016).

Overview of Permafrost

Although permafrost is only found in cold climates, it covers about one quarter of the Earth's surface and as much as 80% of Alaska (Washburn, 1979). Scientists believe permafrost may have originated during the Pleistocene period of glaciation which occurred about 1,000 to 10,000 years ago (Shankel, 1985). The surface layer of permafrost soil is known as the active layer and undergoes seasonal freeze and thaw

cycles (Brown, Hinkel, & Nelson, 2000; Lemke, Ren, Alley, Allison, & Carrasco, 2007).

"The depth of annual thaw depends on vegetation cover, soil type, soil moisture, and

solar aspect" (Bjella, 2012, p. 12). This layer plays a major role in cold environments due

to fact that all biological activity takes place in this thin layer (Hinzman, Kane, Gieck, &

Everett, 1991). Figure 4 depicts the temperature regime of permafrost soil during multiple

seasons.

Permafrost is also defined in different ways around the world. In North America,

any frozen soil or rock, regardless of moisture levels, that has remained below 0°C is

defined as permafrost. However, in Asia, specifically Russia, soils must maintain some

moisture and water/ice in order to be termed "permafrost". Additionally, rock and

bedrock are never termed permafrost in Russia, as they do not change characteristics

from the frozen to thawed states (V. Romanovsky, personal communication, 13 May

2016).
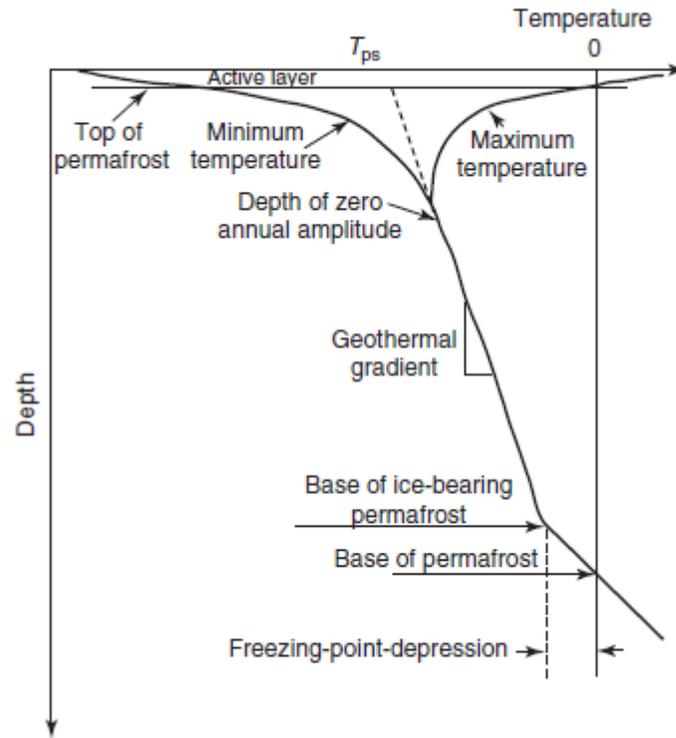
Figure 4: Temperature Regime of Permafrost Soils (Curry & Webster, 1999)

Permafrost can be classified in different ways as seen in Figure 5. "In the Northern Hemisphere, permafrost is usually divided into continuous and discontinuous zones" (Washburn, 1979, p. 332). In the continuous zone, the permafrost exists laterally under the ground surface until its lower boundary and occurs in about 90% of the ground. However, there is a possibility of widely separated thawed portions within this zone, which are known as taliks. In discontinuous permafrost zones, there is more thawed soil than frozen soil. This is due to the ground temperature in these areas being higher and closer to freezing. This discontinuous nature is a result of water flow, vegetation type, and thermal properties of the subsurface materials (Curry & Webster, 1999; Shankel, 1985).
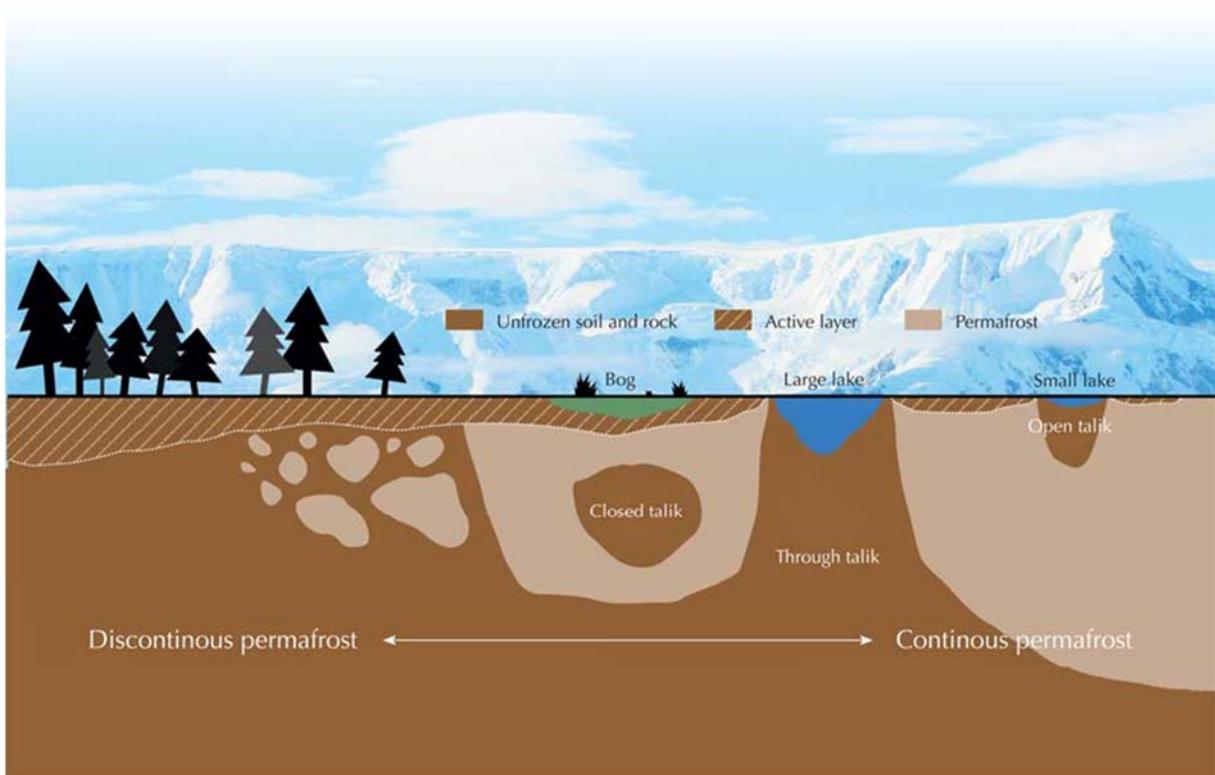
Figure 5: Permafrost Types (www.scienceinschool.org)

Permafrost is also classified as epigenetic or syngenetic. In epigenetic permafrost, the frozen state was formed in previously-deposited soil (Bjella, 2012). On the other hand, syngenetic permafrost was formed concurrently with the deposition of soil (Bjella, Tantillo, Weale, & August, 2008). These two types of permafrost react differently to Arctic infrastructure. For one, ice wedges are formed differently between the two types. In epigenetic permafrost, ice wedges have a typical wedge shape, as seen in Figure 6 below. Alternatively, in syngenetic permafrost the ice wedges will have an atypical shape (CRREL, 2012). These two types of permafrost also have different crystalline structures that will react differently on infrastructure foundations (Stephani, Fortier, Shur, Fortier, & Doré, 2014).

Figure 6: Ice Wedge Example in USACE CRREL Permafrost Tunnel in Fox, Alaska

Climate Changes Effects on Permafrost

Many scientists have concluded permafrost degradation is occurring around the arctic. They predict a large loss of permafrost by the year 2100 and that a large majority of this will occur in Central Alaska compared to Northern Alaska (Esch & Osterkam, 1990; Jorgenson & Osterkamp, 2005; Torre Jorgenson, Racine, Walters, & Osterkamp, 2001; Osterkamp, 2005; Survey, 2015; "Thawing Permafrost Threatens Alaska's Ecosystem, University of Alaska Fairbanks Researcher Says," n.d.; Washburn, 1979). Models predict that nearly 38% of the boreal and arctic permafrost will be reduced by 16% to 24% by the end of 2100. Additionally, northern latitude tundra and boreal forests are experiencing higher rates of warming compared with other parts of the world (Survey, 2015). The IPCC predicts that near-surface permafrost in high northern latitudes will be

affected by a global temperature increase. Their predictions are more ominous, stating that near surface (<3.5 m depth) permafrost will decrease by 37% to 81% by the end of 2100 under their RCP2.6 and RCP8.5 emission scenarios (IPCC, 2013). The IPCC also concluded, with high confidence that permafrost temperatures have already increased in most northern regions since the early 1980s (after the cooling period). The report stated a warming of 3°C has been observed from 1980 to the mid-2000s in Northern Alaska (IPCC, 2013).

Of particular concern to Eielson AFB is the fact that the central region of Alaska is more vulnerable to near-surface permafrost degradation than northerly regions (Pastick et al., 2015). Since discontinuous permafrost tends to be warmer than continuous permafrost, any warming in the air temperature will have a great affect on it (Osterkamp, 2005). "Additional warming will cause more of it to thaw and a warming of several degrees would cause most of it to begin thawing (Osterkamp, 2005, p. 188). This is interesting due to some researchers predicting that the colder, continuous, North Slope permafrost may be degrading at a faster rate than Central Alaska. However, Dr. Romanovsky, a professor at the University of Alaska's Permafrost Laboratory, suggests that the permafrost in Central Alaska has reached its latent heat of fusion and is undergoing an unobservable phase change. However, even though the temperature is not changing, this is of particular concern as changes are still taking place in the chemical structure of the soil (V. Romanovsky, personal communication, 19 April 2016).

However, some scientists remain unconvinced of these changes. Brewer and Jin (2008) claimed that, although there has been a warming of the upper layer of permafrost over the last 50 years, there has been no thawing of the permafrost during that same

period, since the thaw depths have gone unchanged (Brewer & Jin, 2008). However, as stated above, the differences in permafrost warming could be due to the permafrost undergoing unobservable changes.

Permafrost Degradation

Permafrost degradation generally refers to a naturally or artificially caused decreased in the thickness and/or areal extent of permafrost. This degradation has been observed in numerous areas along the discontinuous permafrost zone in the past few decades, which has moved the southern permafrost boundary northward (Lemke et al., 2007).

As the surfaces of permafrost warms within the active layer, the heat penetrates through the permafrost and eventually reaches its base. When the base of the permafrost starts to thaw, it is known as basal thawing. This is extremely common for discontinuous permafrost. In ice-rich permafrost, as the ice melts and the permafrost thaws, the ground surface subsides and causes thaw settlement. This thaw settlement does not occur uniformly and creates hills and wet depressions which are known as thermokarst terrains and can be seen in Figure 7 (Jorgenson & Osterkamp, 2005; Lemke et al., 2007).

Figure 7: Polygonal Bumps near UAF

As active layer thicknesses change over time, it can have a negative impact on permafrost soils. Climate change is causing the active layer to increase in thickness and vertically degrade the permafrost and underlying ice. As soils thaw downward during warmer months, this heat is penetrating the permafrost table and causing degradation (Jorgenson & Osterkamp, 2005). The change in active layer thicknesses is the result of heat flow from the surface to the soil layers, which can be caused by increased air temperatures, surface cover changes, soil disturbances, etc. (Brown et al., 2000; Davis, 2001).

Permafrost is being affected by not only the changing climate, but also anthropogenic processes. There are sixteen permafrost degradation types which include, but are not limited to: thermokarst lake, thermokarst basin, thaw sink, glacial thermokarst, collapse-scar fen, collapse-scar bog, thermokarst pit, polygonal thermokarst mounds, irregular thermokarst mounds, thermokarst gullies and water tracks, sinkholes

and pipes, thermos-erosional niche, collapsed pingo, and nonpatterned. The most
common types of degradation found in Central Alaska are collapse-scar bogs, irregular
thermokarst mounds, thermokarst lakes, thermokarst gullies, and thaw slumps (Jorgenson
& Osterkamp, 2005).

Most often, the degradation of permafrost is caused by anthropogenic processes.
As cities expand, populations change, infrastructure is built, and land is cleared, the
surrounding ecosystems and soils are affected. The clearing of vegetation, whether
through fires, floods, or human impacts, greatly changes the characteristics of the active
layer and permafrost conditions. This change is evident in Figure 8 below. As the surface
conditions changed at the Fairbanks Experiment Station, the thickness of the active layer
changed concurrently (Wagner, n.d.).
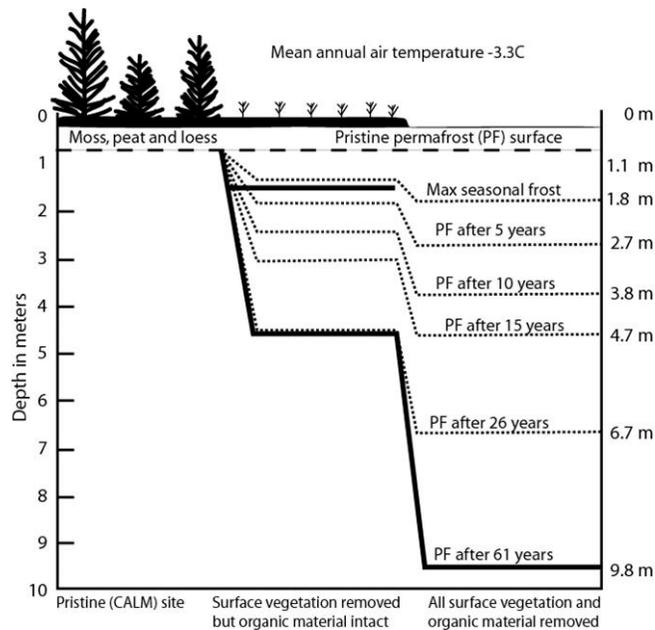
Figure 8: Graphic Illustration of the Linell Plots at Fairbanks Permafrost Experiment Station

(Wagner, n.d.)

25

The population of Fairbanks and Eielson has shifted over the past 100 years, leading to anthropogenic impacts on permafrost soils. Eielson AFB is located in the southeast portion of the North Star Borough near Fairbanks. In Alaska as a whole, the first census in 1880 counted 33,426 people living in the entire state. However, as of the 2013 census, this population has slowly increased to nearly 740,000. In Fairbanks, the census counted 30,215 souls in 2000 and 32,204 souls in 2013. This is a positive change of 1,969 over these 13 years. In the North Star Borough, this number changed from 82,840 in 2000 to 99,632 in 2013, or roughly 16,800 additional people. However, during this same period Eielson AFB saw a negative shift from 5,388 to 2,593 (Fallis, 2013).

These changes are important due to the effects of anthropogenic activities on the surrounding environment. Environmental warming was observed immediately around numerous cities around the world. As these cities expanded, so did their impacts on the environment. In particular, a phenomenon known as the heat island effect was observed, which is a warming of the environment immediately surrounding a city. This warming was a result of added infrastructure, increased automobile emissions, and added industrial areas/factories (Bornstein, 1968). According to this research, as Fairbanks and Eielson AFB expanded, they may have impacted the temperatures in and around the area. This warming of the surface air temperatures would have had a negative impact on the permafrost soils.

North Slope Permafrost Degradation

This research would be remiss to leave out the impacts of climate change on the North Slope of Alaska, as the DoD has multiple interests in this area. In a recent GAO report (2015), the surveyors concluded multiple long-range radar stations (LRRS) were

experiencing permafrost degradation at an alarming rate. These stations are located along the coast very close to the shoreline. As the atmospheric temperature is increasing in the region, sea ice is being affected in the Arctic Ocean. Essentially, the sea ice, which protected the coastline from erosion, is not forming until later in the year, after the major fall storms. This change is leaving the coastline vulnerable to strong winds, waves, and rain. As the coastline erodes, the permafrost layers are being uncovered and subjected to these atmospheric conditions, causing an increase in the rate of thawing (Duffy, 2015).

USACE performed an experiment in Shishmaref, Alaska, where coastal erosion was a major concern to the local residents. They installed thermistors along the coastline to study permafrost temperatures and determine the best courses of action in order to protect the coastline from continued erosion. They also studied soil temperature fluctuations during the fall storms, to see if these storms had an impact on the permafrost temperatures due to the lack of sea ice (Azelton & Zufelt, 2007). This article, however, was written in the early stages of research and did not provide any findings.

Additional research was conducted in Barrow, Alaska to monitor the ground temperature at varying depths. The team installed a series of thermistors at varying depths in the area (Brewer & Jin, 2008):

> Since deepening of the active layer and/or permafrost thaws only when the temperatures are above freezing for an extended period of time, the annual change in the thawing index tends to provide far greater insights regarding the near-surface permafrost than do the changes in the annual average air temperatures. (Brewer & Jin, 2008, p. 193)

Active Layer and Permafrost Modeling

Due to a lack of understanding of the climate-permafrost relationship, the 1990

IPCC encouraged scientists to begin researching the effects of temperature variations,

seasonal snow cover, surficial sediments, and bedrock types on permafrost conditions

(IPCC, 1990a; Riseborough et al., 2008). A number of methods have been devised for

theoretically calculating active layer thickness over time and to model climate-permafrost

interactions theoretically (Anisimov et al., 1997). "Process-based permafrost models

determine the thermal state of the ground based on principles of heat transfer, and can be

categorized using temporal, thermal, and spatial criteria" (Riseborough et al., 2008, p.

138). All of these models use some version of basic heat flow theory to attempt to model

the climate-permafrost relationship (Riseborough et al., 2008). These methods have

grown over time as more information has become available of this relationship.

Permafrost soils and active layers are caused by seasonal temperature changes and

heat flow from the air through the soil layers. Basic heat flow theories are based on three

natural laws:

1. Heat flows from a material with a higher temperature to a material with a
   lower temperature (i.e. hot to cold).

2. The amount of heat in a material is proportional to its temperature and mass.

3. The rate of heat flow across an area is proportional to its size and to the
   temperature gradient (Jumikis, 1966, p. 45).

Additionally, the depth of freezing or thawing heavily depends on soil characteristics,

such as thermal conductivity, volumetric unfrozen water content, layer thickness, and

actual temperatures (Riseborough et al., 2008).

Temperature gradients can be analyzed linearly or non-linearly through soil layers. Figure 6 below shows a linear temperature gradient through snow and frozen soil. dT/dX_{sn} shows the change in temperature with respect to the depth of snow. $dT/d\xi$ shows the temperature change with respect to depth in the frozen soil. The temperature is coldest at the surface of the snow. It increases in temperature through the snow until it reaches the soil surface. From here, the temperature continues to increase through the frozen ground until it reaches unfrozen soil, T_f. In permafrost this can either be the thawed soil between the active layer or the talik below the permafrost layer.
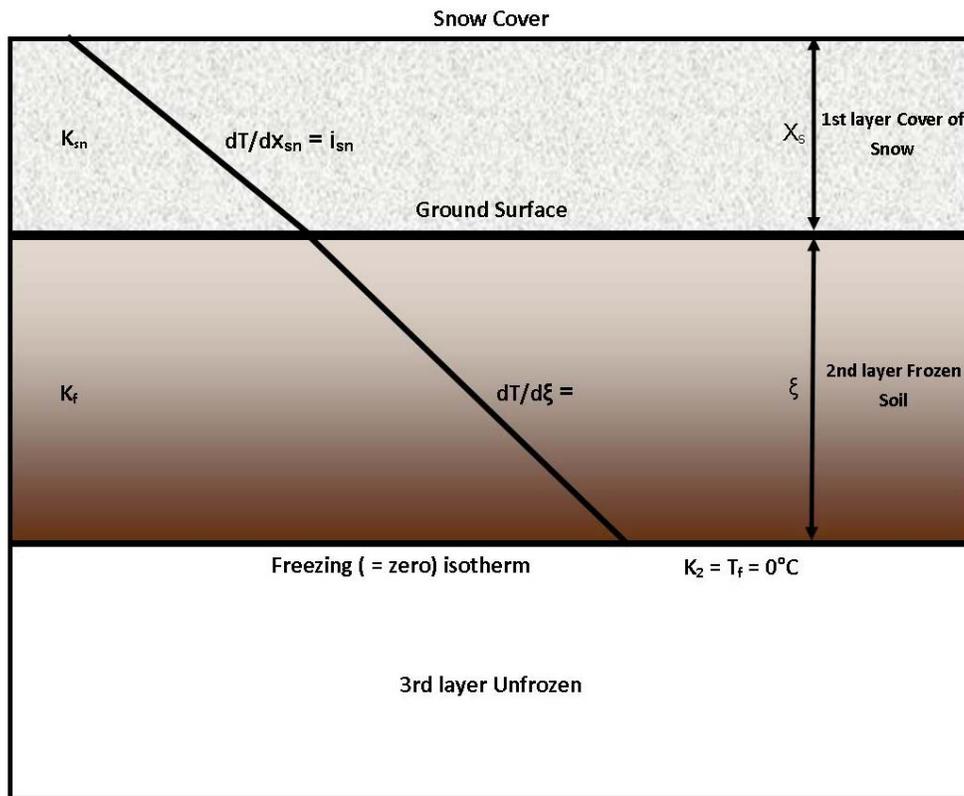
Figure 9: Thermal Gradients (Jumikis, 1966)

Specific analytical models that look at the thermal behavior of the ground when undergoing freezing or thawing processes are limited in their ability to realistically model

29

real-world conditions. Some of these limitations include, ignoring seasonal variations in the ground surface temperatures, changes in snow cover, and temperature dependent thermal properties of soils. However, there are two ways to overcome these limitations. For one, approximate analytical models can make simplifying assumptions of these conditions. Another possibility is to use a numerical technique to solve more complex problems (Riseborough et al., 2008).

One of the simplest analytical methods is known as Stefan's Formula, which calculates the depth of frost penetration in a soil type as a function of time. The simplest form of this equation is given as (Jumikis, 1966, p. 107):

$$\xi = \sqrt{\frac{2K_1}{L\rho_i}(T_f - T_s)t} \qquad (1)$$

Where ρ_i is the density of ice, K_1 is the thermal conductivity of frozen soil in Cal/(m)(hr)(degree), L is the latent heat of fusion of water (ice), T_f is freezing temperature (0°C), T_S is the soil surface temperature when it is $< T_f$, and t is time in hours.

Although this method is simple, it assumes that the soil is homogeneous and the temperature gradient in the frozen zone is linear (Jumikis, 1966; Kudryavtsev et al., 1977; Stendel & Christensen, 2002). A similar, more complex method has been used, and is known as the Neumann Equation. It was developed by Franz Neumann while he was studying the process of ice formation on water surfaces. His equation differs from Stefan in that it takes into account the frozen part of the soil and the unfrozen soil beneath the freezing isothermal surface (Jumikis, 1966).

In 1977, Kudryavtsev proposed another method which calculates the maximum annual depth of thaw propagation and the mean annual temperature at the base of the active layer. His method takes into account, the atmospheric temperature, vegetation cover, soil moisture, snow cover, and soil thermal properties. The method assumes a periodic steady state with phase change and can be used in a variety of climate conditions (Anisimov et al., 1997; Riseborough et al., 2008). Kudryavtsev assumes that the following equation can describe the annual variations of the air temperature (Anisimov et al., 1997, p. 64).

$$T_a(t) = \overline{T_a} + A_a cos(2(t/P))$$ (2)

Where $\overline{T}$ is the mean annual air temperature, A_a is the annual amplitude of the air temperature, t is time, and P is the period of temperature cycle (typically 1 year). The model also assumes that the mineral soil is a homogeneous medium and has different thermal properties in frozen and thawed states. It also assumes that the mineral layer is covered by three other layers, which include an organic-rich surface horizon, vegetation, and snow (Anisimov et al., 1997; Riseborough et al., 2008). Therefore, the depth of seasonal thawing and freezing is given by the following equation (Kudryavtsev et al., 1977, p. 116):

$$Z = \frac{2(A_s - \overline{T_z}) \times \left(\frac{\lambda \times P \times C}{\pi}\right)^{1/2} + \frac{(2A_z \times C \times Z_c + Q_L \times Z) \times Q_L \left(\frac{\lambda \times P}{\pi \times C}\right)^{1/2}}{2A_z \times C \times Z_c + Q_L \times Z + (2A_z \times C + Q_L) \times \left(\frac{\lambda \times P}{\pi \times C}\right)^{1/2}}}{2A_z C + Q_L}$$ (3)

Z is the depth of thawing or freezing; A_s is the annual amplitude of the surface temperature (°C); $\overline{T_z}$ is the mean annual temperature at the depth of seasonal thawing

31

(°C); λ and C are the thermal conductivity and volumetric heat capacity of the soil (W m^{-1} °C^{-1}, and J m^{-1} °C^{-1}); P is the period of the annual temperature cycle (1 yr, expressed in seconds); and Q_L is the volumetric latent heat of fusion (J m^{-3}) (Anisimov et al., 1997, p. 65).

Although these models theoretically model active layer changes and permafrost temperatures with respect to time, they make many assumptions and are limited in their realism, as aforementioned. UAF attempted to fill this gap and more realistically model soil temperatures by creating the GIPL 1.0, and most recently the GIPL 2.1 permafrost modeling tool ("GIPL 2.0," 2010; Romanovsky & Marchenko, 2009). "The GIPL model was developed specifically to assess the effect of changing climate on permafrost". GIPL 1.0 was created as "quasi-transitional, spatially distributed, equilibrium model for calculating the active layer thickness and mean annual ground temperature" (Romanovsky & Marchenko, 2009, p. 2). It has been used to evaluate the changing climate's effect on arctic permafrost (Romanovsky & Marchenko, 2009). The GIPL 2.0 model built on these concepts by simulating soil temperature dynamics, as well as the depth of seasonal freezing and thawing. It accomplishes this by calculating one-dimensional, non-linear heat equations with phase changes numerically (Marchenko, Romanovsky, & Tipenko, 2008). The GIPL 1.0 model and version 2, GIPL 2.0 make use of Stefan and Kudryavtsev's approaches (Marchenko et al., 2008; Panda et al., 2014; Romanovsky & Marchenko, 2009).

Active Layer Indices

Degree day calculations have been widely used in calculations on mechanical systems. These are usually categorized as heating or cooling degree days (Büyükalaca,

Bulut, & Ylmaz, 2001). In contrast, for permafrost calculations thawing and freezing degree days have proven useful. Thawing degree days (DDT) are defined as days with an average temperature greater than 0°C. Conversely, freezing degree days (DDF) are days with an average temperature equal to or less than 0°C. The following equations were used to calculate degree days (Christensen & Kuhry, 2000, p. 29,650):

$$Degree\text{-}Days = Temperature(^{o}C) \times 1 \ Day \qquad (4)$$

An average year in Fairbanks, Alaska has roughly 1,800 thawing degree days. These warm temperatures penetrate into the soils. The rate of penetration depends on the thermal conductivity of the soil, the amount of water in the soil, and whether or not the ground and water is frozen. The warmer temperatures melt all of the ice in the active layer first, then penetrates through the frozen soil (Davis, 2001).

Degree Days has also been used in calculating a normalized permafrost index, *F*, which is given by the following equation (Christensen & Kuhry, 2000, p. 29,650):

$$F = \frac{\sqrt{DDF}}{\sqrt{DDT}+\sqrt{DDF}} \qquad (5)$$

The permafrost index was used to create permafrost distribution maps in Eastern Russia (Nelson & Outcalt, 1987) and across the Arctic (Stendel & Christensen, 2002). Thresholds were set by Nelson & Outcalt (1987) as 0.5, 0.6, and 0.67 to represent sporadic permafrost, discontinuous permafrost, and continuous permafrost, respectively (Nelson & Outcalt, 1987).

Arctic Infrastructure

The degradation of permafrost has major ecological and engineering implications, which can range from local changes in hydrology and vegetation to possible increases in global greenhouse gases (Panda, 2011). It is important to note that thawing permafrost is a slow and incremental process that will not cause major issues in days or hours to infrastructure. The effects of sinkholes are not identical to thawing permafrost, though many people may have this concern (Bjella, 2012). Thawing starts from top down and then moves from the bottom up. The thawing rates are slow and generally about 10 cm per year near the surface and fewer than 2 cm per year at the base. Due to this slow rate, it requires decades to millennia to completely thaw discontinuous permafrost (Lundardini, 1996; Osterkamp, 2005; Osterkamp, 1983).

When planning construction on permafrost soils, it is imperative that the engineers understand the strength and deformation characteristics of the frozen soils, which are temperature dependent. In order to do this, active layer thicknesses (maximum thaw depth) and permafrost temperatures must be determined prior to finalizing designs (A. Instanes & Anisimov, 2008).

Permafrost degradation has known to negatively impact different types of infrastructure, from roads to buildings. Within the vertical construction realm, different foundation types are typically encountered. These range from shallow foundations to piles and caissons. One study looked at the adverse impacts of climate change on pile foundations. The study found that over the course of seven years from 2000 to 2007, there was a loss of roughly 100 kN of adfreeze bond strength along the pile foundations due to increasing temperatures in Norway (A. Instanes & Anisimov, 2008). Foundation

failures and differential settlement can be observed around the Fairbanks, Alaska region. One house beside Farmer's Loop Road in Fairbanks showed signs of differential settlement and can be observed in Figure 10 below. This settlement is likely due to the impacts of cleared vegetation along with the construction of the facility and nearby road.
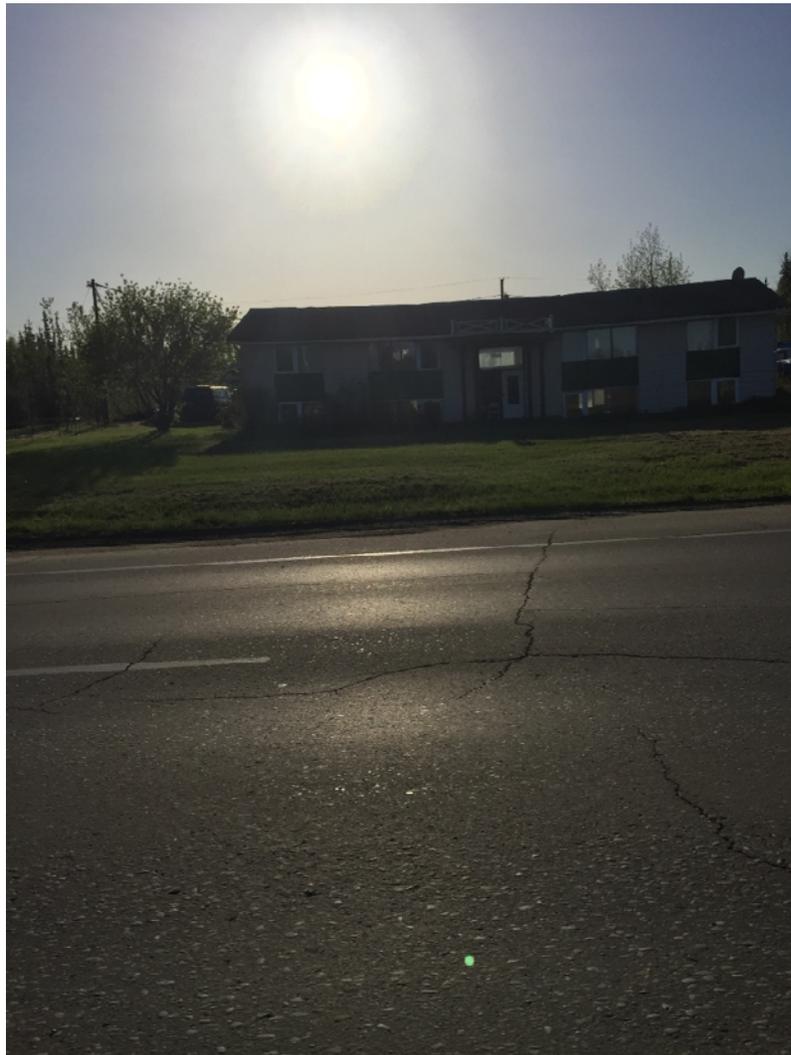
Figure 10: House along Farmer's Loop Road in Fairbanks, AK

Current Practices

Many different construction methods have been explored to try and prevent permafrost deterioration. These methods can be broken into two categories: active and

passive cooling techniques. Active techniques seek to cool the soil, while passive techniques prevent heat transfer between the infrastructure and the soil (Wei, Guodong, & Qingbai, 2009).

A number of passive methods exist and have been widely used in the construction industry. Currently, a minimum distance of 8 feet between the bottom of a foundation and the surface of the permafrost has been used. This allows enough distance to prevent heat transfer from facility to the permafrost surfaces (K. Bjella, personal communication, 13 May 2016). However, there are many concerns that passive methods may not be adequate to combat the changing climate's effects on soil temperature, especially in areas where warm, discontinuous permafrost exists (Wei et al., 2009). Due to these conclusions, many projects have been completed using active cooling techniques.

Recent Advancements

Active cooling techniques aim at "actively" cooling the soils beneath foundations and pavements. In a study conducted along the Qinghai-Tibet Railroad (QTR), the scientists looked at a number of measures to cool down the roadbed. These methods focused around controlling the amount of solar radiation, heat convection, and heat conduction, as well as a combination of these.

The first few methods studied concentrated on adjusting the amount of solar radiation that reached the ground surface. The first study utilized an awning over the roadbed. The ground surface temperatures were studied over a one-year period. At the end of the year, the readings were compared to a nearby unshaded ground surface location. The next study implemented the installation of shading boards on the embankment slopes. This particular research was performed in Beiluhe, China. Similar to

the awning, the surface of the embankment slope was studied over the course of a year and compared with untreated embankment slopes.

The results under the two types of solar radiation methods varied slightly with shading boards being more effective than awnings. In areas where the awnings were installed, after a year the surface mean temperature was 8-15°C lower than the uncovered ground. The maximum difference was also found to be 24°C. Additionally, the awning was found to be effective at protecting the roadbed from thawing, as the active layers (thawing depth) differed by about 0.9 meters between the ground under the awning and the uncovered ground. On the other hand, shading boards resulted in mean annual slope surface temperatures on the embankments below the boards that were 3.2°C lower than outside the board, as well as 1.5°C lower than the natural ground surfaces. Shading boards could also help the embankment fill from becoming loose by reducing the number of freeze-thaw cycles, protect the embankment from wind and erosion caused by rain.

The next method focused on modifying and controlling heat convection. In this method, crushed rock was placed over the permafrost ground to act as a thermal semi-conductor. Much like the above methods, the mean annual ground temperatures were studied under the crushed rock and compared to untreated ground. Next, PVC and concrete ventilation ducts were installed along the railroad in Beiluhe. To study the effectiveness of these ducts, the temperature inside the ducts was taken and compared with the atmospheric air temperature around the embankment. Shuttered ventilation ducts were also examined by comparing the mean annual ground temperature at a depth of 3.5 meters of the treated ground with untreated ground.

The final study under the convection umbrella analyzed thermosiphons. This method is generally accepted in preventing thawing permafrost under manmade structures and has been adopted in permafrost regions all over the world. Thermosiphons are one of the more expensive approaches but were considered in this case study. Seven, nine, or twelve-meter thermosiphons were installed vertically or diagonally into the shoulders of the railroad for 34 kilometers and were spaced approximately three meters apart. Again, the mean annual ground temperature in the treated area was compared to the controlled, untreated ground.

Each of the three types of heat convection techniques also had an impact on the ground temperature in the treated areas. Crushed rocks showed a cooling impact on the ground beneath it, but the magnitude of the results was less than predicted. The air in winter is colder than the permafrost, which causes a Raleigh-Bernard convection effect between the crushed rocks. This results in the permafrost losing heat during this period. Additionally, in the summer, the colder air is heavier and sinks through the rocks to the ground. During this period, the main form of heat transfer takes place as conduction. Wind also plays a role as it is stronger in the winter months and helps force stronger convection during this period. The bad results were likely caused by the difference in the mean annual ground temperature in the different regions. It was also concluded that fine soil particles entered the crevices between the rocks and reduced the porosity of the rock layer, which reduced the cooling effect.

The concrete and PVC ventilation ducts were found to be somewhat effective at reducing the ground temperature to an acceptable level. However, the air inside the ducts was measured at 1.6-1.8°C higher than the air temperature, and the embankment

temperature was measured at 4ºC higher than the air temperature. This temperature was compared with the natural ground surface temperature, which was 2.5ºC higher than the air temperature. Due to these results, shuttered ducts were examined and determined to be more effective. The mean annual ground temperature, which was taken at 3.5 meters below the embankment, was measured to be 0.45ºC lower than the embankments installed with open ventilation (Wei et al., 2009). It was concluded that the thermosiphons lowered the ground temperature, as well as moved the permafrost table upwards. In addition, the modeling also helped show that the cooling effect would be higher when the thermosiphons are installed at an angle of 25-30 º on the side of the slopes. However, these thermosiphons alone cannot fully prevent the permafrost in the embankments from thawing over a period of 50 years, where the air temperature is -3.5ºC (Zhi, Yu, Wei, Jilin, & Wu, 2005).

The control of heat conduction was the final area studied. In order to perform this study, the engineers were required to find a thermal semi-conductor material that had a greater thermal conductivity in the frozen state than when it was in the thawed state. Layers of water-absorbing material, which were separated by layers of air, were placed in a sealed container. Water was then added to the container and frozen. The thermal conductivity of the two states was measured. However, these experiments were conducted in controlled environments in a laboratory and were not applied to the railroad construction. When studying heat conduction, the laboratory was able to find a material which could be studied further out in the field. When the material and water froze, the thermal conductivity of the material changed from 0.11 W/m K to 1.2 W/m K, which is an increase of approximately 10 times.

Engineers also examined the possibility of using combined controlled measures by looking at different combinations: dry bridging, shading boards and crushed-rock revetments, and thermosiphons combined with insulating board. These methods were studied and measured using the mean annual ground temperature of the treated ground and compared with the untreated ground. The results of each experiment produced different outcomes and helped show the engineers which methods worked better in permafrost regions for road and railroad construction. For example, dry bridging was installed for a total of 125 km, "in ice-rich and extremely unstable permafrost sections" (Wei et al., 2009, p. 8). The foundation of the bridges consisted of different 1.2 meter in diameter piles which were driven 25-30 meters into the ground.

Of the three combined control measures studied, dry bridging was found to be the most effective method at preventing deformation of the railroad and preventing permafrost thaw. Since the initial installation of the dry bridges prior to 2009, the average deformation of the railroad track had only been 2 millimeters on average, and a maximum deformation of 5 millimeters. Dry bridging also helped lower the ground temperature as it acted as a sunshade and allowed air to move freely through the openings. This resulted in mean annual surface ground temperature beneath the bridges to be lower than the unshaded ground. Combining thermosiphons and insulating board was not studied on the railroad but was simulated. The model created, which assumed a 2°C temperature rise due to global warming, showed this method will not be an effective construction method as the embankments will become structurally compromised (Wei et al., 2009).

Chapter Summary

Although many studies have been conducted on permafrost and climate change, the future of our climate, as well as any impacts on arctic infrastructure, still remains unclear. This research will seek to further climatologists' knowledge of the potential futures of our climate. The literature review also looked at the characteristics of permafrost soils and ways that have been studied to determine the impacts of the climate on our permafrost soils. UAF's GIPL 2.1 Model was identified from this review of literature to be a useful tool for this research. Although this model has been used at numerous other locations, this research will be the first time it has been used on a USAF installation. Additionally, linear regression methods were researched as they apply to atmospheric sciences and archived surface weather data.

III. Methodology

Chapter Overview

This chapter describes the data used in this research, as well as the methods that were used to analyze the data. The data consisted of historical USAF weather observations, SNAP data, geotechnical data, and historical snow cover observations. The methodology is broken into two major parts, with the first being a regression analysis of different climate/permafrost variables and the second focusing around active layer modeling. For the first phase, simple linear regression was used to analyze the historical data and determine climate trends over the roughly 70 years. The next portion of this research calculated active layer thicknesses numerically using UAF's GIPL 2.1 model.

Data Collection

Multiple data sources were used for this research effort. The first set of weather observations was collected from a USAF weather station on Eielson AFB in Alaska (Platform PAEI/ICAO). The observations were taken using multiple weather station types from 1944 to 2016. The total number of observations ranged from 70,000 per decade to over 200,000 per decade. The high number of observations is due to the fact that multiple measurements were taken each day. These measurements and records included:

1. Station
2. Year
3. Month
4. Day
5. Observation Type
6. Time of day

7. Winds
8. Visibility
9. Surface temperatures
10. Dew points
11. Sky conditions
12. Ceiling
13. Remarks
14. Snow Cover

As with any real data, numerous errors were found in both the temperature and snow depth data sources provided by the 14th Weather Squadron. For the weather observations, missing temperature and dew point data were observed over large portions of some years in the data sets. Additionally, the methods of recording the time of day and time of year changed throughout the years and was dealt with by changing all temperature and snow cover data points to days of the year. The days were numbered from 1 to 365 (366 for leap years).

Specifically, the years 1944 to 1946 contained a large amount of missing data and were removed from this analysis. For example, in 1944 measurements did not begin until 15 November and continued until 31 December. In 1945 and 1946, the data abruptly ends on 7 June and doesn't begin again until 1 October 1946. Additionally, due to the date (3 March 2016) this data was collected from the 14th Weather Squadron, 2016 was excluded. Large sections of missing data would skew the mean annual air temperatures off, either negatively or positively. Years that contained more observations in the winter months while missing summer observations had much lower averages than those that contained more observations in the summer months with missing winter observations.

Additionally, years 1971 and 1972 had missing temperature recordings in the PAIE observation platform on Eielson AFB. In order to fill these gaps for the GIPL 2.1

model and the regression analysis, daily observations were obtained for Fairbanks, Alaska weather station PAFB for 1971 and Fort Greely, Alaska station PABI for 1972. Although the temperatures would not be exactly the same as Eielson AFB, it was assumed that these values were within 1°C to 2°C.

Due to the nature of the timeline, this data contained a number of threats to external validity which were considered (Shadish, Cook, & Campbell, 2002). For one, instrumentation changed a number of times over the roughly 70 years of observations. As time progressed, so did the technology in the instrumentation. These improvements led to more accurate readings in the data. Unfortunately, this data did not record the particular instrument used in these observations and could not be accounted for in the statistical analysis.

Furthermore, the population changes mentioned in the Literature Review Section of this report may have had an impact on the measurements. As humans move and expand footprints, surrounding environments are impacted. This impact comes from new infrastructure, such as roads and airports, structures, and pollution. The warming of the area around urban sprawl is known as a heat island effects, and can be seen in many cities around the world (Bornstein, 1968).

The projection data set consisted of SNAP projections published by UAF's International Arctic Research Center. This data provided mean monthly air temperatures and monthly snow averages for various IPCC emission scenarios. The data used in this study was based off of CMIP5 model outputs from the IPCC Fifth Assessment Report's RCP4.5 mid-range emissions scenario (Christensen et al., 2013; "SNAP Data Sources," n.d.). These projections, however, come with high potential error. The projections

represent scientific interpretations of the potential future of our environment, but one major natural event could change these projections drastically.

The scientist's at UAF's International Arctic Research Center tried to reduce uncertainty wherever possible. For one, normal changes in weather patterns can throw off trends observed in a warming climate. The global circulation model (GCM) used in this data attempted to match these actual swings. The scientists attempted to best model actual predictions by averaging values across years to reduce uncertainty caused by natural variability. Additionally, they averaged values across multiple GCM models to determine a best-case scenario. Finally, they calibrated the GCM models against actual measured data to ensure high correlation between predicted values and actual data ("SNAP Data Sources," n.d.).

Regression Modeling

Simple linear regression is a probabilistic technique that was used. Simple linear regression is a method used in statistics to analyze a relationship between two continuous quantitative variables, the independent variable and dependent variable (McClave, Benson, & Sincich, 2014). In this study, six dependent variables were analyzed against the independent variable, years:

1. Thawing Days
2. Freezing Days
3. Thawing Degree Days
4. Freezing Degree Days
5. Normalized Permafrost Index
6. Temperature

The periods of interest were 1947 to 2015 and 2016 to 2100. This technique showed linear trends in data over a specified period of time. McClave, Bensen, and Sincich

(2014) described the five steps required to create this model. The models are built in the following form (McClave, Benson, & Sincich, 2014, p. 604),

$$y = \beta_0 + \beta_1 x_1 + \varepsilon \qquad (6)$$

Where y is the dependent variable (surface temperature), x_1 is the independent variable, β_0 and β_2 are the regression coefficients, and ε is the random error component (McClave et al., 2014). There are three assumptions which are required in order to properly apply simple linear regression. The random error component of the model must be, "normally distributed with a mean of zero, have constant variance, and be probabilistically independent" (Cook, 2006, p. 18).

Regression modeling has been used when looking at weather patterns and environmental changes in the past. Witt (2013) describes a basic method of using simple linear regression modeling to simulate the changes of arctic sea ice over time. The regression line was used to see the direction of sea ice growth or degradation (Witt, 2013). This same methodology was applied to the weather data gathered from the USAF.

Throughout the experiment, $\alpha=0.01$ is used to establish a 99% confidence. The Bonferroni correction, which is a method of adjusting P-values when multiple dependent variables are studied, is applied to avoid surpassing the overall experiment-wise alpha (McClave et al., 2014). Since only one factor existed, $\alpha=0.01$ was used throughout the testing. Two statistical programs were used in this analysis, Microsoft Excel® and JMP®.

In order to perform the regression analysis, the data points were averaged by year to create mean annual temperatures. Regression requires several assumptions to be met and the following assumptions are checked prior to conducting the regression analysis.

Testing for Normality

In order to test for normality, the Goodness-of-Fit Test (Shapiro-Wilk W Test) was used on the six variables of interest, shown in Appedix B. The following hypotheses were used in this test.

H_o: *The variables' residuals are normally distributed*

H_a: *The variables' residuals are not normally distributed*

H_o is the null hypothesis, which states that the variables' residuals are normally distributed. H_a is the alternative hypothesis and states that the variables' residuals are not normally distributed (Graboski, Bierhaus, Cantu, & Schmidt, 2016; McClave et al., 2014).

Testing for Constant Variance (Breusch-Pagan Test)

When testing for constant variance, the Breusch-Pagan (BP) Test was used. In order to perform these tests, the Sum of Squares of the Error (SSE), Sample Size (N), and Degrees of Freedom (Df) were recorded from a Two Way Analysis of Variance. From here, the Sum of Squares of the Model (SSM) was recorded using the squares of the variables' residuals. The following equation was used to determine the test statistic (T.S.) and corresponding P-value for this test:

47

$$T.S. = \frac{\dfrac{SSM}{2}}{\left(\dfrac{SSE}{n}\right)^2} \tag{7}$$

H_o: *The variances between the Mean Annual Air Temperatures residuals are equal*

H_a: *The variances between the Mean Annual Air Temperatures are not equal*

H_o is the null hypothesis, which states that the variances in the variables' residuals are equal to one another. H_a is the alternative hypothesis and states that the variances in the variables' residuals are not equal to one another (Graboski et al., 2016; McClave et al., 2014).

Independence (Durbin-Watson Test)

The next test looked at independence between the residuals.

H_o: *There is independence between the Mean Annual Air Temperatures' residuals.*

H_a: *The Mean Annual Air Temperatures' residuals are dependent upon one another.*

The null hypothesis, H_o, states that there is independence between the residuals. On the other hand, the alternate hypothesis states that the residuals are dependent upon one another. The Durbin-Watson test has two assumptions that must be fulfilled in order to be a valid test. For one, the data must be in the order it was collected. Next, the data points have to be evenly spaced (Graboski et al., 2016; McClave et al., 2014). For these data, the points are evenly spaced yearly between 1947 and 2015. Therefore, this data fulfills the assumptions of this test.

Forecasting

Using the abovementioned regression equation (Equation 6), a forecast model for temperature was created and compared with the projections in the 2013 IPCC report. A

linear projection was made based on the IPCC projections. The linear regression model was then plotted against these projections to make the comparison. This was accomplished using Microsoft Excel®.

For each of the dependent variables a linear trend line was used to predict values into the future between the years 2016 and 2100. It is understood by the researchers that this is a very simplistic forecast model with a lot of variance in the actual values that could be encountered. However, if trends continue as observed in the past 68 years of data, these futures are one of the many possible outcomes for Alaska's environment.

Validating Models

In order to validate the model, absolute percent error (APE) and confidence intervals were used on the 68 years of data. The APE was calculated using the following equation:

$$APE = \frac{Actual\ Mean\ Annual\ Air\ Temp - Predicted\ Mean\ Annual\ Air\ Temp}{Actual\ Mean\ Annual\ Air\ Temp} \tag{8}$$

This statistic showed the prediction accuracy for the linear regression used. In the case of this research, it focused around the independent variable, years, on the dependent variables of interest (McClave et al., 2014).

Empirical coverage was also considered when looking at the final model. A 99% prediction interval and 99% confidence interval, as well as a predicted value, were all calculated from the regression line. From here, the actual values were compared with the confidence intervals. When the actual value was within the 99% confidence interval, this was identified as a success. The percentage of successes was recorded and also used to validate the usefulness of the model (McClave et al., 2014). A success was recorded as a

1 and a failure was recorded as a 0 in JMP®. Bar charts were used to graphically

represent the number of successes as compared to the number of failures and are

displayed in Appendix D.

Active Layer and Permafrost Modeling

As the surfaces of permafrost warms within the active layer, the heat penetrates

through the permafrost and eventually reaches its base, resulting in permafrost

degradation. The changes in the active layer thicknesses are critical to understanding the

state of the permafrost beneath it (Lemke et al., 2007). A number of methods have been

devised for theoretically calculating active layer thickness and associated permafrost

temperatures over time. Stefan's Formula, Neuman's Theory, and Kudryavtsev's

Equations (Anisimov et al., 1997; Jumikis, 1966; Kudryavtsev et al., 1977). For the

purpose of this study, Stefan's Formula was used and compared with UAF's GIPL 2.1

model.

Stefan's Formula

Stefan's Formula helps provide an approximate result by calculating heat

conduction to determine active layer thicknesses. However, some unrealistic assumptions

need to be made. For one, it assumes negligible sensible heat effects, which is usually

true when latent heat is larger than sensible heat effects. This is usually only true in soils

with high water content, but not in dry soils (Bonan, 1989). This equation also assumes

that temperature gradients in the soil are linear in nature (Bonan, 1989; Jumikis, 1966).

The following equation takes the latent heat of fusion of ice relative to the amount of

water in the soil into consideration, as well as the volumetric heat capacities of ice and solids in the soil (Jumikis, 1966).

The version of Stefan's Formula used in this study is given as follows (Jumikis, 1966, p. 107):

$$\xi = \sqrt{\frac{2K_1(T_f - T_s)t}{Q_L + \frac{T_f - T_s}{2}C_{vf}}} \tag{9}$$

Where:

K_1 = Thermal conductivity of frozen soil in Cal/(m)(hr)(degree)

Q_L = The latent heat of fusion of water (ice) in calories

T_f = Freezing temperature (0°C), T_S is the soil surface temperature when it is $< T_f$

t = Total number of hours of days with an average temperature ≤0°C

C_{vf} = The volumetric heat capacity of frozen soil.

In order to calculate C_{vf}, the following equation must be used (Jumikis, 1966, p. 108):

$$C_{vf} = \gamma_s\left[c_{ms} + \frac{(c_{mi})(\omega)}{100}\right] \tag{10}$$

Where:

γ_s is dry weight of soil obtained from UFC 3-220-10N Table 6

c_{ms} = 0.20 and is the heat capacity of dry soil in cal/(g)(°C) (Jumikis, 1966, p. 108)

c_{mi} = 0.50 and is the heat capacity of ice in cal/(g)(°C) (Jumikis, 1966, p. 108)

ω = the moisture content of water in soil in % of dry weight of soil

The total amount of latent heat of fusion for converting water into ice is calculated

as follows (Jumikis, 1966, p. 108):

$$Q_L = (80) \left(\frac{\omega}{100} \right) (\gamma_s) \qquad (11)$$

Where ω and γ_s are the same as above. The following data was inputted for the Stefan

Formula:

Table 1: Small Heated Facility Stefan Equation Inputs

Small Heated Facility/Surround Vegetation Untouched: Project B			
Variable	**Value**	**Units**	**Source**
K(1)	2.0	[Cal/(cm)(hr)(°C)]	Jumikis, 1966, p. 232: Thermal Conductivity of Various Substances
T(f)	0	°C	Freezing Temperature
T(s)	Mean Annual Air Temp	°C	Excel® =AVERAGE(Average Daily Temps of days ≤T(f))
t	Winter Season Length	hours	Sum of the hours of winter (days with T(s)<0°C
Q(L)	51.26	Cals	Equation 11
C(vf)	0.26	[cal/cm^3]	Equation 10
C(ms)	0.2	[cal/(g)(°C)]	Given: Jumikis, 1966 p. 108
C(mi)	0.5	[cal/(g)(°C)]	Given: Jumikis, 1966 p. 108
ω	50%	%	From USACE Geotechical Data
γ(s)	1.28	g/cm^3	From UFC 3-220-10N Table 6, p. 7.1-22

Table 1 describes the methodology used in this calculation. Working through the

table, a more detailed description is required. The Thermal Conductivity of Frozen soil

was determined by looking at the graph on page 232 in Jumikis (1966) based on 50%

porosity of the soil, 1.28 g/cm³ dry weight of soil from UFC 3-220-10N, and to find a

value of 2 [Cal/(cm)(hr)(°C)]. T(f) is a given value of 0°C for freezing at standard-

temperature-and-pressure (STP). T(s) was taken by taking the mean of the average daily

temperatures for days with an average daily temperature less than or equal to T(f).

Equations 10 and 11 were used to determine the volumetric heat capacity of frozen soil

(C_{vf}) and the total amount of latent heat of fusion for converting water into ice (Q_L),

respectively. These values were also compared with those provided by Dr. Romanovsky

at UAF (V. Romanovsky, personal communication, 26 October 2016).

The depth of freezing was plotted over the period of 1947 to 2015 using Microsoft

Excel®. The described regression techniques were then applied to these data sets to

determine linear trends for the historical data.

Degree Day Calculations

In permafrost calculations thawing and freezing degree days have proven useful.

A thawing degree day (DDT) is defined as a day with an average temperature greater

than 0°C. Conversely, a freezing degree day (DDF) is a day with an average temperature

equal to or less than 0°C (Christensen & Kuhry, 2000). The following equations were

used to calculate degree days (Christensen & Kuhry, 2000, p. 29,650):

$$Degree\,Days = Temperature(^oC) \times 1\,Day \qquad (12)$$

Degree Days were also used to calculating a normalized permafrost index, *F*,

which is given by the following equation (Christensen & Kuhry, 2000, p. 29,650):

$$F = \frac{\sqrt{DDF}}{\sqrt{DDT}+\sqrt{DDF}} \qquad (13)$$

Thresholds were set by Nelson & Outcalt (1987) as 0.5, 0.6, and 0.67 to represent

sporadic permafrost, discontinuous permafrost, and continuous permafrost, respectively

(Nelson & Outcalt, 1987).

The normalized permafrost indexes and degree days (DDF and DDT) were

plotted over the period of 1947 to 2015 using Microsoft Excel®. The described

regression techniques were then applied to these data sets to determine regression lines for the historical data.

Seasonal Calculations

Seasonal calculations were determined using a similar method to the DDF and DDT. For the purposes of this research, a winter day was defined as a day with a mean air temperature of 0°C or less. A summer day was defined as a day with a mean air temperature greater than 0°C. The calculations were given by the following formulas:

$$\textit{Thawing-Days} = \sum \textit{\#Days(>0°C)} \tag{14}$$

$$\textit{Freezing-Days} = \sum \textit{\#Days(≤0°C)} \tag{15}$$

Once the total number of days was calculated for each season, the yearly values were plotted on a line graph from 1947 to 2015 in Microsoft Excel®. Following this, the regression techniques described were applied to determine a regression line for the data.

GIPL 2.1

In order to more accurately predict active layer thicknesses and permafrost temperatures, UAF's GIPL 2.1 model was used. This model has been widely accepted across the permafrost field of study and is being taught in various geophysics courses at the University of Alaska Fairbanks. UAF's model results have also been published a number of times in the Proceedings of the International Conferences of Permafrost (Marchenko et al., 2008; Panda et al., 2014; Panda, 2011; Riseborough et al., 2008; Treat, Wisser, Marchenko, & Frolking, 2013).

Additionally, this model has been validated using actual measurements around the Arctic (Marchenko et al., 2008; Nicolsky, Romanovsky, & Tipenko, 2007; Panda, 2011). In one study, 15 boreholes were available for validation. Out of these 15 boreholes, most of the models resulted in very small errors and within 1-2°C of the actual temperature (Marchenko et al., 2008). Additionally, model runs were completed at various stations across Alaska. These also resulted in very small variations from measured soil temperatures, usually within 1-2°C of the actual measured temperature (Panda, 2011). Furthermore, Nicolsky et al. (2007), along with a team of scientists tested the model near Dalton Highway in Alaska and found the model to calculate temperatures within 0.3-0.5°C of the actual measured temperatures at various depths (Nicolsky et al., 2007).

"The GIPL 2.0 model takes air temperature, snow depth, surface organic layer properties, moisture, thermal conductivity, and heat capacity of different soil layers as input and simulates daily average soil temperature at desired depths" (Panda, 2011, p. 72). Heat conduction is assumed to be the dominate process, allowing the use of a one-dimensional heat equation with phase change. GIPL 2.0 is a numerical model that solves the abovementioned one-dimensional non-linear heat equations with phase changes. The heat equation assumes that the system is only one-dimensional where heat only moves vertically through the strata, and that the soil temperatures are homogenous in the horizontal direction and all other dimensions. This assumptions is made possible by using a finite element analysis, where the layers of soil are non-infinitely thin and homogenous. Modeling the process of soil freezing/thawing is accomplished by using the unfrozen water content curve and soil thermal properties, which are specific for each geographical

location, layer of soil, and soil type (Marchenko et al., 2008). Additionally, it is assumed that no internal sources of sinks of heat exist in the soil and temperature changes that impact the soil only occur at the soil surface. Other assumptions are: the migration of water is negligible through the soil, there are no changes in topography and soil properties in the lateral direction, frost heave and thaw settlement is negligibly small, and there is no ice lens formation during soil freezing and thawing. Lastly, the model assumes that, "the special enthalpy formulation of the energy conservation law makes it possible to use a coarse vertical resolution without loss of latent heat effects in the phase transition zone even in cases of fast temporally and spatially varying temperature" (Marchenko et al., 2008, p. 1126).

The GIPL 2.1 model makes use of the Enthalpy formulation of the one-dimensional Stefan Formula (as cited in Marchenko et al., 2008). The model uses "the quasi linear heat conduction equation, which expresses the energy conservation law" (Marchenko et al., 2008, p. 1126):

$$\frac{\partial H(y,t)}{\partial \tau} = div(\lambda(y,t)\nabla t(t,\tau)), y \in \Omega, \tau \in \psi \tag{16}$$

Where H(y, t) is the enthalpy:

$$H(y,t) = \int_0^t C(y,t)\,dt + L\phi(y,t) \tag{17}$$

Where:

$C(y,t)$ = The heat capacity

L = The latent heat

$\lambda(y,t)$ = The thermal conductivity

$\phi(y,t)$ = The volumetric unfrozen water content

56

t = Temperature (°C)

y = Depth (m); the depth domain in this simulation is $0 \leq \Omega \leq 20$

τ = Time; ψ is the time interval with initial temporal step of 24 hours (Marchenko et al., 2008; Panda, 2011).

Modeling Steps

The GIPL 2.1 model was used for two portions of this research, to model past permafrost conditions and project permafrost changes between 2016 and 2100 using IPCC emissions scenario RCP 4.5 projected temperatures and consistent facility temperatures. A total of six scenarios were used for this research on two separate MILCON projects:

1. Historical data with undisturbed conditions
2. SNAP data on native soils
3. Consistent foundation temperatures on excavated soils

The two MILCON projects were on Eielson AFB: The first project is a large, heated facility where preexisting vegetation will be removed and the second is a small, heated facility where the surrounding vegetation will remain in place.

The historical temperatures were used to show active layer changes to the undisturbed soils over the period of 1947 to 2015 at either borehole location, or project site. The final temperature gradients from these model runs were used for the predictions. The first two forecast model runs looked at active layer changes (1) if the soil and vegetation remained untouched from 2016 to 2100 and (2) the IPCC RCP 4.5 emissions scenario were to become true on both project sites. The last two model runs looked at the impacts of infrastructure on the active layer thickness and permafrost. The large, heated

57

facility was assumed to be kept at 15°C over the course of a year with a temperature loss of roughly 4°C through a 12" (30.5 cm) concrete slab (Dhananjay & Abhilash, 2014). The small, heated facility was assumed to be kept at 11.8°C for the entire year, as stated in the design specifications (Green, 2016) with a 3°C temperature loss through the 8" (20 cm) concrete slab.

In order to calibrate the model, initial temperatures were provided by UAF's GIPL for a typical borehole in the Fairbanks area. Due to the absence of actual soil temperatures, it was not possible to calibrate to known values at these boreholes. The initial temperatures at various depths can be observed in Table 2 below. One hydrological year's temperatures and snow cover data (1 September to 31 August) were then used and repeated 40 times to signify 40 years. Since the beginning period for the historical models start in 1947, the hydrological year used was 1 September 1947 to 31 August 1948. The GIPL model was then run for both boreholes (two different cross sections of soil) for this 40 hydrological year period. The final temperatures at the various depths were then recorded and used as the new initial temperatures for 1947.

Table 2: Initial Conditions Provided by UAF

DEPTH	TEMPERATURE	DEPTH	TEMPERATURE
-1.5	7.78	10	-2.118
0	7.78	11	-1.987
0.1	3.695	12	-1.872
0.2	1.139	13	-1.775
0.3	0.186	14	-1.691
0.4	-0.074	15	-1.628
0.5	-0.205	16	-1.578
0.6	-0.323	18	-1.484
0.7	-0.434	20	-1.395
0.8	-0.539	22	-1.311
0.9	-0.639	24	-1.229
1	-0.735	26	-1.151
1.2	-0.916	28	-1.075
1.4	-1.085	30	-1.002
1.6	-1.241	34	-0.859
1.8	-1.387	38	-0.721
2	-1.522	42	-0.587
2.5	-1.818	46	-0.456
3	-2.058	50	-0.328
3.5	-2.247	55	-0.171
4	-2.389	60	-0.017
4.5	-2.488	65	0.068
5	-2.551	70	0.151
6	-2.582	80	0.308
7	-2.521	90	0.445
8	-2.404	100	0.559
9	-2.262		

A total of five files are required to run the model, which are listed as follows:

BOUND, GRID, INIT, INPUT, and SNOW. Each of these files were saved in .pbz

format and contain a wealth of information that must be inputted into the model. The first

file, BOUND, consisted of temperature data.

Roughly 68 years of historical temperature data taken at Eielson AFB was available for the historical model of this research. Each day was given a number starting from 1 to n. Day 1 was representative for 1 January 1947. However, the first day used in this model was 1 September 1947, or day 274. This day was chosen due to the absence of snow on the ground, which provided more accurate initial conditions for heat transfer from the air to the ground. In the BOUND file, the days starting on 1 September 1947 to 31 December 2015 were recorded, as well as their corresponding average daily temperatures. Boundary conditions were also set in this file, including: lower boundary condition of gradient of temperature, value of temperature gradient at the lower boundary at 0.01 K/m, number of points for output data at 52 and number of nodes in the depth grid, which was set from 20 to 269.

The GRID file was used to set an output temperature grid at various soil depths. The range set was 1.5 meters above the soil surface down to a depth of 100 meters in 269 depth increments. 1.5 meters above the surface was used as the upper boundary due to the maximum depth of snow observed on Eielson AFB to be roughly 1.3 meters over 70 years of data.

The INIT file was used to set the initial soil conditions, or temperatures. The range of depths corresponded to the grid set in the GRID file. This range was from 1.5 meters above the soil surface to 100 meters below the surface. The initial temperatures used for this file were provided by GIPL for a nearby borehole. These temperatures were calibrated by the methods discussed above.

For the INIT file for each run, different values were used based on a point in time. Once the calibration was complete, the temperatures for each borehole were used as the

1947 initial condition. From here, the model was run over the 68 year period from 1 September 1947 to 31 December 2015 using the historical USAF weather data. At the conclusion of each of these runs, the final temperature conditions were recorded and used as the initial conditions for 1 January 2016. From here, the two initial condition files were run for each borehole from 1 January 2016 to 31 December 2100.

The SNOW file contained snow data over the same period as the BOUND file previously mentioned. This data started at day 274 and continued to 31 December 2015. Each day was matched exactly with the temperature data. Snow density was assumed to be 140 kg/m^3 as is usually observed in the Fairbanks area (V. Romanovsky, personal communication, 26 October 2016). The analysis using the SNOW file was nearly identical to the INIT file described above.

Finally, the INPUT file was used to input soil characteristics into the model. For this file, the geotechnical data, project specifications, and design drawings provided by USACE for two aforementioned MILCON projects were used. Each of the soil layers was categorized based on typical soil nomenclature (ML, OL, GP, etc.) in accordance with UFC 3-220-10N (UFC, 2005). Where the organic layer thickness was recorded in the geotechnical reports, thicknesses of moss, dead moss, and organic material were assumed. For example, on the large, heated facility the specified organic layer thickness was recorded as 0.06096 meters. It was assumed that the top 0.021 meters was moss, the next .0146 meters was dead moss, and the last organic layer was .02536 meters thick. However, for the purposes of this model, the organic layers were grouped together and assumed to be uniform throughout. The next layers' thicknesses were taken directly from

the geotechnical reports. The two boreholes used to gather the data are included in Appendix E.

UAF's Permafrost Laboratory was crucial in providing typical properties experienced in the Fairbanks area. The above mentioned method was used to divide the soil into layers. The basic properties of each layer were sent to the laboratory. Dr. Vladimir Romanovsky, a permafrost expert and author of numerous published articles on the subject matter, provided the INPUT files necessary for this model run. The input values used for the various runs are as follows:

Table 3: Soil layer parameters which were used in the GIPL 2.1 model to simulate soil and permafrost temperatures in the upper 20 m of the ground surface (Panda, 2011, p. 74)

Soil Layer (m)	Moisture (fraction of 1)	Thawed Heat Capacity	Frozen Heat Capacity	Ratio of Frozen to Thawed Thermal Conductivity
Snow				
Snow Properties	0	0.84 X 10^6	0.84 X 10^6	1.0
Small, Heated Facility (Native Soils)				
0.00 - 0.045 (organic layer)	0.24	2.6 X 10^6	2.2 X 10^6	1.4
0.045 - 1.83 (wet silt)	0.50	2.5 X 10^6	1.7 X 10^6	1.8
1.83 - 2.65 (organic silt)	0.45	2.5 X 10^6	1.7 X 10^6	1.7
2.65 - 9.75 (wet silt)	0.40	2.5 X 10^6	1.7 X 10^6	1.5
9.75 - 12.95 (massive ice)	0.99	2.5 X 10^6	1.7 X 10^6	4.0
12.95 - 14.94 (frozen organic silt)	0.45	2.5 X 10^6	1.7 X 10^6	1.8
14.94 - 20.0 (wet silt)	0.45	2.5 X 10^6	1.7 X 10^6	1.8
Small, Heated Facility (Post-Construction)				
0.00 - 3.05 (gravel/classified fill)	0.30	2.5 X 10^6	1.7 X 10^6	1.3
3.05 - 9.75 (wet silt)	0.40	2.5 X 10^6	1.7 X 10^6	1.5
9.75 - 12.95 (massive ice)	0.99	2.5 X 10^6	1.7 X 10^6	4.0
12.95 - 14.94 (frozen organic silt)	0.45	2.5 X 10^6	1.7 X 10^6	1.8
14.94 - 20.0 (wet silt)	0.45	2.5 X 10^6	1.7 X 10^6	1.8
Large, Heated Facility (Native Soils)				
0.00 - 0.061 (organic layer)	0.30	2.2 X 10^6	1.7 X 10^6	1.3
0.061 - 1.52 (silty sand)	0.35	2.5 X 10^6	1.7 X 10^6	1.1
1.52 - 2.29 (wet gravels)	0.35	2.5 X 10^6	1.7 X 10^6	1.1
2.29 - 6.09 (wet poorly graded gravel)	0.38	2.5 X 10^6	1.7 X 10^6	1.3
6.09 - 7.62 (wet sand)	0.35	2.5 X 10^6	1.7 X 10^6	1.2
7.62 - 20.0 (frozen gravel)	0.38	2.5 X 10^6	1.7 X 10^6	1.3
Large, Heated Facility (Post-Construction)				
0.00 - 1.83 (gravel/classified fill)	0.30	2.5 X 10^6	1.7 X 10^6	1.1
1.83 - 2.29 (wet gravels)	0.35	2.5 X 10^6	1.7 X 10^6	1.1
2.29 - 6.09 (wet poorly graded gravel)	0.38	2.5 X 10^6	1.7 X 10^6	1.3
6.09 - 7.62 (wet sand)	0.35	2.5 X 10^6	1.7 X 10^6	1.2
7.62 - 20.0 (frozen gravel)	0.38	2.5 X 10^6	1.7 X 10^6	1.3

Where:

Moisture = volumetric water content as a fraction of 1

Thawed and frozen volumetric heat capacity = J/m^3K [J = Joules, m = meter, K=Kelvin]

Thawed and frozen thermal conductivity = W/mK [W=Watts, m=meter, K=Kelvin]

When running the future models, SNAP data was given in average monthly temperatures for 2016 to 2100. Two emissions scenarios were provided, RCP 4.5 and RCP 8.5. As previously discussed, the RCP 4.5 scenario was selected, as it is as close to the USAF historical temperature regression and more accurately projects the expected future outlines in this research. For snow cover, historical data was used from 1948 to 2015. However, for months with a temperature above 0°C, the measured snow depth was converted to 0 meters. When the temperature was ≤0°C, monthly historical snow levels were used from the years 1948 to 2015. It is assumed that there is no trend of snow precipitation into the future. Since the historical data only covered a period of 68 years, the remaining 16 years were recorded as a repeat of 1948 to 1964.

Summary

This chapter explored the data sources available for analysis in this research. The general concept of this methodology was to gain some understanding of possible climate and soil temperature trends in order to predict possible impacts on USAF infrastructure. Various variables that have been accepted by permafrost scientists were calculated using these calculation methods. Trends were determined from these variables using simple linear regression. Next, three separate data sets were inputted into an advanced numerical

permafrost modeling program to study active layer thicknesses and permafrost

temperatures with respect to time.

IV. Analysis and Results

Chapter Overview

The methods proposed in Chapter III were used to analyze climate data, as well as soil temperatures with respect to time. Linear regression was used to analyze the six different permafrost variables. Next, The Stefan Formula and GIPL 2.1 numerical permafrost model provided active layer and permafrost modeling over most of the 20th and 21st century. Although the future of our environment is unknown, the regression and permafrost modeling methods used provides some insight into a likely scenario if 20th century trends continue through the year 2100.

Analysis

A number of assumptions were made in this study. For one, the mean annual air temperatures were indicative of the actual changes in the air temperature over time. Second, the measuring equipment gathered the air temperatures and dew points within 1°C of the actual temperature at the specified time. The GIPL 2.1 model used in this report is also assumed to be accurate as it is based on well-established heat transfer equations and has been proven valid and useful in various studies around the Arctic (Marchenko et al., 2008; Nicolsky et al., 2007; Panda, 2011).

Additional assumptions are required for the IPCC emissions scenarios. This research assumed moderate accuracy of the projections. However, it is understood that the future is unknown. A single volcanic eruption, or change in the sun has the potential of changing the Earth's environment and climate drastically.

66

The assumptions made when performing the regression modeling are described in the following sections. This research assumed constant variance, independence, and normality for the data sets analyzed. When forecasting, a linear projection was assumed to adequately model the potential future climate for Eielson AFB. However, it is understood that this model takes a simplified approach to forecasting and could easily change based on realistic futures when other variables are taken into consideration, such as solar cycles, volcanic activity, etc..

For the GIPL 2.1 model, a number of assumptions were made for this research. For one, in the projection models, it was assumed that the vegetation around the boreholes will remain the same for the natural state and surrounding the constructed facility once built. For the two facilities examined, it was assumed that each facility use will remain the same between initial construction through 2100 and that the temperatures in these facilities will remain constant throughout the same period. The data run for this model only looks at one geographical point and is assumed to be representative of the soils for the entire foundation area.

Method Implementation

The following sections explain the steps that were used in implementing the proposed method. Microsoft Excel (2010) was the platform most often used for data collection and graphing results. JMP® was the platform used when running the regression models for six permafrost variables (Thawing Days, Freezing Days, Thawing Degree Days, Freezing Degree Days, Normalized Permafrost Index, and Temperature). UAF's GIPL 2.1 Model provided the platform for active layer and permafrost modeling.

Data Collection

The proposed methodology for data collection required a large quantity of historical weather data which was easily accessible through online databases and the 14th Weather Squadron in Asheville, North Carolina. The USAF has been recording temperature data on Eielson AFB for nearly 72 years. However, two whole years were missing from the USAF database, 1971 and 1972. These data gaps were filled using www.weatherunderground.com. The database from www.weatherunderground.com had 1971 for Eielson AFB station PAEI, as well as For Greely, Alaska station PABI. These surface weather observations included temperatures, dew points, and snow data from 1945 to 2015 which were used for this research.

The GIPL 2.1 model used data from multiple databases. The historical data was recorded on Eielson AFB and included temperature and snow depths, among other variables, that were used in the historical analysis of this research from 1947 to 2015. UAF's SNAP data was provided by UAF's GIPL and included IPCC RCP 4.5 and RCP 8.5 emissions scenarios from 2006 to 2100. The GIPL model also required soil characteristics which were gathered from USACE geotechnical reports of borehole soil characteristics for the two MILCON projects studied.

Temperature Regression Modeling

When analyzing the 68 years of temperature data from the surface weather observations, simple linear regression was used. This method showed a linear relationship of the data. As can be seen in Figure 11, a slight increase was observed in the surface air temperatures over time. The regression line shows an observed annual average

temperature of -3.36°C in 1947 and -2.90°C in 2015, or a positive change of 0.46°C over the 68 years.

The data passed constant variance, but statistically failed independence and normality, which can be seen in Appendix B. However, independence can be explained due to the nature of this data. Temperature measurements are by their very nature, independent upon one another. The average temperature of one year does not depend on the temperature of the previous year. Therefore, the mean annual air temperatures used in this analysis pass independence based on the type of data. Normality, on the other hand, was considered a "reasonable" pass based on a visual look at the histogram of the data.
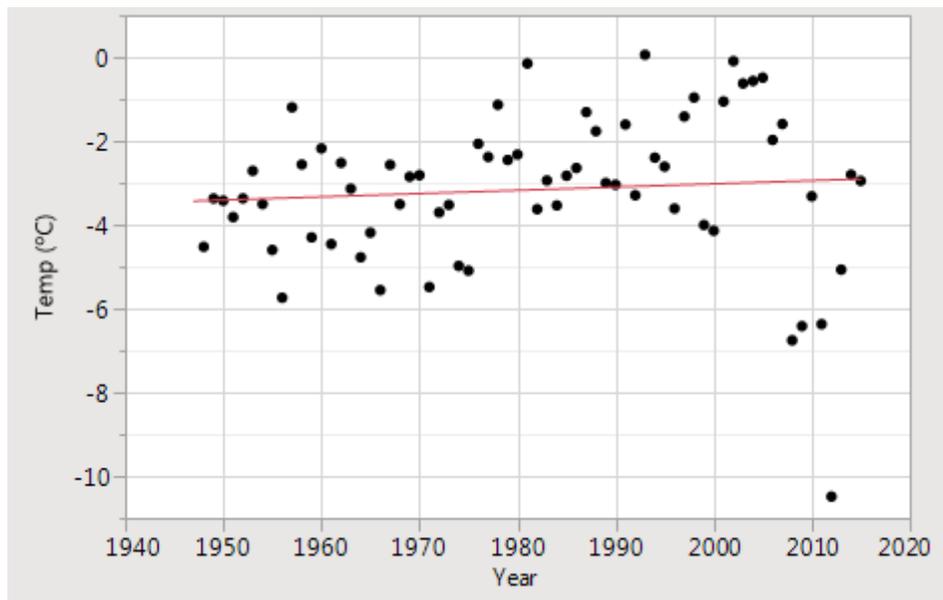
Figure 11: Temperature Regression Model

However, it is important to note that the R^2 for this analysis was only 0.006, which means that only 0.6% of the variance can be explained by the model. However, this is not surprising as the temperatures shifted within a few degree most years. This upward and downward fluctuation will result in higher residuals and SSE calculations. Figure 12 shows the trend continuing into the future using Microsoft Excel® from the

20th century and into the 21st century. The upward linear trend was continued to 2100 which shows warming to approximately -2.3°C with a 99% confidence interval of -4.9°C to 0.3°C. This range shows that the temperature is projected to increase, but instead could decrease from the mean annual air temperature of -2.9°C in 2015.
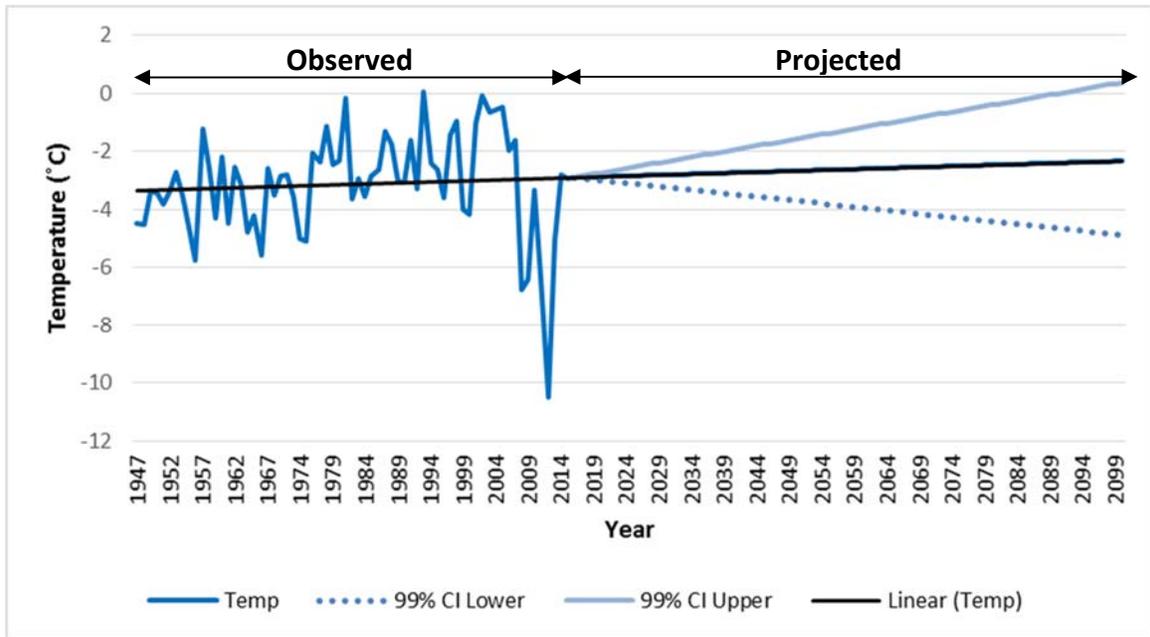
Figure 12: Temperature Regression
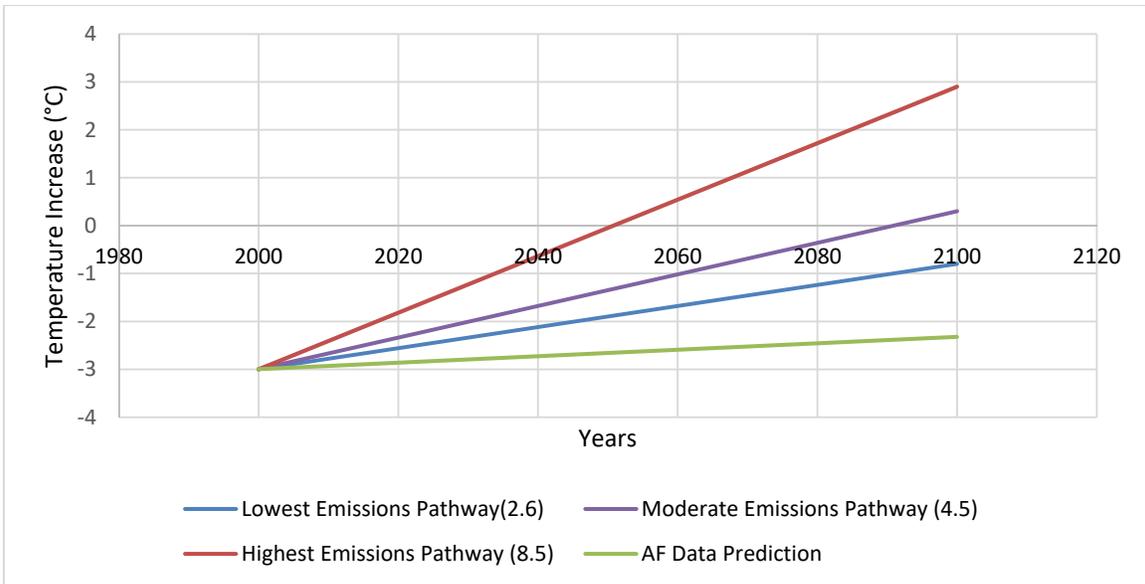
Figure 13: IPCC Comparison Chart

From the IPCC's Fifth Assessment Report in 2013, RCP 2.6 most closely models a possible future climate for Eielson AFB. Although this emissions scenario is most statistically similar to the actual data observed, due to the availability of data, RCP 4.5 was used in this analysis. Figure 13 also supports the first IPCC report from 1990 which concluded a change of 0.45±0.15°C relative to the years 1880 to 1990 by the year 2099 (IPCC, 1990b). The IPCC changed these projections in their additional reports due to political drivers and the availability of additional information.

The following regression was performed on the SNAP projection data provided by UAF's Permafrost Laboratory. The assumption tests were based on $\alpha = 0.01$, or a 99% confidence interval. Both of these data sets passed all three assumptions. Thawing days failed normality with a p-value of 0.0030 and independence with a p-value of 0.0094, but passed constant variance with a p-value of 0.93427. All of these test results are recorded in Appendix B. Although normality and independence failed, the histogram of normality was considered "normal enough" and passed visually. Additionally, as with the previous

71

regression model, the nature of the data is in itself independent. Therefore, the data is independent upon one another and passes this test.
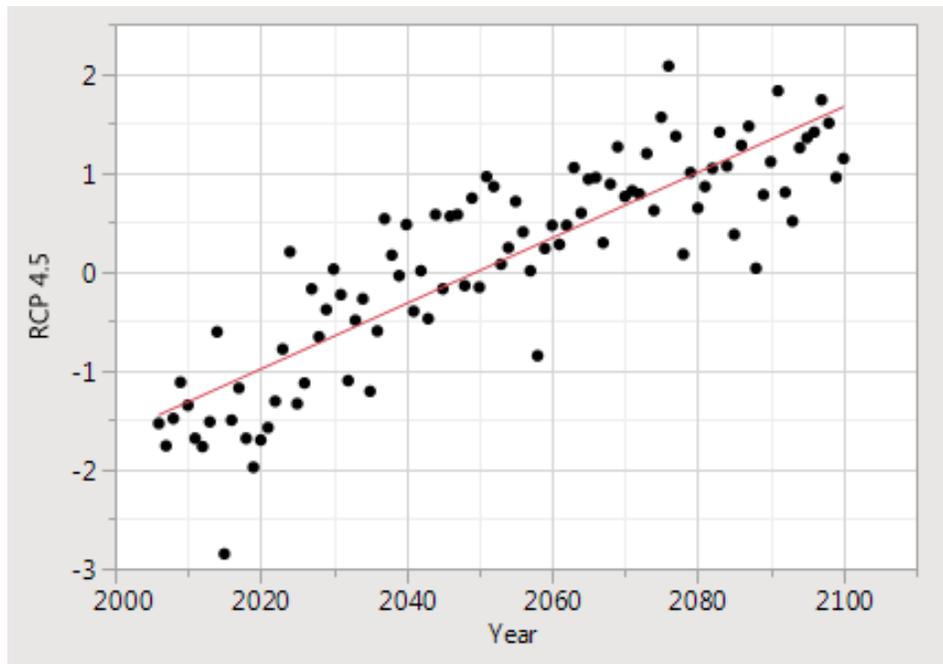
Figure 14: SNAP RCP 4.5 Projection Temperature Regression

Seasonal Length Regression Modeling

The methods described in Chapter III were used to calculate the seasonal length for each year. When analyzing the results for the 68 years of data, simple linear regression was used for both the thawing days and freezing days. As can be seen in Figure 15 and Figure 16, positive and negative linear trends can be observed in the thawing days and freezing days, respectively.

The assumptions tests were based on $\alpha = 0.01$, or a 99% confidence interval. Both of these data sets passed all three assumptions. Thawing days passed normality with a p-value of 0.0752, independence with a p-value of 0.0171, and constant variance with a p-value of 0.8729. Freezing days passed normality with a p-value of 0.7564, independence

with a p-value of 0.4999, and constant variance with a p-value of 0.91804. All of these

test results are recorded in Appendix B.
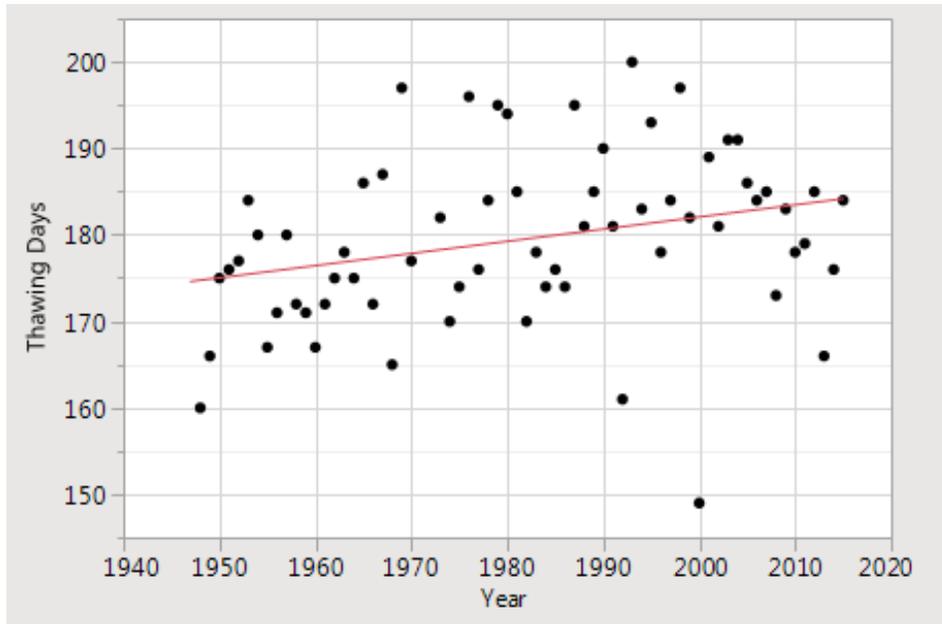
Figure 15: Thawing Days Regression
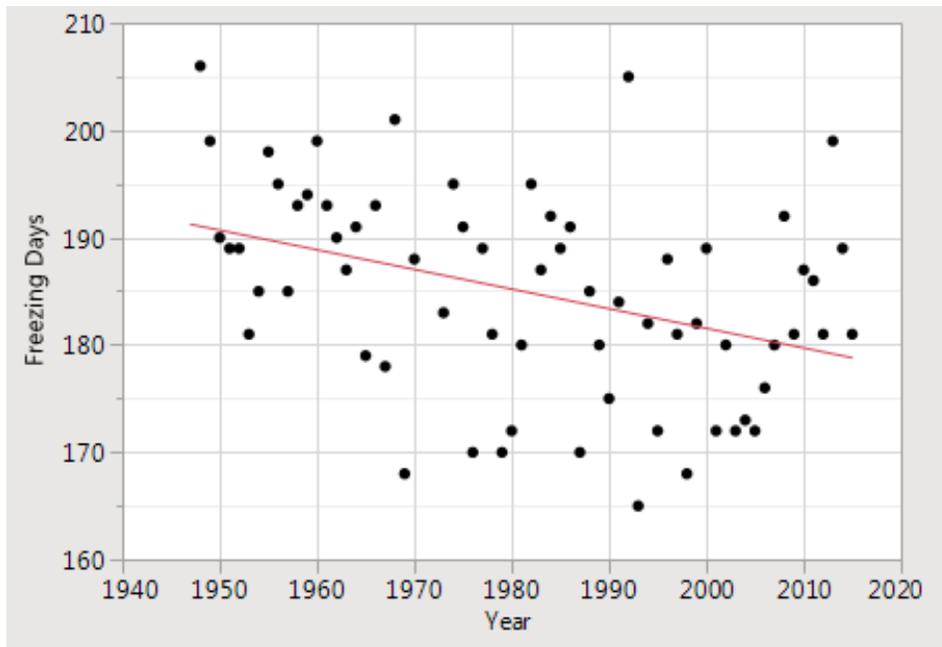
Figure 16: Freezing Days Regression

For the thawing days regression, the R^2 was around 0.084356 and for freezing

days regression was 0.152438, which shows that nearly 9% to 15% of the variability in

the data can be explained as compared to the total variation in the data. 0 and 100%

would show that the model explains none of the variability of the response data around its

mean or all of the variability, respectively (McClave et al., 2014). The p-values

calculated also provide evidence that the independent variable "years" are statistically

significant predictors of the dependent variables, thawing and freezing days.

The thawing days regression model showed an upward linear trend, with a

regression line of:

$$Thawing\text{-}Days = -99.08257 + 0.1405807 \qquad (18)$$

The freezing days regression model showed a downward linear trend, with a regression

line of:

$$Freezing\text{-}Days = 547.24125 - 0.182847 \qquad (19)$$

Thawing days had predicted values of 174.628 thawing days in 1947 and 184.188

thawing days in 2015. This equates to an increase of 9.56 thawing days over 68 years.

The freezing days regression models shows a downward linear trend, with a predicted

value of 191.239 freezing days in 1947 and 178.805 freezing days in 2015. This equates

to a decrease of 12.4 freezing days over 68 years. Based on these trends, the number of

days of thawing surpassed the number of days of freezing around 1999, as observed in

Figure 17. In essence, summers were getting longer while winters were getting shorter.

However, the regression line, which are shown as the black lines in Figure 17 are shallow

and show that the seasons are not changing at an alarming rate.

The increase in summer lengths and decrease in winter lengths would have major

repercussions on permafrost soils, as they require longer winters and colder temperatures

to prevent thickening of the active layer. As the number of thawing days increase and

freezing days decrease, the depth of thaw will increase and active layer will thicken and

cause permafrost degradation, as discussed above. However, it is important to note that

these regressions are only over a 68 year period and future trends may not follow these

linear relationships.
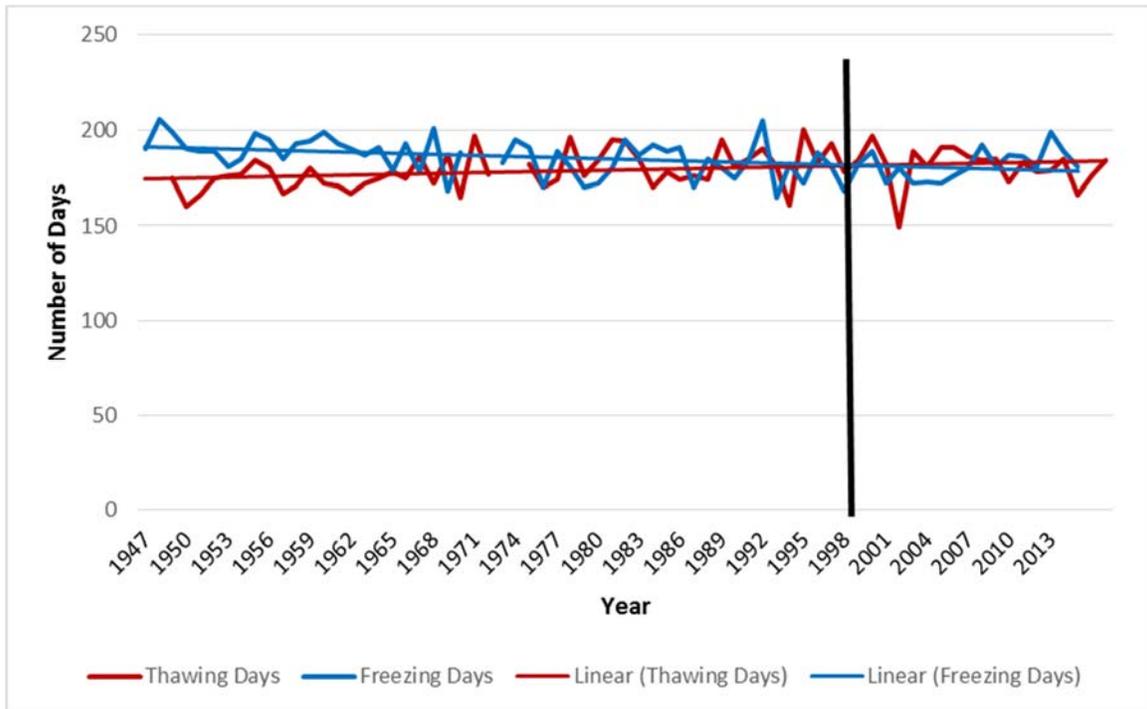
Figure 17: Length of Seasons Regression

Degree Days Regression Modeling

The methods described in Chapter III were used to calculate freezing and thawing

degree days. When analyzing the results for the 68 years of data, simple linear regression

was used for both the freezing and thawing degree days. As can be seen in Figure 18 and

Figure 19, positive and negative linear trends can be observed in the thawing degree days

and freezing degree days, respectively. This is nearly identical to the previous seasonal length results.

These tests were based on α = 0.01, or a 99% confidence interval. Both of these data sets passed all three assumptions. Thawing degree days passed normality with a p-value of 0.4128, independence with a p-value of 0.0234, and constant variance with a p-value of 0.8479. Freezing days passed normality with a p-value of 0.7153, independence with a p-value of 0.1671, and constant variance with a p-value of 0.97045. All of these test results are recorded in Appendix B.
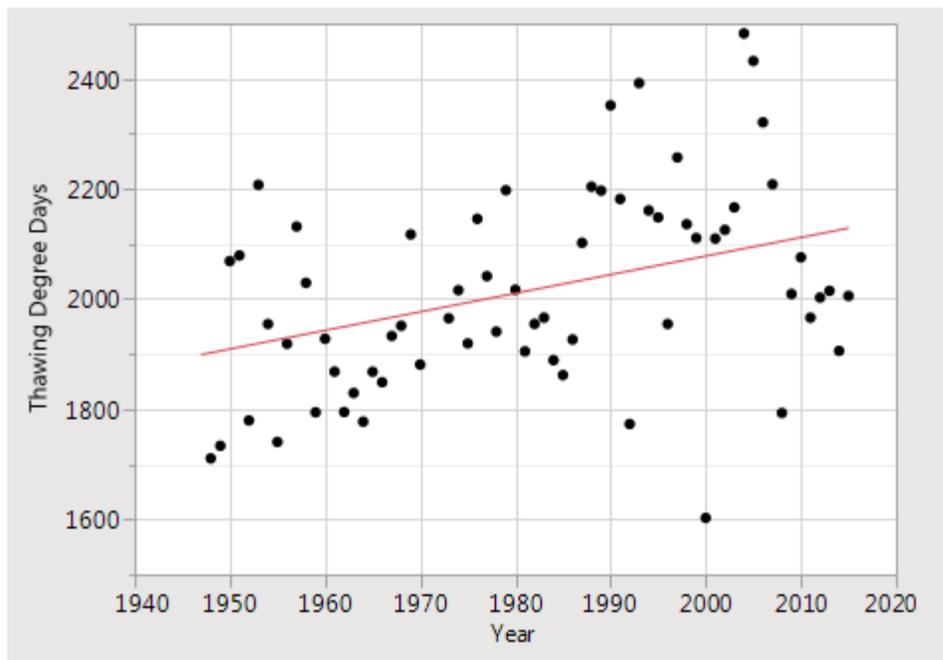
Figure 18: Thawing Degree Days Regression
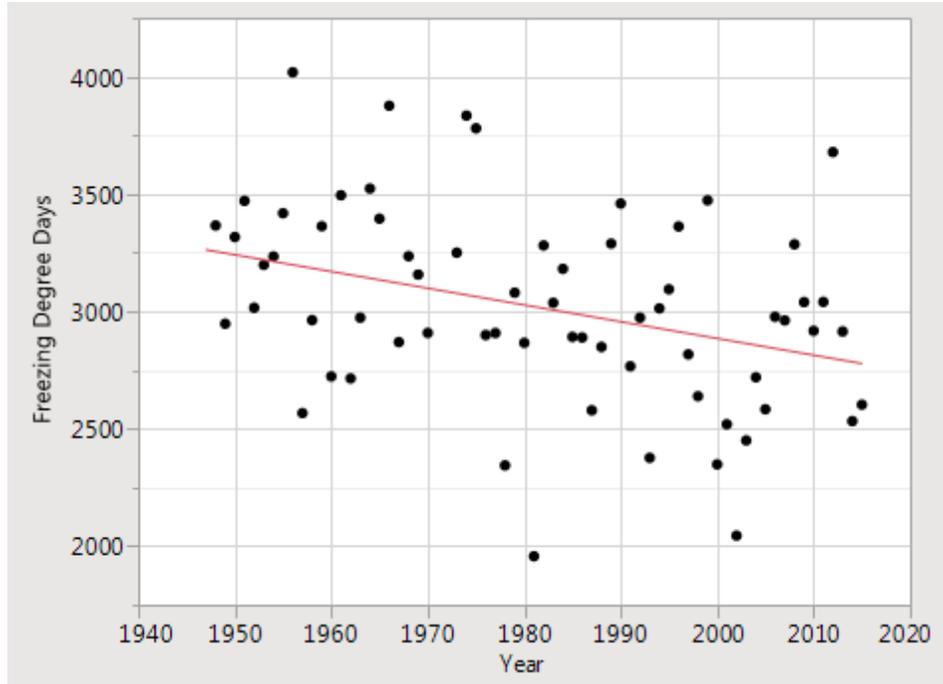
Figure 19: Freezing Degree Days Regression

For the thawing degree days regression, the R^2 was around 0.142802 and for

freezing degree days regression was 0.121601, which shows that nearly 13% to 14% of

the variability can be explained in the data. The p-values calculated also provide evidence

that the independent variable "years" are statistically significant predictors of the

dependent variables, thawing and freezing degree days.

The thawing degree days regression model showed an upward linear trend, with a

regression line of:

$$TDD = -4672.991 + 3.3756388 \times Year \tag{20}$$

The freezing degree days regression model showed a downward linear trend, with a

regression line of:

$$FDD = 17144.762 - 7.129665 \times Year \tag{21}$$

As mentioned in Chapter III, degree days are calculated by multiplying the temperature on any given day by the time, in days, and summing these daily values for the entire calendar year (Christensen & Kuhry, 2000). The thawing degree days regression model shows an upward linear trend, with a predicted value of 1899.378 thawing degree days in 1947 and 2129.922 thawing degree days in 2015. This equates to an increase of 230.5 thawing degree days over 68 years. The freezing degree days regression models shows a downward linear trend, with a predicted value of 3263.304 freezing days in 1947 and 2778.486 freezing degree days in 2015. This equates to a decrease of 484.8 freezing degree days over 68 years. If this trend continues in a linear fashion, the number of thawing days will surpass the number of freezing days around the year 2077, as can be observed in Figure 20. However, with the 99% confidence intervals shown, the crossing could occur as early as 2047 or well past 2100.

As with seasonal lengths, the increase in thawing degree days and decrease in freezing degree days has major repercussions on permafrost soils, as soils require more freezing than thawing in the active layer to maintain permafrost conditions. As the number of thawing degree days increase and freezing degree days decrease, the active layer will thicken and cause permafrost degradation, as discussed above. However, it is important to note that these regressions are only over a 68 year period and future trends may not follow these simple linear relationships.
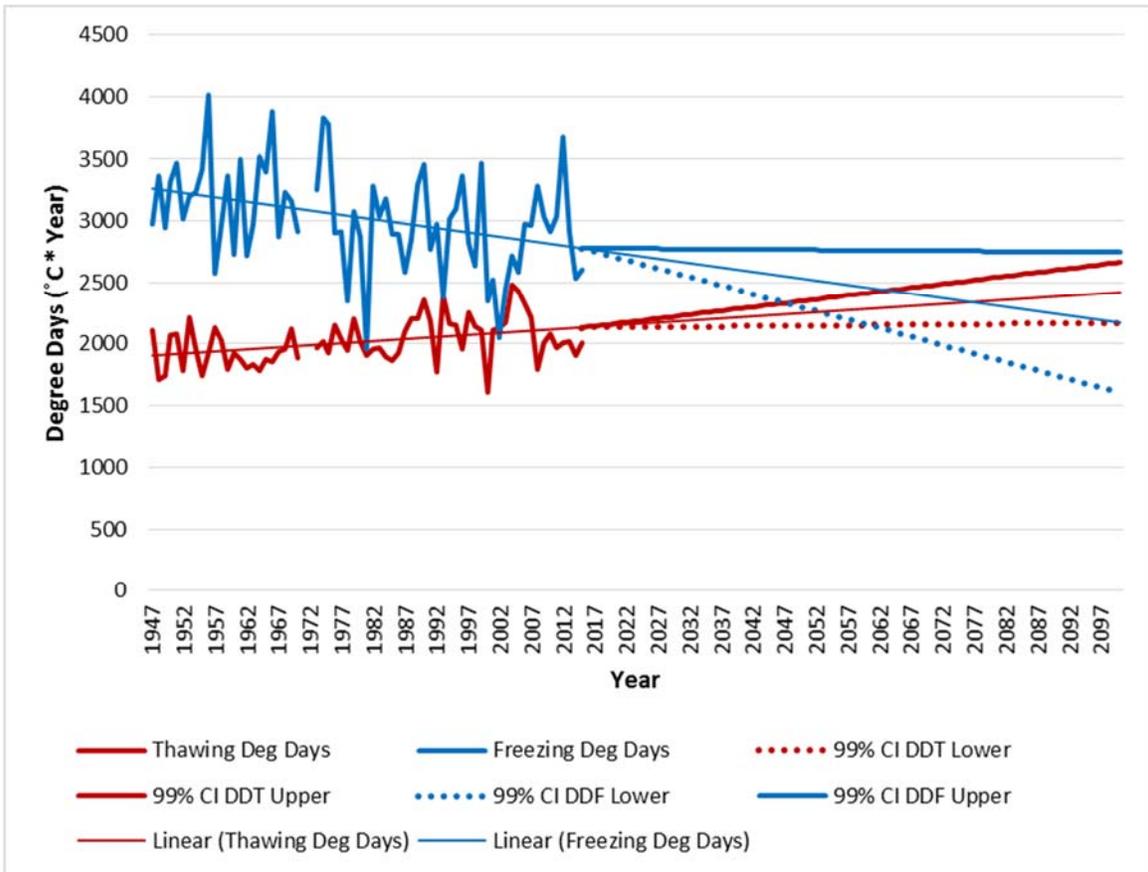
Figure 20: Degree Days

Normalized Permafrost Index Regression Modeling

The methods described in Chapter III were used to calculate the normalized permafrost index. When analyzing the results for the 68 years of data, simple linear regression was used to determine a trend in these calculations. As can be seen in Figure 21, a negative linear trend can be observed in the permafrost index over time.

These tests were based on $\alpha = 0.01$, or a 99% confidence interval. Both of these data sets passed all three assumptions. Thawing degree days passed normality with a p-

value of 0.6253, independence with a p-value of 0.0456, and constant variance with a p-value of 0.90621. All of these test results are recorded in Appendix B.
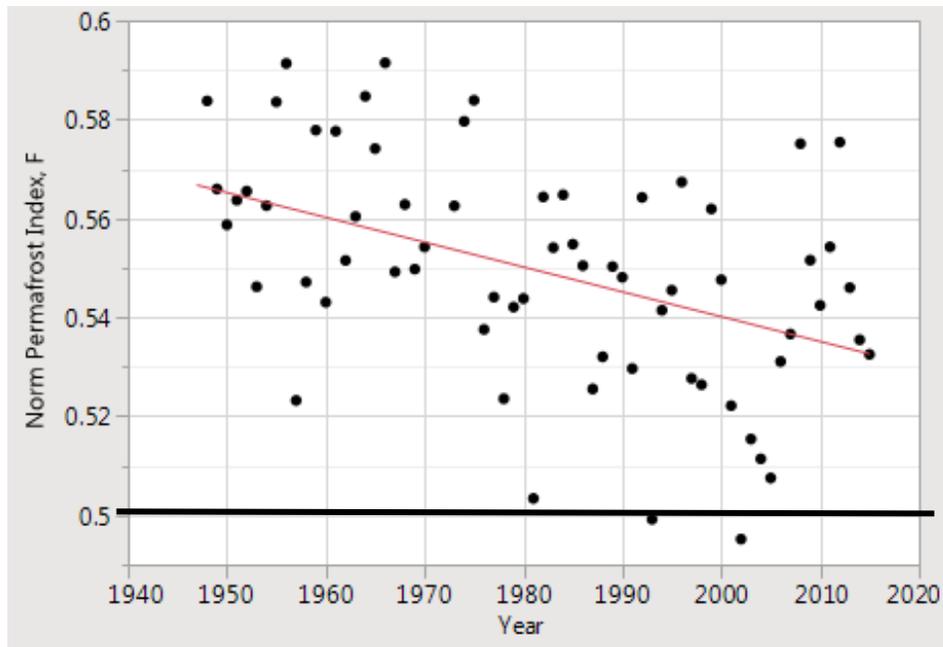
Figure 21: Normalized Permafrost Index Regression

For the Normalized Permafrost Index regression, the R^2 was around 0.205495, which shows that nearly 21% of the variability can be explained in the data. The p-values calculated also provide evidence that the independent variable "years" are statistically significant predictors of the dependent variable, the normalize permafrost index.

The normalized permafrost index regression model shows a downward linear trend, with a predicted permafrost index of 0.5667 in 1947 and 0.5326 in 2015. This equates to an index change of 0.0341 over 68 years. As discussed above, a permafrost index of 0.5 is indicative of sporadic permafrost regions, while 0.6 is indicative of discontinuous permafrost regions (Nelson & Outcalt, 1987). As the index moves farther from 0.6 and closer to 0.5, a region will likely start to encounter permafrost degradation from increased active layer thicknesses. For these results, Eielson AFB is starting to

experience a shift away from discontinuous permafrost to an area of sporadic permafrost. However, it is important to note that this data is only over a 68 year window and trends could easily shift in the opposite direction in the future. When projected out to the year 2100, the line reaches the sporadic level of F = 0.5 anywhere from 2050 to well past 2100 (Figure 22). It is important to note that 2075, where the linear regression crosses, is roughly the same year the number of thawing degree days surpassed freezing degree days according to the regression line presented. This is due to the fact that this index is calculated from DDF and DDT.

The results from this calculation are in accordance with generally accepted permafrost maps (Figure 19). Eielson AFB resides within the discontinuous permafrost zone. In these areas, permafrost soils can be encountered throughout the soil. One location may experience an extremely shallow permafrost table, while none may be encountered only inches or feet away (Osterkamp & Jorgenson, 2009).
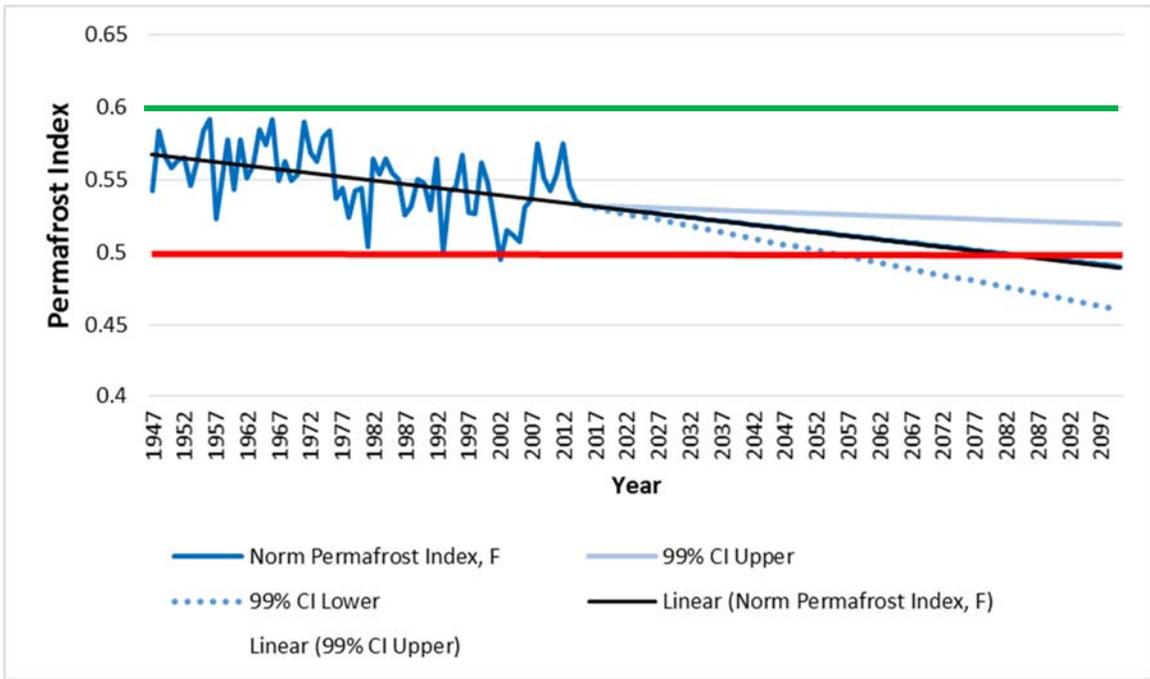
Figure 22: Normalize Permafrost Index
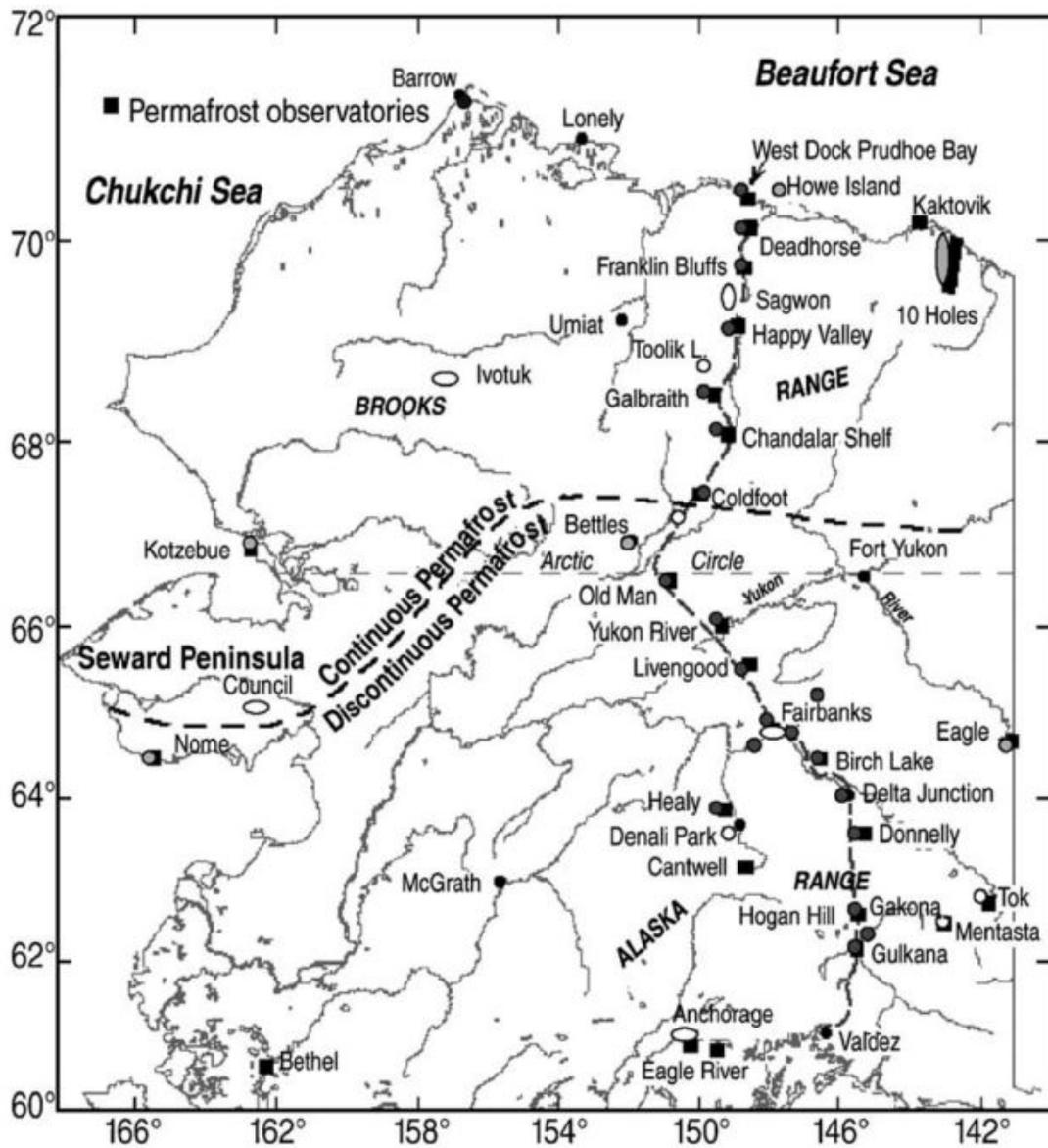
Figure 23: Permafrost Map (Osterkamp, 2005)

GIPL 2.1 Modeling

The following sections describe the six GIPL 2.1 runs using two different

boreholes and various scenarios. The input variables were changed on each .pbz file

based on the characteristics of each scenario. The following graphs were all completed

using output data from the GIPL 2.1 converted into Microsoft Excel®.

Large, Heated Facility (1947-2015) Historical

Figure 24 shows modeled temperatures at various depths around the permafrost table of the borehole location. The results show that temperature increases can be observed at 12 to 17 meters over the entire period studied. This change indicates some permafrost degradation took place during this period. Figure 25 furthers this argument by showing the change in the modeled permafrost table over the 67 years researched.

The permafrost table started around 12 meters in 1947. It then shifted downwards in 1950 and stayed at this depth for 8 years before shifting down another 1 meter in 1958. The permafrost continued this degradation through the 20th century until it ended up around 20 meters in 2015. These results show steps over time of permafrost degradation with a total change of 8 meters. Figure 25 also shows active layer thicknesses year-by-year. The active layer generally stayed around 1 meter to 2 meters during this time.

An increase in the active layer thickness is observed between the years 2007/2008 until 2015 in Figure 25. This same change was also observed in Figure 24, with an abrupt decrease in soil temperatures from 12 meters deep to 16 meters deep. These changes were observed at both borehole locations and are likely a result of downward shifts in the mean annual air temperature during this same period. The observed temperatures changed from a measured average of -1.6°C in 2007 to -6.8°C in 2008. The temperature remained between -6°C and -10°C between 2008 and 2013, as can be seen in Figure 12.
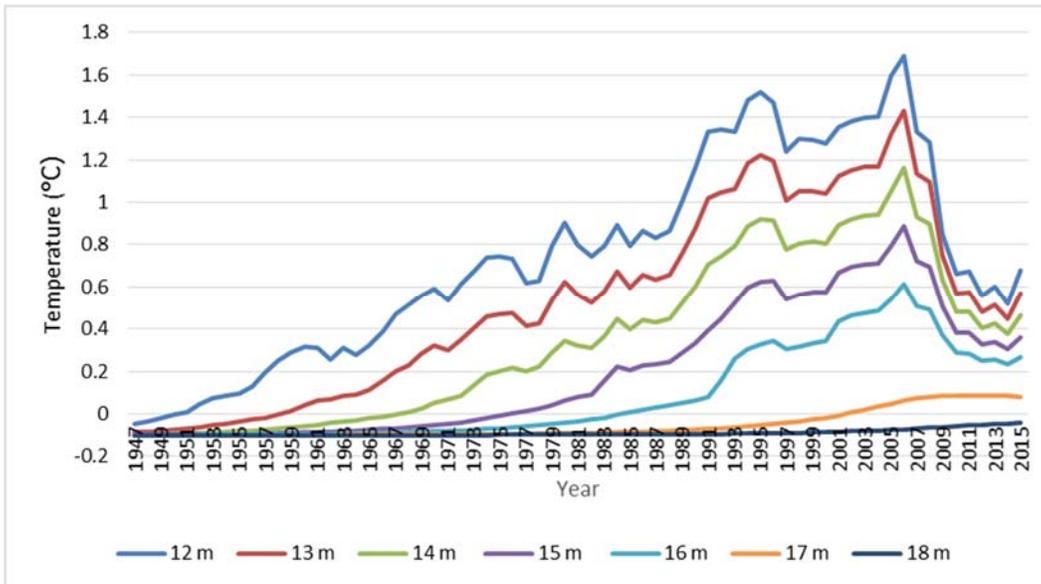
Figure 24: Large, Heated Facility Permafrost Temperatures (Historical)
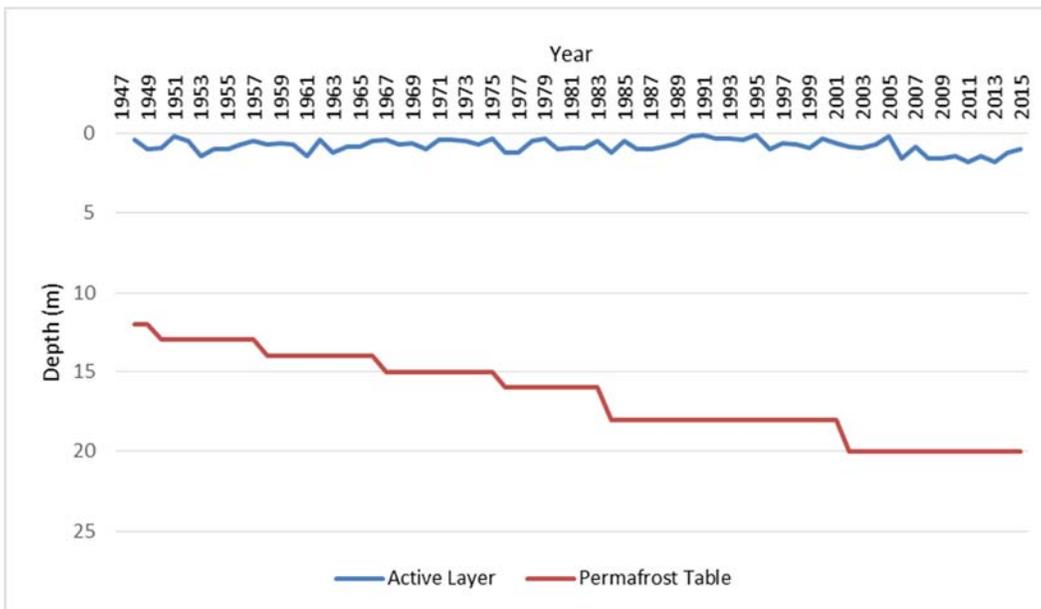
Figure 25: Large, Heated Facility Active Layer/Permafrost Table (Historical)

Although the modeled permafrost table is 20 meters as compared to a measured depth of 10 meters from the USACE borehole in Appendix C, this disparity can be easily explained due to the location of Eielson AFB. As previously discussed in this chapter, the base is located in the discontinuous permafrost zone. One borehole could be located

85

directly on top of a wedge of ice, while no ice may be found within inches of the second bored location.

Large, Heated Facility (2016-2100) Projections

This section of the research looked at permafrost projections from 2016 to 2100. Two scenarios were studied, which included undisturbed conditions using climate projections and a constructed facility with a 12" Portland cement concrete (PCC) slab at 11°C over excavated soil layers. This method displayed anthropogenic impacts on the permafrost soils.

Figure 26 shows modeled temperatures at various depths around the permafrost table of the borehole location. The results show that temperature increases can be observed at 20 to 30 meters throughout the duration of this analysis. The first meter of permafrost begins thawing in 2025, where the temperature in that layer rises above freezing (0°C). These changes indicates severe permafrost degradation over this period. Figure 27 furthers this argument by showing the change in the modeled permafrost table over the 85 years researched using SNAP projection data.
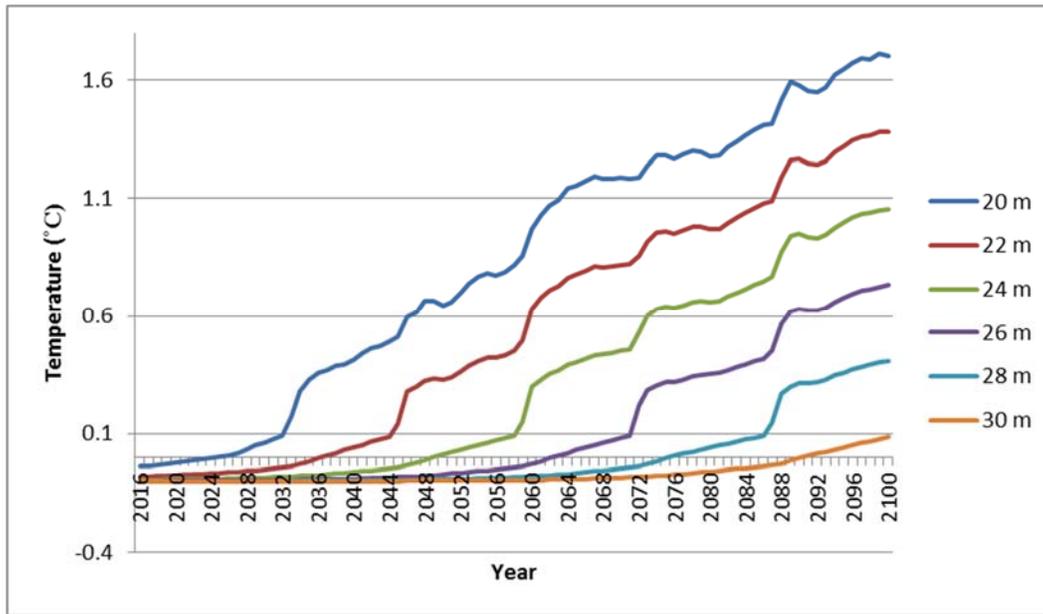
Figure 26: Large, Heated Facility Permafrost Temperatures (Natural Projection)

Overall, the permafrost was reduced by 14 meters over the course of the 85 years analyzed. The bottom of the permafrost remained around 65 meters over the entire duration. The permafrost table began at 20 meters and remained at the depth until year 2025, where degradation dropped it to 22 meters. The downward stepping pattern remained throughout the duration of the analysis. In 2100, the permafrost table depth was observed at 34 meters. Figure 27 also shows active layer thicknesses year-by-year. The active layer generally stayed around 0 meters to 1 meters during this time. This reduction in the active layer is indicative of warmer temperatures, longer summers, and shorter winters. The active layer is driven by freezing and thawing depth (Brown, Hinkel, & Nelson, 2000; Lemke, Ren, Alley, Allison, & Carrasco, 2007). As winters are reduced in duration and intensity, the depth of thaw becomes shallower, which reduces the overall depth of the active layer.

87
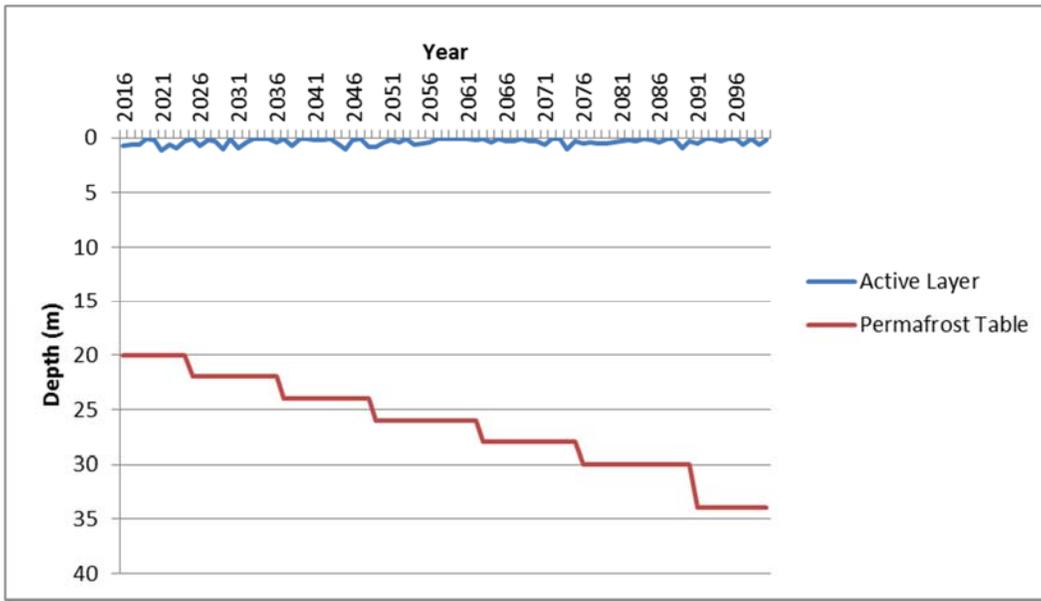
Figure 27: Large, Heated Facility Active Layer/Permafrost Table (Natural Projection)
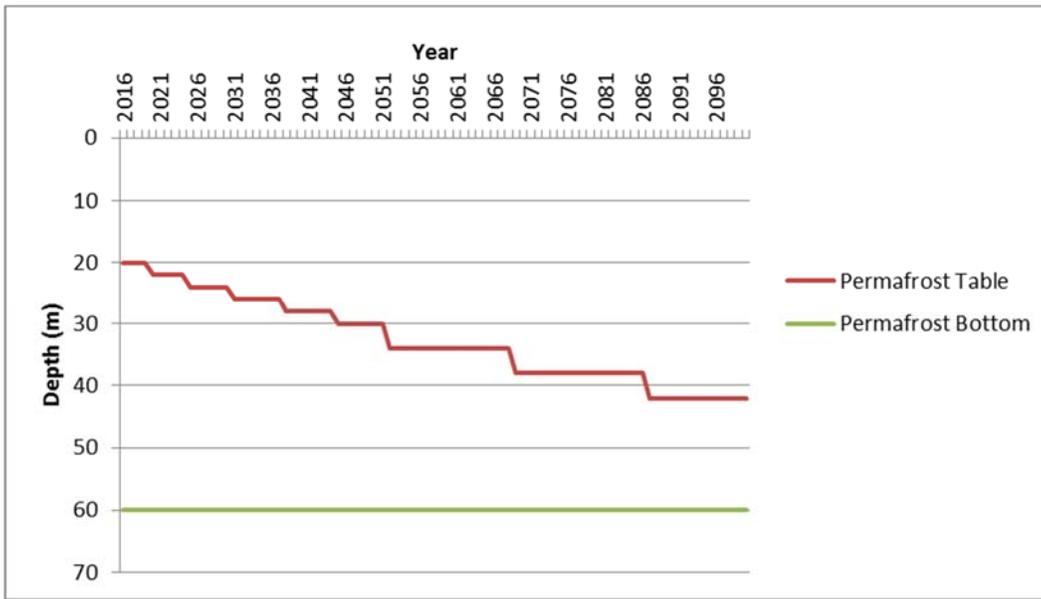
Figure 28: Large, Heated Facility Active Layer/Permafrost Table (Post Construction)

The results in Figure 27 were compared with Figure 28 as the graphs showed natural projections compared with post-construction conditions, respectively. The impacts of climate change were easily observed with a permafrost table change of 14

88

meters over the course of 85 years. When analyzing the post construction results, a permafrost thickness reduction of 24 meters was observed.

These results show that the change in soil layers, along with the added heat from a foundation will cause the permafrost to degrade an additional 10 meters over the course of 85 years. This means that an additional 10 meters of soil that was once frozen and suitable for construction, will thaw and become unstable. Gravels could likely experience liquefaction during earthquake events and the silts present will become a moist, muddy substance. For construction, these changes are likely to result in differential settlement of structures, which pose threats to military operations.

Small, Heated Facility (1947-2015) Historical

Figure 29 shows modeled temperatures at various depths around the permafrost table of the borehole location. The results show that temperature increases can be observed at 10 meters, 11 meters, and 12 meters over the period of 1956 to 2015. This change indicates some permafrost degradation took place during this period. Figure 30 furthers this argument by showing the change in the modeled permafrost table over the 67 years researched.

Starting in 1955, the permafrost table shifted downwards 1 meter and stayed at this depth for roughly 24 years. Again in 1979, the surface shifted downward another 1 meter to 12 meters. The surface maintained at 12 meters until 1999 when it shifted again to 13 meters. These results show steps over time of permafrost degradation with a total change of 3 meters. Figure 30 also shows active layer thicknesses year-by-year. The active layer generally stayed around 1 meter to 2 meters during this time. There is also a

slight increase in the permafrost table during the period of 2011 to 2015 (Figure 30), as well as a decrease in temperature at various depths in Figure 29.

As stated previously, these temperature changes were observed at both borehole locations. The decrease in temperature at 10 to 12 meters depth and an increase in the permafrost table from 2008 until 2015 is most likely correlated to the mean annual air temperature shifts during this same period. The observed temperatures shifted from a measured average of -1.6°C in 2007 to -6.8°C in 2008. The temperature remained between -6°C and -10°C between 2008 and 2013, as can be seen in Figure 12.
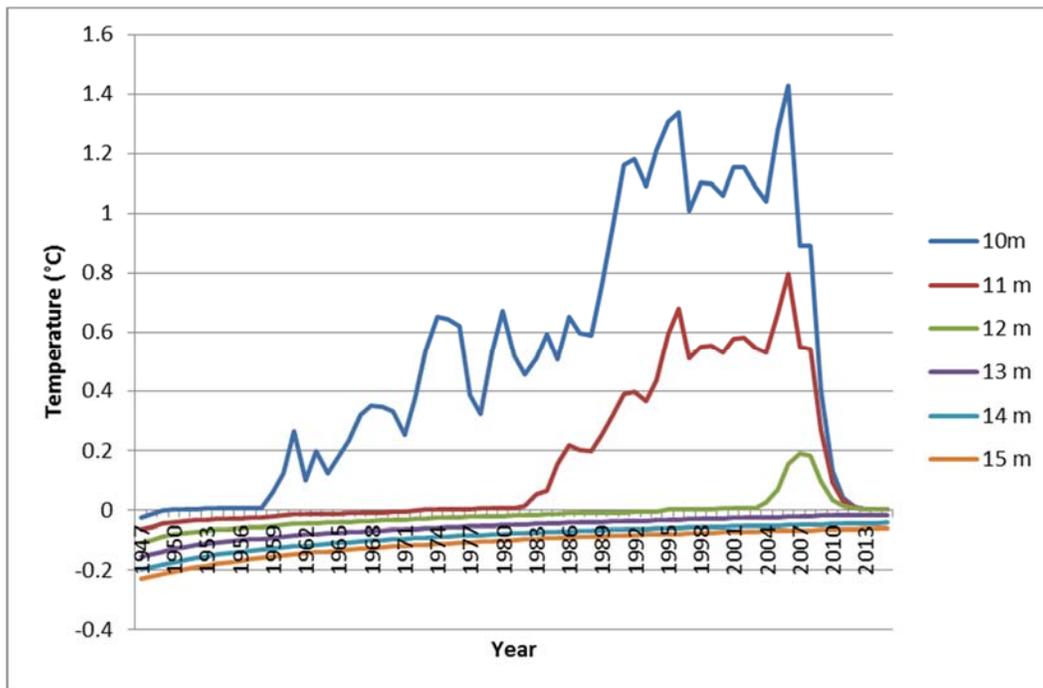
Figure 29: Small, Heated Facility Permafrost Temperatures (Historical)
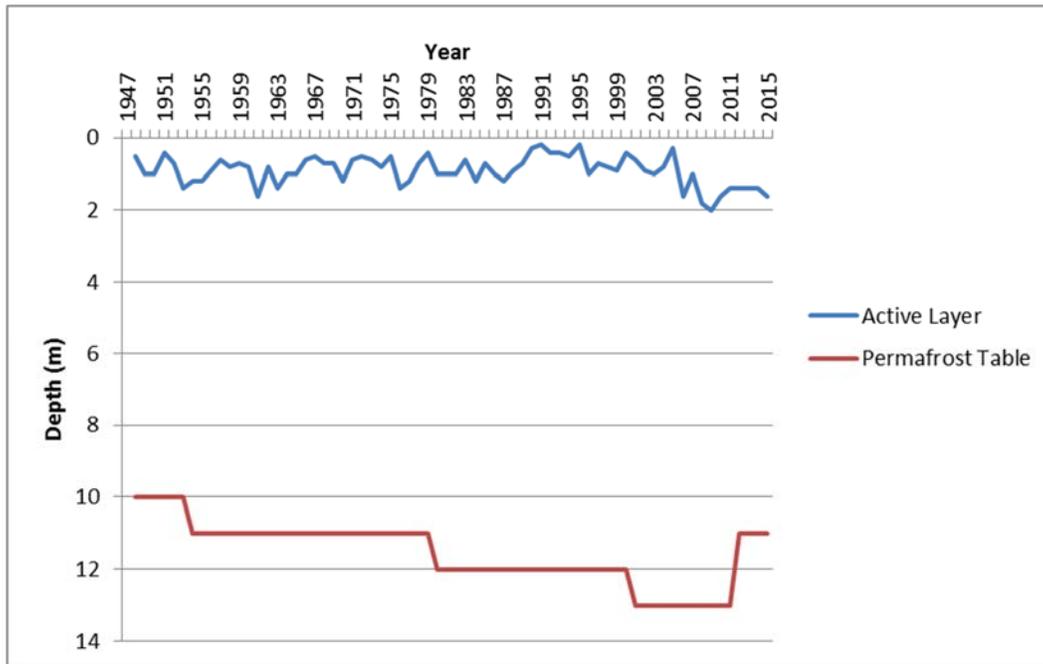
Figure 30: Small, Heated Facility Active Layer/Permafrost Table (Historical)

The final permafrost table was modeled to be between 10 and 11 meters, which is in-line with the actual observed permafrost table observed in the borehole displayed in Appendix A and E. This provides some additional validity to the model used in this research.

Small, Heated Facility (2016-2100) Projections

This section of the research looked at permafrost projections from 2016 to 2100. Two scenarios were studied, which included undisturbed conditions using climate projections and a constructed facility with an 8" PCC slab at 8.8°C over excavated soil layers. This method displayed anthropogenic impacts on the permafrost soils.

Figure 31 shows modeled temperatures at various depths around the permafrost table of the borehole location. The results show that temperature increases can be observed at 10 to 20 meters starting in 2019 and continuing throughout the duration of

this analysis, or around 2100. These changes indicates severe permafrost degradation

over this period. Figure 32 furthers this argument by showing the change in the modeled

permafrost table over the 85 years researched using SNAP projection data.
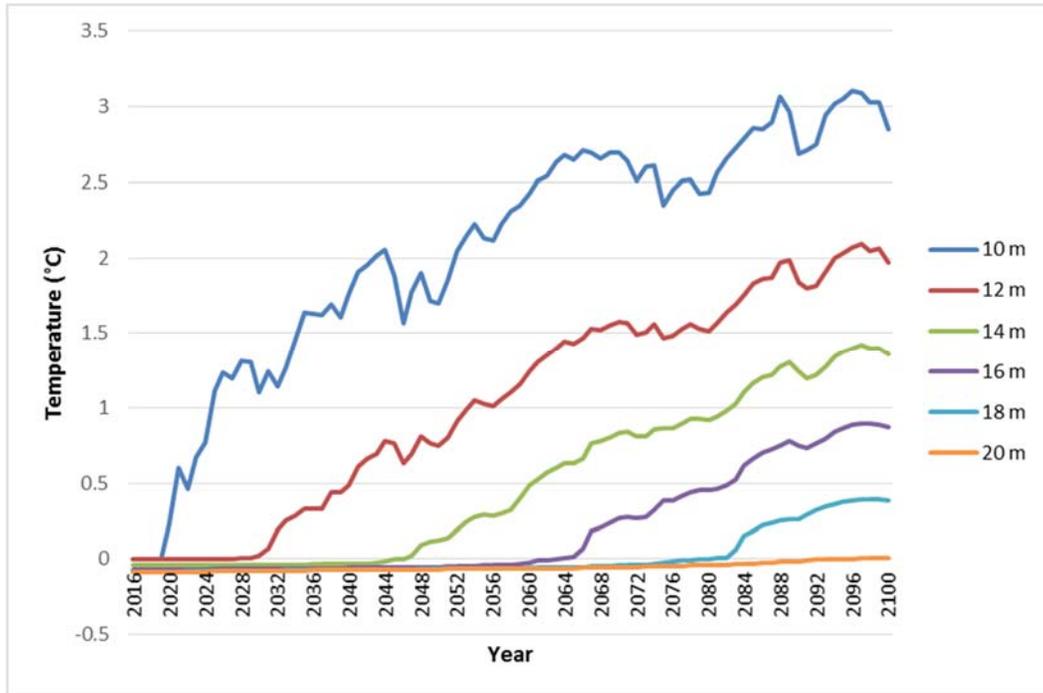
Figure 31: Small, Heated Facility Permafrost Temperatures (Natural Projection)

Overall, the permafrost was reduced by 10 meters over the course of the 85 years

analyzed. The bottom of the permafrost remained around 65 meters over the entire

duration. The permafrost table began at 12 meters and remained at the depth until year

2030, where degradation dropped it to 13 meters. The downward stepping pattern

remained throughout the duration of the analysis. In 2100, the permafrost table depth was

observed at 22 meters. Figure 32 also shows active layer thicknesses year-by-year. The

active layer generally stayed around 0 meters to 2 meters during this time. This reduction

in the active layer is indicative of warmer temperatures, longer summers, and shorter

winters. The active layer is driven by freezing and thawing depth (Brown, Hinkel, &

Nelson, 2000; Lemke, Ren, Alley, Allison, & Carrasco, 2007). As winters are reduced in duration and intensity, the depth of thaw becomes shallower, which reduces the overall depth of the active layer.
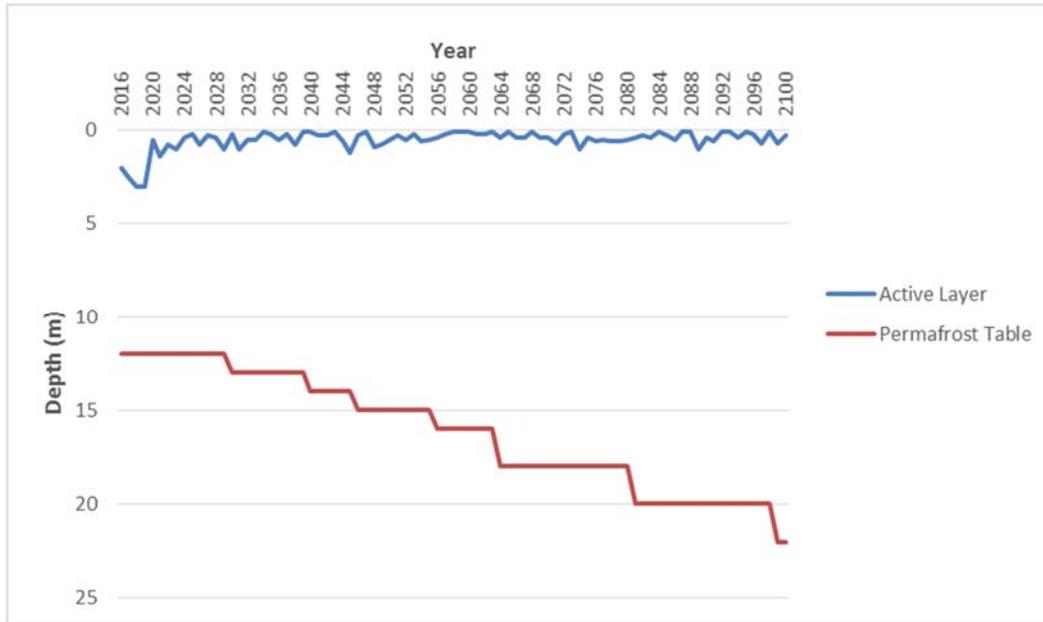
Figure 32: Small, Heated Facility Active Layer/Permafrost Table (Natural Projection)
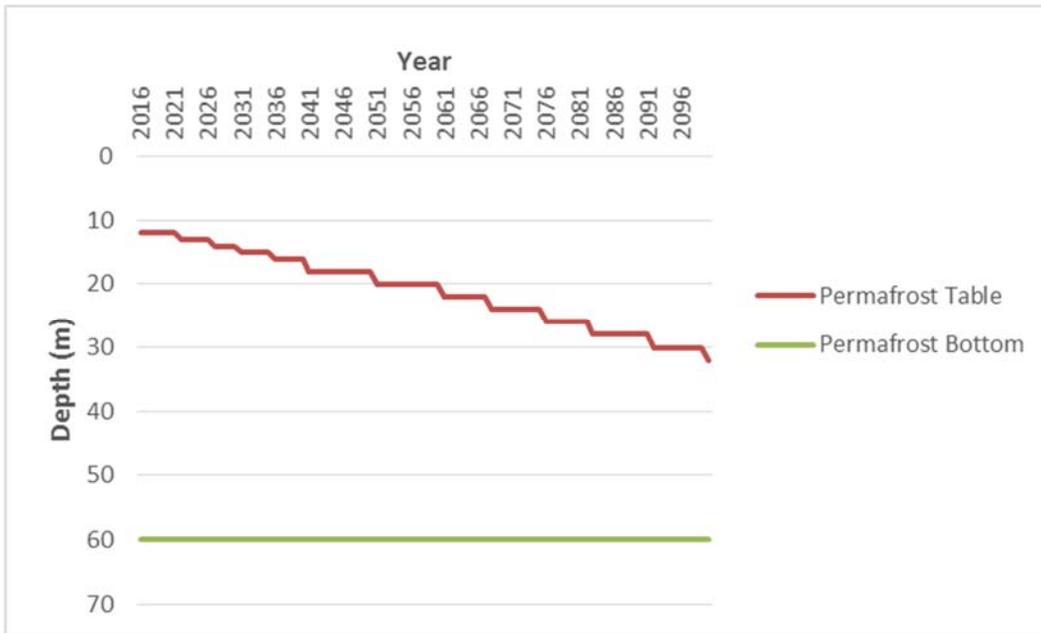
Figure 33: Small, Heated Facility Active Layer/Permafrost Table (Post Construction)

The results in Figure 32 were compared with 33 as the graphs showed natural projections compared with post-construction conditions, respectively. The impacts of climate change were easily observed with a permafrost table change of 10 meters over the course of 85 years. When analyzing the post construction results, a permafrost thickness reduction of 20 meters was observed.

As with the large, heated facility, these results show that the change in soil layers, along with the added heat from a foundation will cause the permafrost to degrade an additional 10 meters over the course of 85 years. This means that an additional 10 meters of soil that was once frozen and suitable for construction, will thaw and become unstable. Gravels could likely experience liquefaction during earthquake events and the silts present will become a moist, muddy substance. For construction, these changes are likely to result in differential settlement of structures, which pose threats to military operations.

94

Additionally, the results from the small, heated facility and the large, heated facility showed different thawing rates. As can be seen in the Figures 21, 23, 25, and 27, the rate of thawing was generally slower in the small facility than the larger facility. This could be caused by a number of factors, such as the soil layers, type of soil, temperature of the facility, and foundation type. Different types of soils have various soil characteristics and respond to temperature changes differently, which is a result of thermal conductivity, heat capacitance, etc. These results show that some permafrost soils may be better to utilize for construction over others.

Stefan's Equation Results

The mathematical model, GIPL 2.1, was compared with the Stefan Equation for the small heated facility from 1947 to 2015 and the results are provided in Figure 34 below.
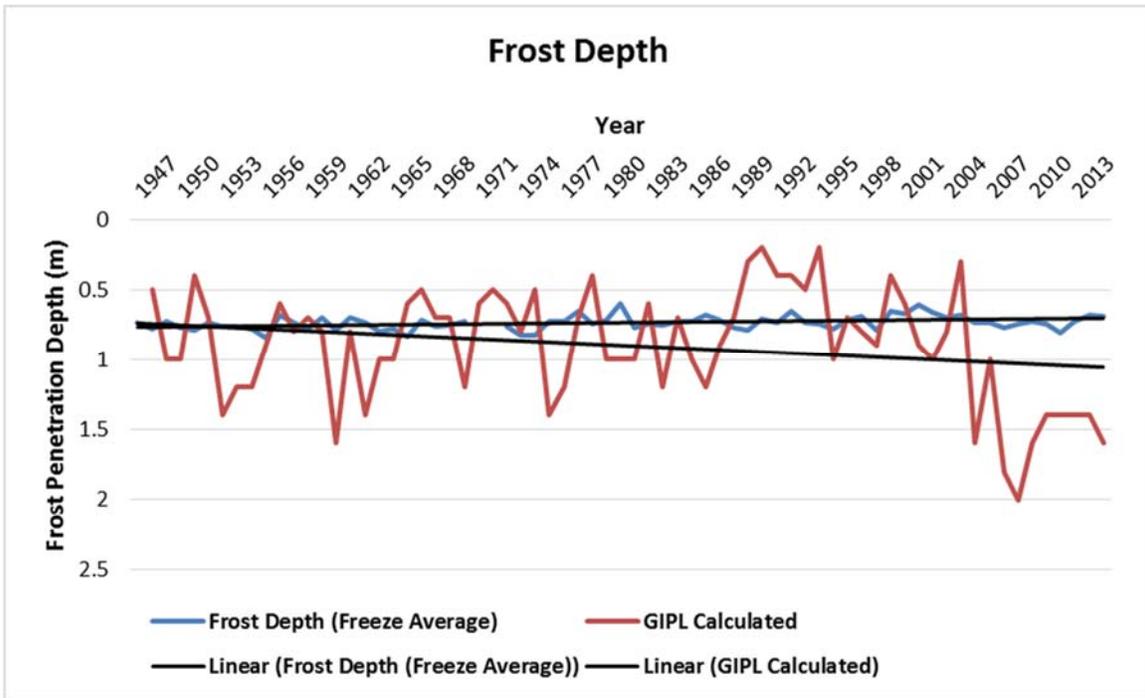
Figure 34: Stefan Equation Results

Stefan's Equation resulted in active layer thicknesses around 0.60 meters to 0.90 meters throughout the entire period studied. These were compared to the values calculated in UAF's GIPL 2.1 model. The active layer thicknesses calculated using the Stefan Equation were stayed within 0.5 to 1.0 meters throughout the duration and did not fluctuate as much as those calculated using the mathematical GIPL model, which resulted in values between 0.5 and 1.5 or more. The disparity is most likely caused by the temperatures used in the calculations. The GIPL model calculated active layer thicknesses using daily average temperatures for each day of the year while the Stefan Equation only used temperature averages for the winter season (or days with a temperature at or below freezing). Some months may have seen more extreme negative temperatures, which were not as evident in the seasonal averages. The percent errors between the two sets of results were calculated using Equation 22.

96

$$Percent\ Error = \frac{Actual\ Value\ \text{-}\ Estimated\ Value}{Actual\ Value} \qquad (22)$$
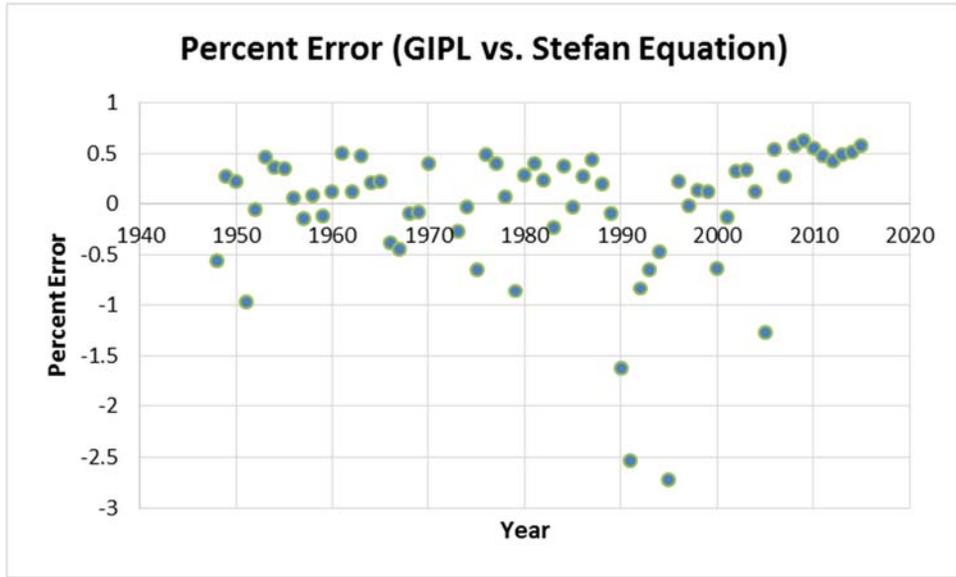
Figure 35: GIPL vs. Stefan Equation

Figure 35 above shows the percent error of the GIPL 2.1 model versus the Stefan

Equation results. These results generally had no more than a 50% percent error, or within

0.5 meters of each other. As discussed in Chapters II and III, the Stefan Equation makes a

number of additional assumptions which are another cause for this disparity. For one, the

ground had different layers of soil, which were not accounted for in the Stefan Equation

due to the homogeneity assumption required.

Summary

This results of this research show potential impacts caused by human activity and

climate change on permafrost soils. The numerical permafrost model used to model soil

temperatures provide significant insight into planning factors for the proposed MILCON

projects on Eielson AFB. The other climate variables studied also provided awareness of

changes that have already taken place in Arctic climates through the 20th century into the

beginning of the 21st. The USAF weather data, UAF SNAP data, and USACE

geotechnical reports proved critical in successful simulations of these variables and soil

temperatures.

V. Conclusions and Recommendations

Chapter Overview

The regression and active layer models used in this research provide an overview of the impacts of climate change on Arctic regions, in particular, Central Alaska. UAF's GIPL 2.1 model provided insight into the impacts of climate change and anthropogenic activities on permafrost soils in this region. The first part of this chapter provides an overview of the conclusions from this research. The next section discusses limitations in this research, as well as the significance of the findings. Finally, the chapter provides some recommendations for planners.

Investigative Questions Answered

Question 1

What is a likely climate scenario for Central Alaska into the year 2100?

Despite the numerous emissions scenarios that the IPCC has published, one scenario mirrors most closely with observed temperatures on Eielson AFB. From the IPCC's Fifth Assessment Report in 2013, RCP 2.6 most closely models a possible future climate for Eielson AFB. Degree Days, Seasonal Lengths, and the Normalized Permafrost Index all support a slight warming trend closely related to climate model RCP 2.6. An increase in thawing temperatures can be observed, as well as shorter winters and longer summers.

Even though the IPCC emissions scenario used in this study is fairly close to the predicted temperature changes based on USAF surface weather observations, there is still a large amount of variability included in the predictions. These IPCC scenarios assume

many constants that could change at any time, such as volcanic activity, solar cycles, etc. If one or more of these assumed constants change drastically, the subsequent catastrophic event could result in unpredicted warming or cooling across the globe. This would lead to extremely different futures for the Earth's climate than what was anticipated based on the models. These deviations would quickly invalidate the projections used in this study.

Question 2

Will climate change have a negative impact on future Air Force assets on Eielson AFB?

If proper construction and mitigation techniques are not used, climate change and anthropogenic processes will continue to negatively impact permafrost soils on base. When inputting recorded USAF weather observations and SNAP projections into UAF's GIPL 2.1 model, permafrost degradation was observed at both locations.

Even without anthropogenic activity at these particular locations, the active layer and permafrost table will be negatively impacted by climate change. These impacts have already been observed when modeling historic soil temperatures. Whenever soils change undergo phase changes (frozen to thawed), their bearing capacities are negatively impacted. Additionally, whenever massive ice is present, thawing of this ice will have severe consequences for the infrastructure relying on its bearing capacity. Essentially, the ice will turn to water and lose all bearing capacity, leading to settlement issues. These changes must be recalculated to ensure proper engineering methods.

Further research will need to be accomplished on the best types of foundation and engineering techniques to use to combat the findings of this research. New construction methods are available that can mitigate differential settlement, foundation cracking, etc.

Question 3

Will permafrost degradation occur at specific construction sites on Eielson AFB?

Permafrost degradation can be seen over the course of the 20th century into the 21st century. This is due to increasing mean annual air temperatures over time and anthropogenic activity. The degradation was observed from the 20th century into the 21st century.

Each of the six scenarios analyzed showed signs of permafrost degradation from a few meters down to 24 meters. The largest amount of degradation was observed in both post-construction analyses. In the small facility, a change of 20 meters was observed between 2016 and 2100 if RCP4.5 comes to fruition. In the large facility, a change of 24 meters was observed using this scenario. These results are compared to the natural projections which showed a change of 14 meters and 10 meters at the large facility and small facility location (with no construction), respectively. The historical analysis also showed degradation at both of these locations. The changes from 1947 to 2015 were calculated to be 12 meters and 3 meters for the large facility and small facility, respectively.

The heat from these facilities penetrated deeper and deeper into the soil each year, causing rising temperatures at various depths. When the heat eventually reached the permafrost table, it began to heat these layers above freezing and cause thawing of ice and soil.

Conclusions of Research

According to the climate variables studied, the amount of heat from thawing degree days (DDT) will surpass freezing degree days (DDF) anywhere from the year 2047 to well past 2100. The Normalized Permafrost Index also supports this conclusion. According to the length of seasons, the number of days above freezing surpassed the number of days at or below freezing around the year 1999. The seasons fluctuated through the year 2015 but continued their moderate linear trends. Overall, the data analyzed support low levels of climate change and moderate warming trends in the Eielson AFB area.

Permafrost degradation without anthropogenic activity was calculated to continue from 1947 through the 21st Century due to temperature increases. The largest amount of degradation was observed in both post-construction analyses. In the small facility, a change of 20 meters was observed between 2016 and 2100 if RCP4.5 comes to fruition. In the large facility, a change of 24 meters was observed using this scenario. These results are compared to the natural projections which showed a change of 14 meters and 10 meters at the large facility and small facility location (with no construction), respectively. The historical analysis also showed degradation at both of these locations. The changes from 1947 to 2015 were calculated to be 12 meters and 3 meters for the large facility and small facility, respectively.

The disparity between permafrost degradation between the natural projection and post-construction trials is due to the addition of facilities and the excavation and removal of unsuitable soils and overlying vegetation. Anthropogenic activity plays a major role in the continued degradation of permafrost. For one, natural canopies that provide shade

from the sun's radiant heat are removed. The vegetation also aids in controlling the amount of heat convection by allowing colder air to pass between bushes and trees (Wei et al., 2009).

The facilities themselves also have detrimental effects on permafrost by projecting heat from the bottom surface of the foundation. If a facility is kept at a particular temperature above freezing throughout the year, that temperature minus the heat loss through the foundation slab, will absorb into the surrounding soils through heat conduction. As the heat penetrates through the layers, the temperatures increase deeper each year and eventually reach the permafrost table. In the results gathered, this heat reduced the permafrost thickness by 20 to 24 meters from 2016 to 2100.

Limitations of Research

This research was met with many challenges and limitations. For one, the availability of data proved to be the largest limitation. The Air Force has only been recording data since 1945, roughly 70 years. This timeline is an extremely small scale compared with the actual age of the Earth. Therefore, the results shown in the temperature and permafrost variables only show a trend over a small period of time. Therefore, the future trends are likely a slight exaggeration of the actual potential future that may be encountered. The SNAP IPCC projections helped mitigate some of these limitations due to the availability of more historical data. The IPCC analyses have temperature measurements back into the latter part of the 19th century.

Additionally, weather observations are heavily reliant upon the tools available at the time. Since these USAF data reach back to the 1940s, the capability of the

measurement tools likely changed over time. Newer technology offered more accurate measurements that were not accounted for in this research. The lack of consideration was due to the fact that the measurement platform was not recorded in the data. Therefore, it was impossible to determine the changes over time.

The research was also forced to make numerous assumptions that are recorded in the methodology section of this research. Some of the largest assumptions are around the projections, as the future is always unknown. The IPCC models make numerous assumptions to attempt to predict the future using time-series analysis. For example, solar cycles are considered constants, as well as volcanic activity, which are both constantly changing with time.

As with any models, they attempt to model reality as closely as possible. The soil temperature outputs are only as accurate as the model used. In this case, GIPL 2.1 was used and was created by permafrost scientists at UAF. The model has proven to be accurate to within 1-3°C of measured soil temperatures at numerous sites (Nicolsky et al., 2007).

Some error was also introduced to the absence of actual temperature measurements at the two borehole locations. To overcome this obstacle, the research used temperature measurements from a nearby borehole in Fairbanks, which was provided by UAF. Calibration techniques were used to overcome this obstacle and are described in Chapter III. However, these temperatures were as accurate as possible in order to perform the analysis.

Lastly, the boreholes are only representative of two points on Eielson AFB and are by no means representative of the base as a whole or entire footprint of a facility.

Therefore, only conclusions could be made based on the permafrost table and soil conditions at these two locations. Due to time constraints, additional boreholes were not analyzed in the model.

Significance of Research

Multiple Executive Orders, GAO reports, as well as the DoD's 2014 Climate Change Adaptation Roadmap require that the Department, in particular the USAF, account for climate change in installation master plans, facility maintenance and repair cost models, and design and construction standards, among others (DoD, 2014; GAO, 2013, 2014, 2016). Although this research focuses on meteorological and geophysical calculations, the results show the impacts of anthropogenic activity and climate change on permafrost soils on Eielson AFB. The information gleamed from these results can help planners develop new design and construction standards for DoD installations in Arctic regions and meet the intent of the DoD's Climate Change Adaptation Roadmap. These new construction methods can either seek to remove, maintain, or improve the permafrost soils in the immediate construction area. The results can also help planners determine lifecycle costs for facilities that are already in existence and are not constructed to newer standards, or for new facilities using various construction standards.

Permafrost degradation is known to result in differential settlement in facilities constructed permafrost soil. This type of settlement can be detrimental to military installations closely tied to operational missions. For example, an aircraft hangar typically houses millions of dollars in military aircraft. Differential settlement can lead to inoperable hangar doors, which may affect mission readiness. It is difficult to deploy an

aircraft if it is stuck inside a hangar. Permafrost also impacts roads around Eielson AFB. For instance roads could be used to transfer critical materials used in case of an emergency. Ignoring permafrost conditions beneath these roads could lead to pavement issues from frost heave and thermokarst terrains, which could make the roads impassable over time.

Although the research only provides a predicted future air and soil temperatures around Eielson AFB, the results can be used to plan foundation types and construction techniques to use. The construction methods and foundation designs heavily affect the costs associated with construction. The results could also help engineers design standardized designs or foundation techniques to use. From these standards, cost factors could be calculated to help financial planners in future projects.

Recommendations for Action

Although this data is specific to Eielson AFB, the methodology should be used to analyze other northern tier bases in accordance with the DoD Roadmap and Executive Orders. GIPL 2.1 is the most accurate permafrost modeling tool available and should be used by DoD geotechnical analysts when constructing on permafrost soils. The particular modeling results from this research should be reviewed by USAF planners prior to finalizing the designs for Eielson AFB's upcoming MILCON projects over the next few years.

The results show consistent permafrost degradation which needs to be accounted for in the MILCON designs. However, these results are only based on a limited data set and only provide a glimpse into the future climate. Numerous studies have been

conducted on active, verses passive cooling techniques. The results have shown that active cooling techniques on foundations have proven most effective at combating the impacts of infrastructure and climate change on permafrost soils (Wei et al., 2009). For example, instead of using slab on grade foundations, piles or caissons should be used on permafrost soils. Additionally, methods such as helical foundations and cooled floors are available and may prove to be more beneficial in preserving the permafrost table over time (Instanes & Instanes, 2006; Shankel, 1985).

Recommendations for Future Research

This research was only focused on two point locations on Eielson AFB. The methodology discussed in this research can be expanded to additional locations and bases around the Arctic. Two areas of interest for the DoD are Thule AFB and the North Slope of Alaska.

This data could also be used to determine suitable engineering designs and standards. In turn, these new standards could be used to develop additional cost factors associated with construction on permafrost soils. This would provide AFCEC planners with knowledge of additional costs from the earliest phases of planning.

Finally, follow-on research could be conducted by analyzing the two MILCON projects researched and determine suitable foundation types. Numerous studies and lessons learned exist on construction techniques in permafrost soils and could be reviewed to aid in this additional research. The foundation types can be used in developing standardized designs discussed above.

Summary

In accordance with President Obama Executive Orders, along with the Secretary of Defense's QDR, and DoD Climate Change Adaptation Roadmap, this research analyzed potential impacts to a major DoD Installation in Alaska, Eielson AFB. This research succeeded in modeling various climate and permafrost variables over the 20th and 21st century. Even though the recorded data only covered roughly 70 years in the 20th century, trends were observed that support the IPCC's "low" emissions scenario (RCP 2.6). Additionally, the modeled active layers and permafrost temperatures showed degradation throughout the entire timeframe studied. Additionally, anthropogenic activity through the disturbance of soils and new infrastructure, resulted in an increase to the rate of permafrost degradation over time. Finally, the methodology from this research can be used at other locations around the Arctic and the results can be used to develop new constructions standards for the DoD in the Arctic region.

Appendix A: Soil Layers

Small, Heated Facility (native soils):
Borehole 11: Permafrost exists at 32' below surface
SURFACE: Grass
0 - .02 m: moss
.02 m - .0356 m: dead moss
.0356 m - .0450 m: organic layer
.0450 m – 1.8288 m: Wet, organic Silt (ML)
1.8288 m – 2.65176 m: wet, silt with organic materials (OL)
2.65176 m – 9.7536 m: wet, silt with trace sand (ML)
9.7536 m – 12.954 m: frozen, massive ICE
12.954 m – 14.9352 m: frozen, organic silt (OL)
14.9352 m – 18.288 m: wet, silt (ML)

Small, Heated Facility (construction):
8" PCC Slab
0 – 3.048 m: classified fill at 95% compaction/clean gravel
3.048 m – 9.7536 m: wet, silt with trace sand (ML)
9.7536 m – 12.954 m: frozen, massive ICE
12.954 m – 14.9352 m: frozen, organic silt (OL)
14.9352 m – 18.288 m: wet, silt (ML)

Large, Heated Facility (native soils):
Borehole 13: Permafrost exists at 35' below surface.
SURFACE: wooded (spruce)
0 - .021 m moss
.021 m - .0356 m dead moss
.0356 m - .06096 m: organic mat
.06096 m – 1.524 m: silty sand (SM)
1.524 m – 2.286 m: wet, gravels (GP-GM)
2.286 m – 6.096 m: wet, poorly graded gravel (GP)
6.096 m – 7.62 m: wet, poorly graded sand (SP)
7.62 m – 10.668 m: wet, poorly graded gravel (GP)
10.668 m – 15.6972 m frozen, poorly graded gravel (PERMAFROST) (GW-GM)

Large, Heated Facility (construction):
12 "PCC Hangar Slab
0 - 1.8288 m: classified fill/clean gravel
1.8288 m – 2.286 m: wet, gravels (GP-GM)
2.286 m – 6.096 m: wet, poorly graded gravel (GP)
6.096 m – 7.62 m: wet, poorly graded sand (SP)
7.62 m – 10.668 m: wet, poorly graded gravel (GP)
10.668 m – 15.6972 m frozen, poorly graded gravel (PERMAFROST) (GW-GM)

Appendix B: Regression Assumption Tests

- **Thawing Days Assumptions:**
  - Normality (Shapiro-Wilk W Test):
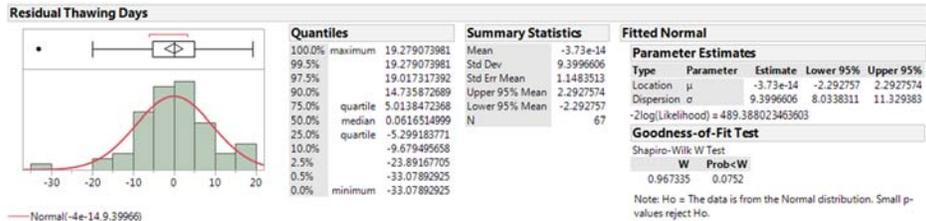
  - Independence (Durbin-Watson Test):

Durbin-Watson			
Durbin-Watson	Number of Obs.	AutoCorrelation	Prob<DW
2.1163442	67	-0.0582	0.6373

  - Constant Variance (Breusch-Pagan Test):

Analysis of Variance

Source	DF	Sum of Squares	Mean Square	F Ratio
Model	1	537.2283	537.228	5.9883
Error	65	5831.3389	89.713	**Prob > F**
C. Total	66	6368.5672		0.0171*

  - SSE: 5831.3389
  - n: 67
  - df: 1

Analysis of Variance

Source	DF	Sum of Squares	Mean Square	F Ratio
Model	1	25970.0	25970.0	1.0039
Error	65	1681551.9	25870.0	**Prob > F**
C. Total	66	1707521.9		0.3201

  - SSM: 25970.0
  - $T.S,. = \dfrac{\frac{SSM}{2}}{\frac{SSE^2}{n}}$
  - P-value: =CHIDIST(T.S., df)

Thawing Days			
N	67	**T.S.**	**P-value**
df Model	1	0.02558	0.87292
SSE	5831.3389		
SSM	25970		

110

- **Freezing Days Assumptions:**
  - Normality (Shapiro-Wilk W Test):
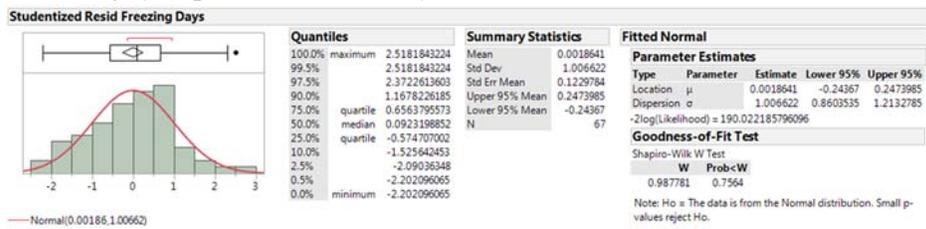
  - Independence (Durbin-Watson Test):

Durbin-Watson	Number of Obs.	AutoCorrelation	Prob<DW
2.0309313	67	-0.0161	0.4999

  - Constant Variance (Breusch-Pagan Test):

Analysis of Variance

Source	DF	Sum of Squares	Mean Square	F Ratio
Model	1	908.8271	908.827	11.6906
Error	65	5053.1132	77.740	**Prob > F**
C. Total	66	5961.9403		0.0011*

  - SSE: 5053.1132
  - n: 67
  - df: 1

Analysis of Variance

Source	DF	Sum of Squares	Mean Square	F Ratio
Model	1	8071.28	8071.3	0.7537
Error	65	696104.39	10709.3	**Prob > F**
C. Total	66	704175.68		0.3885

  - SSM: 8071.28

Freezing Days			
N	67	**T.S.**	**P-value**
df Model	1	0.01059	0.91804
SSE	5053.1132		
SSM	8071.28		

- **Thawing Degree Days Assumptions:**
  - Normality (Shapiro-Wilk W Test):

Residual Thawing Degree Days

Quantiles		
100.0%	maximum	390.72187845
99.5%		390.72187845
97.5%		353.5851518
90.0%		213.19239222
75.0%	quartile	134.13543299
50.0%	median	-18.47487475
25.0%	quartile	-115.8332247
10.0%		-180.3378364
2.5%		-360.9161801
0.5%		-475.357666
0.0%	minimum	-475.357666

Summary Statistics	
Mean	2.851e-13
Std Dev	167.84578
Std Err Mean	20.505626
Upper 95% Mean	40.940802
Lower 95% Mean	-40.9408
N	67

Fitted Normal

Parameter Estimates

Type	Parameter	Estimate	Lower 95%	Upper 95%
Location	μ	2.851e-13	-40.9408	40.940802
Dispersion	σ	167.84578	143.45674	202.30402

-2log(Likelihood) = 875.625870592995

Goodness-of-Fit Test

Shapiro-Wilk W Test

W	Prob<W
0.981366	0.4128

Note: Ho = The data is from the Normal distribution. Small p-values reject Ho.

— Normal(2.9e-13,167.846)

  - Independence (Durbin-Watson Test):

Durbin-Watson

Durbin-Watson	Number of Obs.	AutoCorrelation	Prob<DW
1.5535945	67	0.2072	0.0234*

  - Constant Variance (Breusch-Pagan Test):

Analysis of Variance

Source	DF	Sum of Squares	Mean Square	F Ratio
Model	1	309755.6	309756	10.8285
Error	65	1859365.6	28606	Prob > F
C. Total	66	2169121.1		0.0016*

  - SSE: 1859365.6
  - n: 67
  - df: 1

Analysis of Variance

Source	DF	Sum of Squares	Mean Square	F Ratio
Model	1	3797998990	3.798e+9	2.4530
Error	65	1.0064e+11	1.5483e+9	Prob > F
C. Total	66	1.0444e+11		0.1222

  - SSM: 3797998990.0

Thawing Degree Days			
N	67	T.S.	P-value
df Model	1	0.0368	0.84787
SSE	1859365.6		
SSM	3797998990		

112

- **Freezing Degree Days Index Assumptions:**
  - Normality (Shapiro-Wilk W Test):

    Residual Freezing Degree Days

Quantiles		
100.0%	maximum	879.31784475
99.5%		879.31784475
97.5%		837.87478785
90.0%		518.88571304
75.0%	quartile	218.8368767
50.0%	median	30.36277076
25.0%	quartile	-250.9602053
10.0%		-464.9378437
2.5%		-896.881538
0.5%		-1063.203951
0.0%	minimum	-1063.203951

Summary Statistics	
Mean	1.483e-12
Std Dev	388.89115
Std Err Mean	47.510616
Upper 95% Mean	94.858005
Lower 95% Mean	-94.85801
N	67

    Fitted Normal

    Parameter Estimates

Type	Parameter	Estimate	Lower 95%	Upper 95%
Location	μ	1.483e-12	-94.85801	94.858005
Dispersion	σ	388.89115	332.38283	468.72935

    -2log(Likelihood) = 988.219895127827

    Goodness-of-Fit Test

    Shapiro-Wilk W Test

W	Prob<W
0.986979	0.7113

    Note: Ho = The data is from the Normal distribution. Small p-values reject Ho.

  - —Normal(1.5e-12,388.891)
  - Independence (Durbin-Watson Test):

    Durbin-Watson

Durbin-Watson	Number of Obs.	AutoCorrelation	Prob<DW
1.7967437	67	0.0960	0.1671

  - Constant Variance (Breusch-Pagan Test):

    Analysis of Variance

Source	DF	Sum of Squares	Mean Square	F Ratio
Model	1	1381801	1381801	8.9983
Error	65	9981598	153563	Prob > F
C. Total	66	11363398		0.0038*

    - SSE: 9981598.0
    - n: 67
    - df: 1

    Analysis of Variance

Source	DF	Sum of Squares	Mean Square	F Ratio
Model	1	4081426868	4.0814e+9	0.0800
Error	65	3.3151e+12	5.1e+10	Prob > F
C. Total	66	3.3192e+12		0.7782

    - SSM: 4081426868

Freezing Degree Days			
N	67	T.S.	P-value
df Model	1	0.00137	0.97045
SSE	9981598		
SSM	4081426868		

113

- **Normalize Permafrost Index Assumptions:**
  - Normality (Shapiro-Wilk W Test):

Residual Norm Permafrost Index, F

Quantiles		
100.0%	maximum	0.041280139
99.5%		0.041280139
97.5%		0.0396680965
90.0%		0.0264513388
75.0%	quartile	0.0164105103
50.0%	median	0.0002102095
25.0%	quartile	-0.014139471
10.0%		-0.026928083
2.5%		-0.045039924
0.5%		-0.046306555
0.0%	minimum	-0.046306555

Summary Statistics	
Mean	1.384e-16
Std Dev	0.0200202
Std Err Mean	0.0024459
Upper 95% Mean	0.0048833
Lower 95% Mean	-0.004883
N	67

Fitted Normal

Parameter Estimates

Type	Parameter	Estimate	Lower 95%	Upper 95%
Location	μ	1.384e-16	-0.004883	0.0048833
Dispersion	σ	0.0200202	0.0171111	0.0241303

-2log(Likelihood) = -334.93819485112

Goodness-of-Fit Test

Shapiro-Wilk W Test

W	Prob<W
0.985471	0.6253

Note: Ho = The data is from the Normal distribution. Small p-values reject Ho.

Normal(1.4e-16,0.02002)

  - Independence (Durbin-Watson Test):

Durbin-Watson			
Durbin-Watson	Number of Obs.	AutoCorrelation	Prob<DW
1.6237277	67	0.1774	0.0456*

  - Constant Variance (Breusch-Pagan Test):

Analysis of Variance				
Source	DF	Sum of Squares	Mean Square	F Ratio
Model	1	0.00684201	0.006842	16.8119
Error	65	0.02645330	0.000407	Prob > F
C. Total	66	0.03329531		0.0001*

    - SSE: .02645330
    - n: 67
    - df: 1

Analysis of Variance				
Source	DF	Sum of Squares	Mean Square	F Ratio
Model	1	0.00000029	2.8575e-7	1.0345
Error	65	0.00001795	2.7622e-7	Prob > F
C. Total	66	0.00001824		0.3129

    - SSM: .00000029

Normalized Permafrost Index			
N	67	T.S.	P-value
df Model	1	0.01388	0.90621
SSE	0.0264533		
SSM	0.00000029		

- **Temperature Assumptions (USAF Data):**
  - Normality (Shapiro-Wilk W Test):
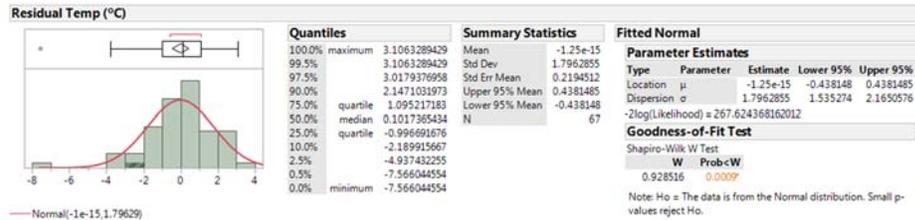
  - Independence (Durbin-Watson Test):

Durbin-Watson			
Durbin-Watson	Number of Obs.	AutoCorrelation	Prob<DW
1.1476813	67	0.4232	<.0001*

  - Constant Variance (Breusch-Pagan Test):

Analysis of Variance

Source	DF	Sum of Squares	Mean Square	F Ratio
Model	1	1.23928	1.23928	0.3783
Error	65	212.95835	3.27628	Prob > F
C. Total	66	214.19763		0.5407

  - SSE: 212.95835
  - n: 67
  - df: 1

Analysis of Variance

Source	DF	Sum of Squares	Mean Square	F Ratio
Model	1	401.0375	401.037	7.9667
Error	65	3272.0582	50.339	Prob > F
C. Total	66	3673.0957		0.0063*

  - SSM: 401.0375

Temperature			
N	67	T.S.	P-value
df Model	1	0.29624	0.58625
SSE	212.95835		
SSM	401.0375		

- **SNAP Data:**
  - Normality:

RCP 4.5

Quantiles		
100.0%	maximum	2.0749999883
99.5%		2.0749999883
97.5%		1.788333265
90.0%		1.3566667817
75.0%	quartile	0.9333332875
50.0%	median	0.2916666267
25.0%	quartile	-0.608333195
10.0%		-1.523333305
2.5%		-1.89166675
0.5%		-2.850000056
0.0%	minimum	-2.850000056

Summary Statistics	
Mean	0.1071053
Std Dev	1.0561098
Std Err Mean	0.1083546
Upper 95% Mean	0.3222458
Lower 95% Mean	-0.108035
N	95

Fitted Normal

Parameter Estimates

Type	Parameter	Estimate	Lower 95%	Upper 95%
Location	μ	0.1071053	-0.108035	0.3222458
Dispersion	σ	1.0561098	0.9243235	1.2320706

-2log(Likelihood) = 278.970827763248

Goodness-of-Fit Test

Shapiro-Wilk W Test

W	Prob<W
0.956208	0.0030*

Note: Ho = The data is from the Normal distribution. Small p-values reject Ho.

  - Independence:

Durbin-Watson

Durbin-Watson	Number of Obs.	AutoCorrelation	Prob<DW
1.5471129	95	0.2212	0.0094*

  - Constant Variance:

Analysis of Variance

Source	DF	Sum of Squares	Mean Square	F Ratio
Model	1	78.26945	78.2695	273.9050
Error	93	26.57513	0.2858	Prob > F
C. Total	94	104.84458		<.0001*

- SSE: 26.57513
- n: 95
- df: 1

Analysis of Variance

Source	DF	Sum of Squares	Mean Square	F Ratio
Model	1	0.101139	0.101139	0.5571
Error	93	16.883557	0.181544	Prob > F
C. Total	94	16.984696		0.4573

- SSM: .101139

SNAP			
N	95	T.S.	P-value
df Model	1	0.0068	0.93427
SSE	26.57513		
SSM	0.101139		

Appendix C: Regression Printouts from JMP®

Whole Model

Regression Plot

Actual by Predicted Plot

Freezing Days Predicted P=0.0011 RSq=0.15
RMSE=8.817
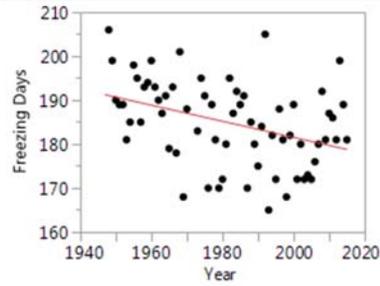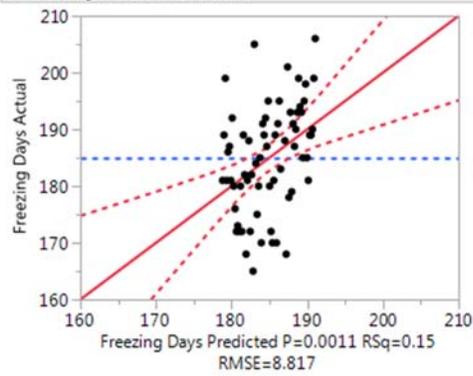
Summary of Fit

RSquare	0.152438
RSquare Adj	0.139399
Root Mean Square Error	8.817041
Mean of Response	184.9701
Observations (or Sum Wgts)	67

Parameter Estimates

Term	Estimate	Std Error	t Ratio	Prob>|t|
Intercept	547.24125	105.9591	5.16	<.0001*
Year	-0.182847	0.053477	-3.42	0.0011*

Residual by Predicted Plot

Whole Model

Regression Plot

Actual by Predicted Plot

Thawing Days Predicted P=0.0171 RSq=0.08
RMSE=9.4717
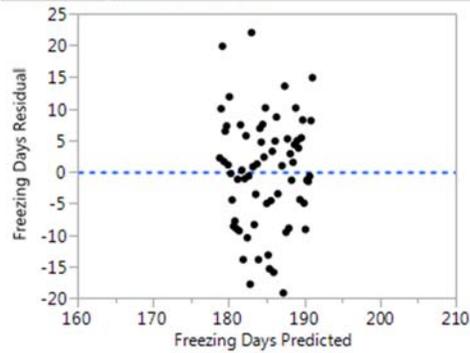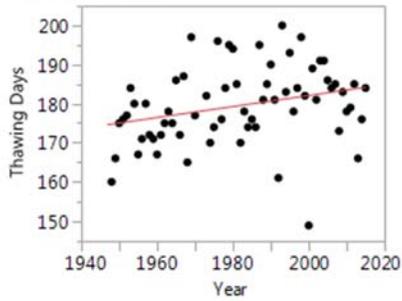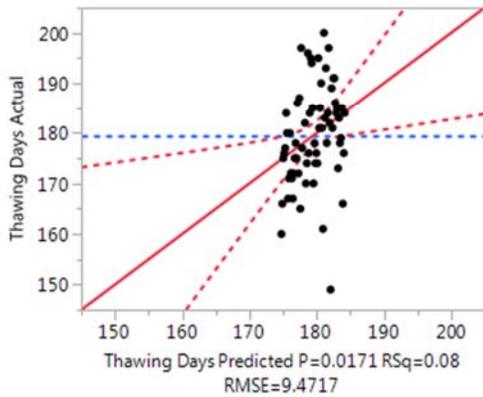
Summary of Fit

RSquare	0.084356
RSquare Adj	0.070269
Root Mean Square Error	9.47169
Mean of Response	179.4478
Observations (or Sum Wgts)	67

Parameter Estimates

Term	Estimate	Std Error	t Ratio	Prob>|t|
Intercept	-99.08257	113.8264	-0.87	0.3872
Year	0.1405807	0.057448	2.45	0.0171*

Residual by Predicted Plot

Thawing Days Predicted

Whole Model

Regression Plot

Actual by Predicted Plot

Thawing Degree Days Predicted P=0.0016
RSq=0.14 RMSE=169.13
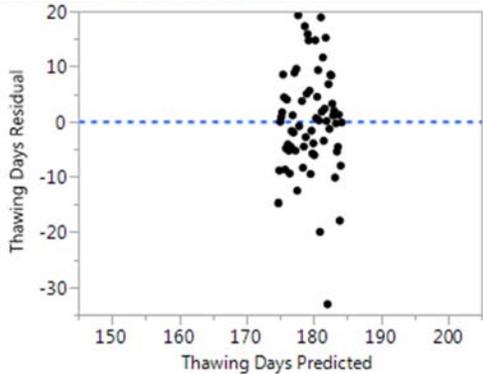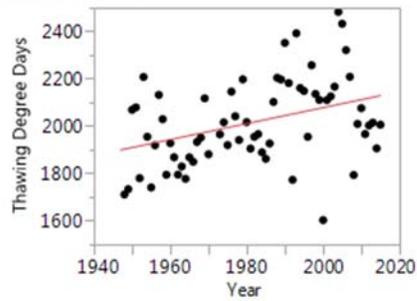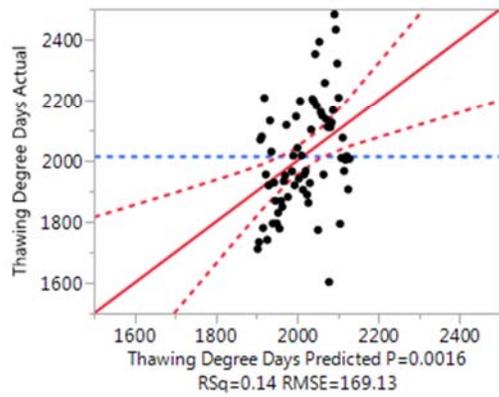
Summary of Fit

RSquare	0.142802
RSquare Adj	0.129615
Root Mean Square Error	169.132
Mean of Response	2015.107
Observations (or Sum Wgts)	67

Parameter Estimates

Term	Estimate	Std Error	t Ratio	Prob>|t|
Intercept	-4672.991	2032.55	-2.30	0.0247*
Year	3.3756388	1.025822	3.29	0.0016*

Residual by Predicted Plot

Thawing Degree Days Predicted

118

Whole Model

Regression Plot

Actual by Predicted Plot

Freezing Degree Days Predicted P=0.0038
RSq=0.12 RMSE=391.87
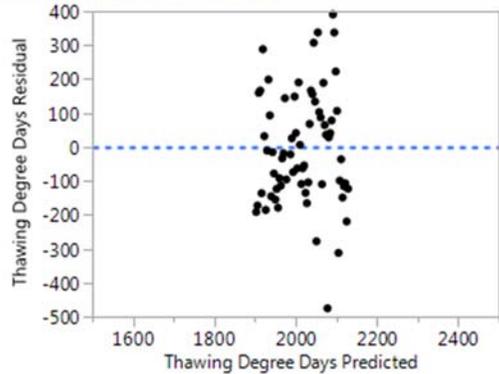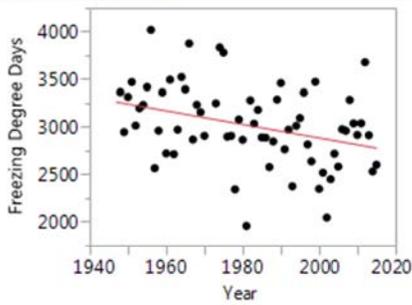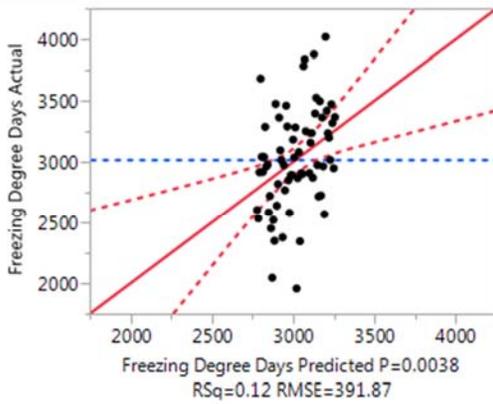
Summary of Fit

RSquare	0.121601
RSquare Adj	0.108087
Root Mean Square Error	391.8712
Mean of Response	3018.873
Observations (or Sum Wgts)	67

Parameter Estimates

Term	Estimate	Std Error	t Ratio	Prob>|t|
Intercept	17144.762	4709.327	3.64	0.0005*
Year	-7.129665	2.376784	-3.00	0.0038*

Residual by Predicted Plot

Whole Model

Regression Plot

Actual by Predicted Plot

Norm Permafrost Index, F Predicted P=0.0001
RSq=0.21 RMSE=0.0202
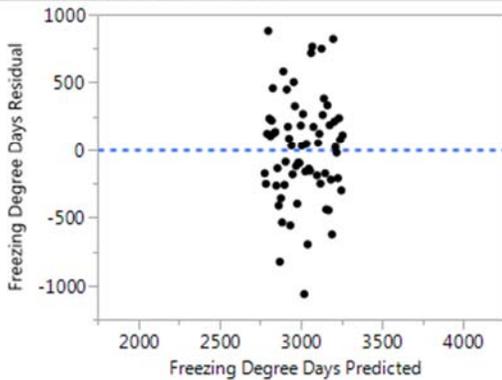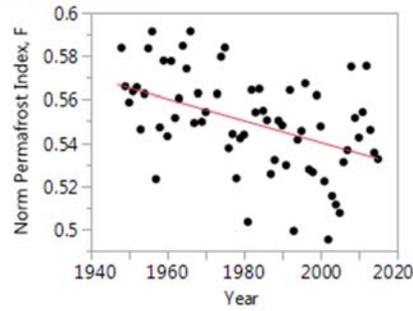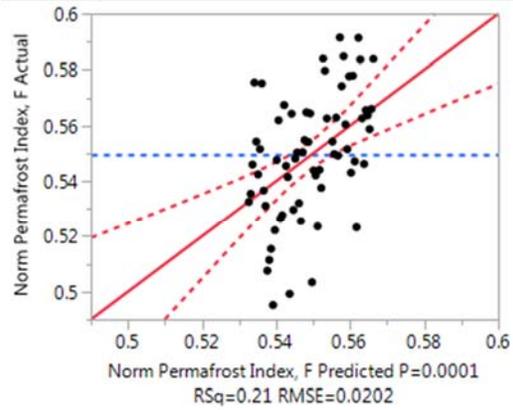
Summary of Fit

RSquare	0.205495
RSquare Adj	0.193272
Root Mean Square Error	0.020174
Mean of Response	0.549558
Observations (or Sum Wgts)	67

Parameter Estimates

Term	Estimate	Std Error	t Ratio	Prob>|t|
Intercept	1.5435553	0.242437	6.37	<.0001*
Year	-0.000502	0.000122	-4.10	0.0001*

Residual by Predicted Plot

Whole Model

Regression Plot

Actual by Predicted Plot

Temp (°C) Predicted P=0.5407 RSq=0.01
RMSE=1.8101
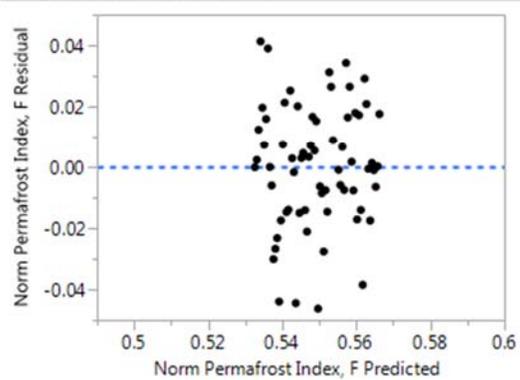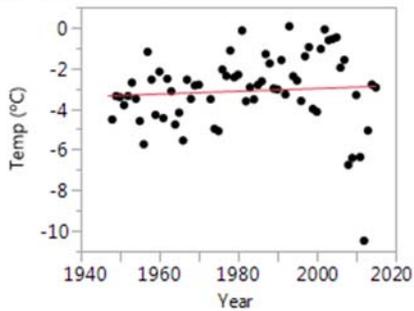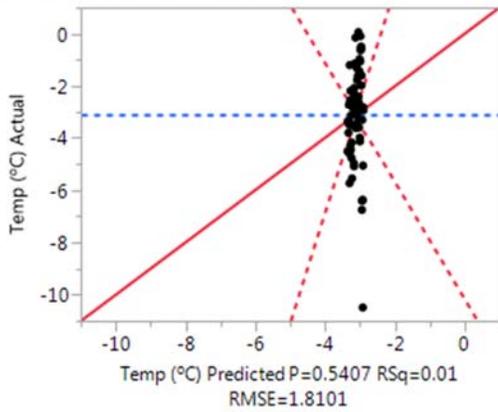
Summary of Fit

RSquare	0.005786
RSquare Adj	-0.00951
Root Mean Square Error	1.81005
Mean of Response	-3.12478
Observations (or Sum Wgts)	67

Parameter Estimates

Term	Estimate	Std Error	t Ratio	Prob>|t|
Intercept	-16.50238	21.75235	-0.76	0.4508
Year	0.006752	0.010978	0.62	0.5407

Residual by Predicted Plot

Whole Model

Regression Plot

Actual by Predicted Plot

RCP 4.5 Predicted P<.0001 RSq=0.75
RMSE=0.5346
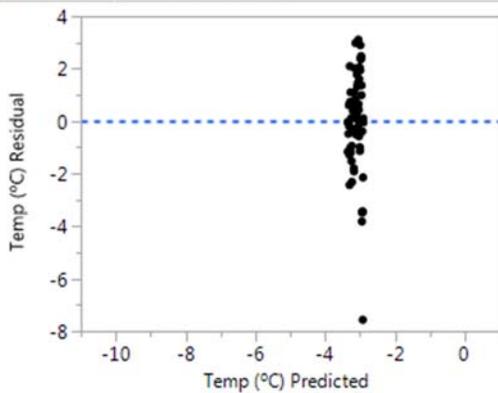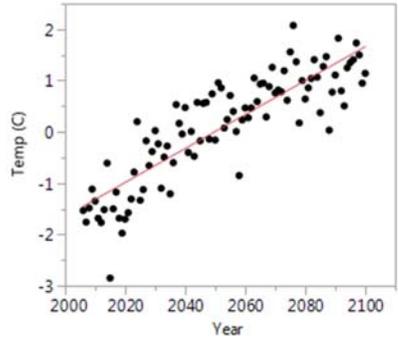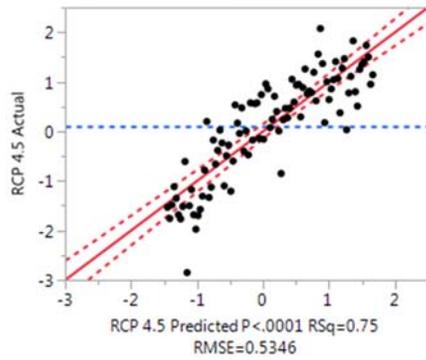
Summary of Fit

RSquare	0.746528
RSquare Adj	0.743803
Root Mean Square Error	0.53456
Mean of Response	0.107105
Observations (or Sum Wgts)	95

Analysis of Variance

Source	DF	Sum of Squares	Mean Square	F Ratio
Model	1	78.26945	78.2695	273.9050
Error	93	26.57513	0.2858	Prob > F
C. Total	94	104.84458		<.0001*

Parameter Estimates

Term	Estimate	Std Error	t Ratio	Prob>|t|
Intercept	-67.84679	4.106324	-16.52	<.0001*
Year	0.0330998	0.002	16.55	<.0001*

Residual by Predicted Plot
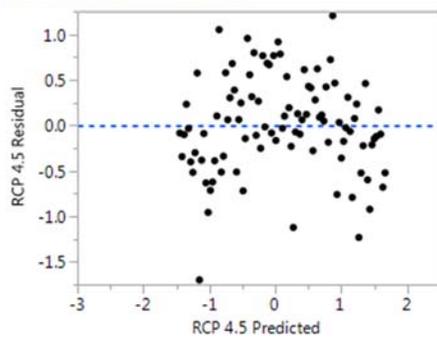
Appendix D: Regression Validation Graphs

APE - Thawing Days
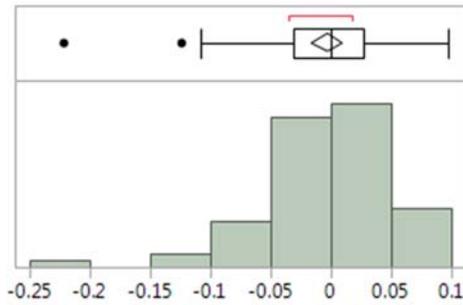
Quantiles			Summary Statistics	
100.0%	maximum	0.0978633197	Mean	-0.002775
99.5%		0.0978633197	Std Dev	0.054165
97.5%		0.0955269719	Std Err Mean	0.0066173
90.0%		0.0756954968	Upper 95% Mean	0.0104367
75.0%	quartile	0.0272491698	Lower 95% Mean	-0.015987
50.0%	median	0.0003387445	N	67
25.0%	quartile	-0.030809208		
10.0%		-0.057092804		
2.5%		-0.153359624		
0.5%		-0.222006237		
0.0%	minimum	-0.222006237		
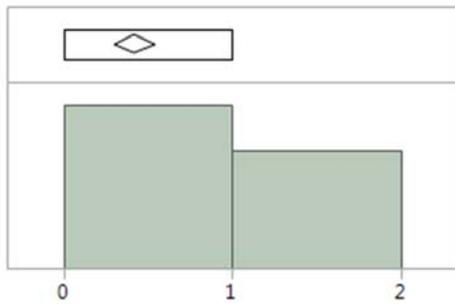
W/I - Thawing Days

Quantiles			Summary Statistics	
100.0%	maximum	1	Mean	0.4179104
99.5%		1	Std Dev	0.4969377
97.5%		1	Std Err Mean	0.0607106
90.0%		1	Upper 95% Mean	0.5391231
75.0%	quartile	1	Lower 95% Mean	0.2966978
50.0%	median	0	N	67
25.0%	quartile	0		
10.0%		0		
2.5%		0		
0.5%		0		
0.0%	minimum	0		

APE - Freezing Days
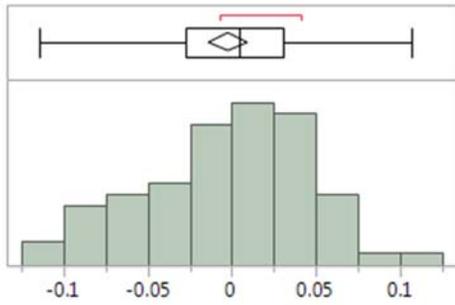
Quantiles			Summary Statistics	
100.0%	maximum	0.1072649368	Mean	-0.002232
99.5%		0.1072649368	Std Dev	0.0479206
97.5%		0.1019300561	Std Err Mean	0.0058544
90.0%		0.0522801636	Upper 95% Mean	0.0094571
75.0%	quartile	0.0304292485	Lower 95% Mean	-0.01392
50.0%	median	0.004382964	N	67
25.0%	quartile	-0.027900007		
10.0%		-0.077800158		
2.5%		-0.10994784		
0.5%		-0.114381912		
0.0%	minimum	-0.114381912		

W/I - Freezing Days

Quantiles			Summary Statistics	
100.0%	maximum	1	Mean	0.3283582
99.5%		1	Std Dev	0.4731602
97.5%		1	Std Err Mean	0.0578057
90.0%		1	Upper 95% Mean	0.4437711
75.0%	quartile	1	Lower 95% Mean	0.2129454
50.0%	median	0	N	67
25.0%	quartile	0		
10.0%		0		
2.5%		0		
0.5%		0		
0.0%	minimum	0		

121

APE - TDD

Quantiles		
100.0%	maximum	0.157389761
99.5%		0.157389761
97.5%		0.146019724
90.0%		0.0967398331
75.0%	quartile	0.0614724435
50.0%	median	-0.009465598
25.0%	quartile	-0.061262339
10.0%		-0.101884963
2.5%		-0.21069422
0.5%		-0.2965556
0.0%	minimum	-0.2965556

Summary Statistics	
Mean	-0.006813
Std Dev	0.084164
Std Err Mean	0.0102823
Upper 95% Mean	0.0137161
Lower 95% Mean	-0.027342
N	67

W/I - TDD
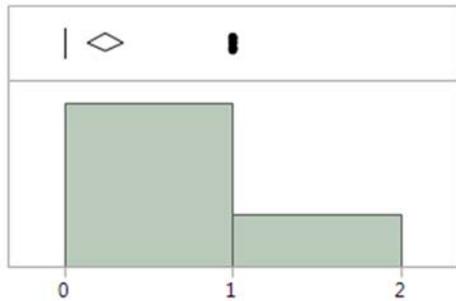
Quantiles		
100.0%	maximum	1
99.5%		1
97.5%		1
90.0%		1
75.0%	quartile	0
50.0%	median	0
25.0%	quartile	0
10.0%		0
2.5%		0
0.5%		0
0.0%	minimum	0

Summary Statistics	
Mean	0.238806
Std Dev	0.4295717
Std Err Mean	0.0524805
Upper 95% Mean	0.3435868
Lower 95% Mean	0.1340252
N	67

APE - FDD
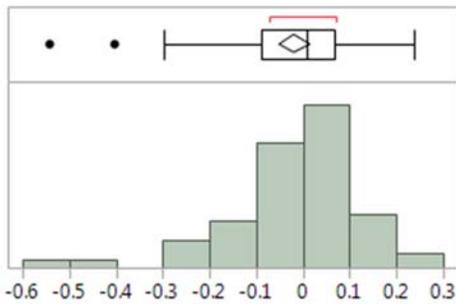
Quantiles		
100.0%	maximum	0.2389974695
99.5%		0.2389974695
97.5%		0.2145317182
90.0%		0.1498329763
75.0%	quartile	0.0681686959
50.0%	median	0.0099976251
25.0%	quartile	-0.087450198
10.0%		-0.180488426
2.5%		-0.445449938
0.5%		-0.543090806
0.0%	minimum	-0.543090806

Summary Statistics	
Mean	-0.017519
Std Dev	0.1405478
Std Err Mean	0.0171706
Upper 95% Mean	0.0167632
Lower 95% Mean	-0.051801
N	67

W/I - FDD
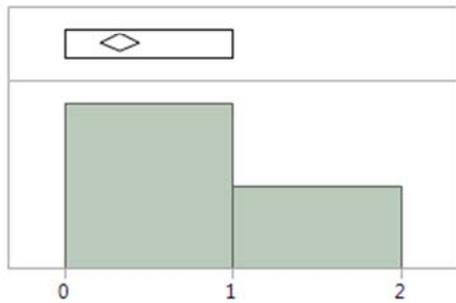
Quantiles		
100.0%	maximum	1
99.5%		1
97.5%		1
90.0%		1
75.0%	quartile	1
50.0%	median	0
25.0%	quartile	0
10.0%		0
2.5%		0
0.5%		0
0.0%	minimum	0

Summary Statistics	
Mean	0.3283582
Std Dev	0.4731602
Std Err Mean	0.0578057
Upper 95% Mean	0.4437711
Lower 95% Mean	0.2129454
N	67

APE - F

Quantiles		
100.0%	maximum	0.0717381228
99.5%		0.0717381228
97.5%		0.0689610717
90.0%		0.0453556794
75.0%	quartile	0.0288548773
50.0%	median	0.0003714178
25.0%	quartile	-0.026575493
10.0%		-0.052403552
2.5%		-0.089994461
0.5%		-0.091988689
0.0%	minimum	-0.091988689

Summary Statistics	
Mean	-0.001331
Std Dev	0.0370398
Std Err Mean	0.0045251
Upper 95% Mean	0.0077035
Lower 95% Mean	-0.010366
N	67

W/I - F
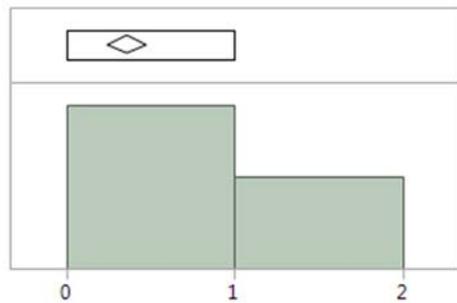
Quantiles		
100.0%	maximum	1
99.5%		1
97.5%		1
90.0%		1
75.0%	quartile	1
50.0%	median	0
25.0%	quartile	0
10.0%		0
2.5%		0
0.5%		0
0.0%	minimum	0

Summary Statistics	
Mean	0.358209
Std Dev	0.4830927
Std Err Mean	0.0590192
Upper 95% Mean	0.4760445
Lower 95% Mean	0.2403734
N	67

APE - TEMP
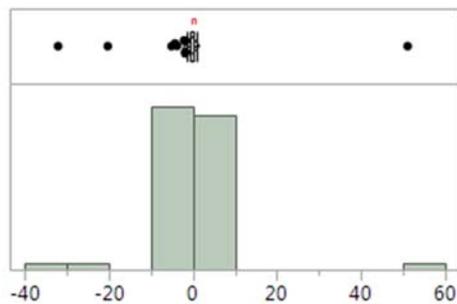
Quantiles		
100.0%	maximum	51.210717489
99.5%		51.210717489
97.5%		15.868415571
90.0%		0.4255487007
75.0%	quartile	0.2490576738
50.0%	median	-0.025045375
25.0%	quartile	-0.500482989
10.0%		-1.897709359
2.5%		-23.87082582
0.5%		-32.15058705
0.0%	minimum	-32.15058705

Summary Statistics	
Mean	-0.355518
Std Dev	7.9232144
Std Err Mean	0.9679747
Upper 95% Mean	1.5771056
Lower 95% Mean	-2.288142
N	67

W/I - TEMP
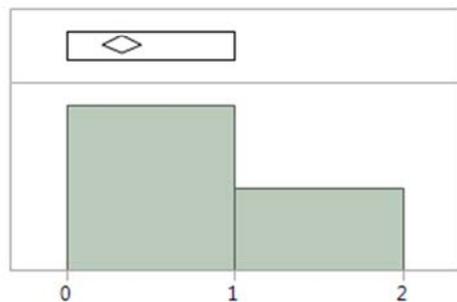
Quantiles		
100.0%	maximum	1
99.5%		1
97.5%		1
90.0%		1
75.0%	quartile	1
50.0%	median	0
25.0%	quartile	0
10.0%		0
2.5%		0
0.5%		0
0.0%	minimum	0

Summary Statistics	
Mean	0.3283582
Std Dev	0.4731602
Std Err Mean	0.0578057
Upper 95% Mean	0.4437711
Lower 95% Mean	0.2129454
N	67

APE - SNAP
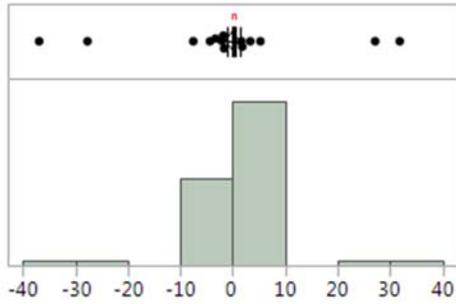
Quantiles

100.0%	maximum	31.83880803
99.5%		31.83880803
97.5%		18.40615845
90.0%		1.1847324728
75.0%	quartile	0.4839883906
50.0%	median	0.1976569893
25.0%	quartile	-0.201622186
10.0%		-0.949974666
2.5%		-19.66484463
0.5%		-36.96789805
0.0%	minimum	-36.96789805

Summary Statistics

Mean	-0.001741
Std Dev	6.5660616
Std Err Mean	0.6736637
Upper 95% Mean	1.3358337
Lower 95% Mean	-1.339316
N	95

W/I - SNAP
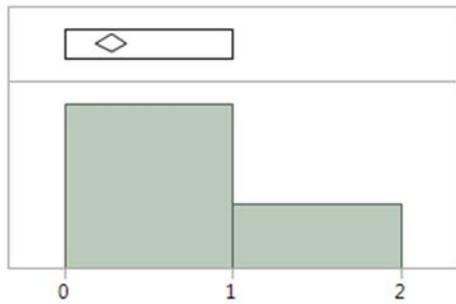
Quantiles

100.0%	maximum	1
99.5%		1
97.5%		1
90.0%		1
75.0%	quartile	1
50.0%	median	0
25.0%	quartile	0
10.0%		0
2.5%		0
0.5%		0
0.0%	minimum	0

Summary Statistics

Mean	0.2736842
Std Dev	0.4482141
Std Err Mean	0.0459858
Upper 95% Mean	0.3649901
Lower 95% Mean	0.1823783
N	95

124

Appendix E: USACE Geotechnical Data

Figure 36: Small, Heated Facility Borehole

PRELIMINARY - PENDING LABORATORY VERIFICATION & QA/QC REVIEW

SOIL PROFILE				SAMPLES			UNCORRECTED BLOWS / ft ■	NOTES TEST RESULTS WATER LEVELS

SOIL PROFILE — SAMPLE DESCRIPTION

VEGETATION: Grass

(Continued)

42.0 - 42.5, Sample 14: Frozen, massive ICE; well bonded (ICE) — ICE

42.5 - 43.5, Sample 14: Frozen, dark brown, ORGANIC SILT; well bonded with excess ice (OL, Nbe) — OL

43.5 - 45.0, Sample 15: Frozen, dark brown, ORGANIC SILT; trace woody debris, well bonded with excess ice (OL, Nbe) — OL

49.0 - 50.5, Sample 16: Moist, grayish-brown, SILT; few sand, organic material and wood debris (ML) — ML

Borehole completed at 50.5 ft.

Samples:
- 14 SS 20/16/14 REC 30 ATT 18/18 — ELEV/DEPTH 42.5
- 15 CA — 61
- 16 SS 2/5/8 REC 13 ATT 18/18 — ELEV/DEPTH 49.0 / 50.5

NOTES:

1) No groundwater observed while drilling.
2) Borehole backfilled with cuttings and imported gravel. Bentonite seal installed from 5 feet to 2 feet below ground surface.
3) Sealed 1-inch Schedule 40 PVC installed to 50.5 feet below ground surface.
4) 140-pound automatic hammer used to advance drive samples.

NOTES TEST RESULTS (49.0-50.5):
Gravel = 0%,
Sand = 6%,
Fines = 94%

BORING METHOD: 4.25 inch I.D. Hollow Stem Auger

DEPTH SCALE: 1 inch to 5 feet
DRILLING CONTRACTOR: Discovery Drilling Inc.
DRILLER: C. Cormier
LOGGED: B. Savikko
CHECKED:
CHECK DATE:

Golder Associates

Figure A-13

Figure 37: Small, Heated Facility Borehole

SOIL PROFILE

SAMPLE DESCRIPTION

SURFACE: Wooded (spruce), next to ditch

DEPTH (ft) | BORING METHOD | ICE BOND | USCS | GRAPHIC LOG | ELEV. DEPTH (ft)

SAMPLES — NUMBER | TYPE | BLOWS / 6 in. | UNCORRECTED BLOWS | REC ATT (in.)

UNCORRECTED BLOWS / ft 10 20 30 40
SALINITY (ppt) Δ
WATER CONTENT (%) Wp — W — Wl 10 20 30 40

NOTES / TEST RESULTS / WATER LEVELS

0.0 - 0.2: ORGANIC MAT

0.2 - 2.5, Sample 1: Moist, brown, SILTY SAND; some fine-grained sand, few gravel, trace organic material (SM) — SM — ELEV 0.2 — 1 GS — PID = 2.9 ppm

2.5 - 4.0, Sample 2: Moist, brown, SILTY SAND; some fine-grained sand, few gravel up to 0.5 inch diameter, trace organic material (SM) — SM — 2 HD — 4/6/10 — 16 — 18/18 — PID = 3.5 ppm, Gravel = 9%, Sand = 44%, Fines = 48%

5.0 - 6.5, Sample 3: Moist, brown, poorly graded GRAVEL with silt and sand; subrounded gravel up to 1 inch diameter, some fine to coarse-grained sand, trace silt (GP-GM) — GP-GM — ELEV 5.0 — 3 HD — 10/10/9 — 19 — 18/18 — PID = 0.7 ppm — 6 ft

Coarse gravel and cobbles inferred by drilling at 2.5 feet

7.5 - 9.0, Sample 4: Wet, brown, poorly graded GRAVEL with sand; subrounded gravel up to 2 inch diameter, some fine to coarse-grained sand, trace silt (GP, NFS) — GP — ELEV 7.5 — 4 HD — 10/8/8 — 16 — 18/18 — PID = 1.1 ppm — 7.5 ft, Gravel = 68%, Sand = 30%, Fines = 2%

10.0 - 11.0, Sample 5: Wet, brown, poorly graded GRAVEL with sand; subrounded gravel up to 2 inch diameter, little to some fine to coarse-grained sand, trace silt, fractured cobble observed in sample (GP) — GP — 5 HD — 7/12/9 — 21 — 12/18 — PID = 0.8 ppm, Gravel = 69%, Sand = 27%, Fines = 4%

15.0 - 16.5, Sample 6: Wet, brown, well-graded GRAVEL with sand; subrounded gravel up to 1.5 inch diameter, some fine to coarse-grained sand, trace silt (GW, NFS) — GW — ELEV 15.0 — 6 HD — 9/7/3 — 10 — 18/18 — PID = 0.4 ppm, Gravel = 63%, Sand = 35%, Fines = 2%

20.0 - 21.5, Sample 7: Wet, gray, poorly graded SAND with gravel; fine to coarse-grained sand, some subrounded gravel up to 2 inch diameter, trace silt (SP) — SP — ELEV 20.0 — 7 HD — 14/14/13 — 27 — 18/18 — PID = 0.8 ppm, Gravel = 42%, Sand = 54%, Fines = 4%

25.0 - 25.2, Sample 8: Wet, gray, poorly graded GRAVEL with sand; subrounded gravel up to 2 inch diameter, some fine to coarse-grained sand, trace silt (GP) — GP — ELEV 25.0 — 8 HD — 11/9/9 — 18 — 2/18 — PID = 0.3 ppm

30.0 - 30.5, Sample 9: Wet, gray, poorly graded GRAVEL with sand (GP) — GP — 9 HD — 11/12/11/12 — 23 — 6/24 — PID = 1.1 ppm

35.0 - 36.0, Sample 10: Frozen, gray, well-graded GRAVEL with silt and sand; subrounded gravel up to 2 inch diameter, some fine to coarse-grained sand, few silt, fractured cobble observed in sample, poorly bonded with approximately 5% visible ice by volume as coatings on particles (GW-GM, Vc) — GW-GM — ELEV 35.0 — 10 HD — 13/19/20/20 — 39 — 12/24 — PID = 0.8 ppm, Gravel = 57%, Sand = 37%, Fines = 6%

Log continued on next page

BORING METHOD: 3.25-inch I.D. Hollow Stem Auger

Golder Associates

DEPTH SCALE: 1 inch to 5 feet
DRILLING CONTRACTOR: Discovery Drilling Inc.
DRILLER: C. Cormier

LOGGED: C. Shonsey
CHECKED: T. Trosper
CHECK DATE: 6/29/2016

Figure A-15

DRAFT

Figure 38: Large, Heated Facility Borehole

SOIL PROFILE

SAMPLE DESCRIPTION

SURFACE: Wooded (spruce), next to ditch

ICE BOND | USCS | GRAPHIC LOG | ELEV. / DEPTH (ft)

SAMPLES — NUMBER | TYPE | BLOWS / 6 in. | UNCORRECTED BLOWS | REC ATT (in.)

UNCORRECTED BLOWS / ft ■ — 10 20 30 40 — SALINITY (ppt) △ — WATER CONTENT (%) — W_P 10 20 30 40 W_L

NOTES / TEST RESULTS / WATER LEVELS

DEPTH (ft)

BORING METHOD

3.25-inch I.D. Hollow Stem Auger

Depth	Description	USCS	ELEV/DEPTH	No.	Type	Blows/6in	Uncorr	Rec/Att	Notes
40.0 – 42.0, Sample 11	Frozen, gray, poorly graded GRAVEL with silt and sand; subrounded gravel up to 3 inch diameter, some fine to coarse-grained sand, few, poorly bonded with no excess ice (GP-GM, Nbn)	GP-GM	40.0	11	HD	17 / 18 / 11	29	8/18	PID = 0.4 ppm
45.0 – 47.0, Sample 12	Frozen, gray, well-graded GRAVEL with silt and sand; subrounded gravel up to 1 inch diameter, some fine to coarse-grained sand, few silt, poorly bonded with approximately 5% visible ice by volume as coatings on particles (GW-GM, Vc)	GW-GM	45.0	12	HD	13 / 23 / 18	41	12/18	PID = 0.6 ppm, Gravel = 51%, Sand = 42%, Fines = 7%
50.0 – 51.5, Sample 13	Frozen, gray, poorly graded GRAVEL with silt and sand; subangular gravel up to 2 inch diameter, some sand, few silt, poorly bonded with approximately 5% visible ice by volume as coatings on particles (GP-GM, Vc)	GP-GM	50.0 / 51.5	13	HD	24 / 22 / 28	50	12/18	PID = 0.3 ppm, Gravel = 55%, Sand = 38%, Fines = 7%

Borehole completed at 51.5 ft.

NOTES:

1) Groundwater observed at 7.5 feet while drilling (WD). Groundwater measured at 6 feet on 6/24/2016.
2) 2-inch Schedule 40 PVC installed to 51.5 feet, hand-slotted from 15 to 21.5 feet.
3) Annulus between borehole and PVC backfilled with cuttings. Bentonite seal installed from 2 to 5 feet below ground surface.
4) 340-pound hammer used to advance sampler.
5) Auger was charged with water when drilling below the water table to control heaving sand conditions.

DEPTH SCALE: 1 inch to 5 feet
DRILLING CONTRACTOR: Discovery Drilling Inc.
DRILLER: C. Cormier

LOGGED: C. Shonsey
CHECKED: T. Trosper
CHECK DATE: 6/29/2016

Golder Associates

Figure A-15

DRAFT

Figure 39: Large, Heated Facility Borehole

Bibliography

Alaska, U. of. (2016). Scenarios Network for Alaska and Arctic Planning. Fairbanks,
Alaska. Retrieved from https://www.snap.uaf.edu

Alexander, R. (2012). *Global Warming: False Alarm* (2nd Editio). Royal Oak, Michigan:
Canterbury Publishing.

Anisimov, O. a., Shiklomanov, N. J., & Nelson, F. E. (1997). Effects of global warming
on permafrost and active layer thickness: results from transient general circulation
models. *Global and Planetary Change*, *15*, 61–77.

Azelton, M., & Zufelt, J. (2007). Permafrost Temperatures and Erosion Protection at
Shishmaref, Alaska. *NICNinth International Conference on Permafrost*, 83–87.

Bjella, K. (2012). Thule Air Base Airfield White Painting and Permafrost Investigation,
(June), 75.

Bjella, K., Tantillo, T., Weale, J., & August, J. L. (2008). Evaluation of the CRREL
Permafrost Tunnel, (August).

Bonan, G. B. (1989). A computer model of the solar radiation, soil moisture, and soil
thermal regimes in boreal forests. *Ecological Modeling*, *45*(4), 275–306.
http://doi.org/10.1016/0304-3800(89)90076-8

Bornstein, R. D. (1968). Observations of the Urban Heat Island Effect in New York City.
Journal of Applied Meteorology, *7*(4), 575–582. http://doi.org/10.1175/1520-
0450(1968)007<0575:OOTUHI>2.0.CO;2

Brewer, M. C., & Jin, H. (2008). Warming of Cold Permafrost in Northern Alaska
During the Last Half-Century. *NICOP 2008: Ninth International Confrerence on
Permafrost*, 189–194.

Brown, J., Hinkel, K. M., & Nelson, F. E. (2000). The circumpolar activer layer

> montitoring (CALM) program: Research designs and initial results. *Polar*
>
> *Geography*, *24*(3), 165–258.

Büyükalaca, O., Bulut, H., & Ylmaz, T. (2001). Analysis of variable-base heating and

> cooling degree-days for Turkey. *Applied Energy*, *69*(4), 269–283.
>
> http://doi.org/10.1016/S0306-2619(01)00017-4

Christensen, J. H., & Kuhry, P. (2000). High-resolution regional climate model validation

> and permafrost simulation for the East European Rusian Arctic. *Journal of*
>
> *Geophysical Research*, *105*(D24), 29,647â€"29,658.

Christensen, J. H., Kumar, K. K., Aldria, E., An, S.-I., Cavalcanti, I. F. a., Castro, M. De,

> … Zhou, T. (2013). IPCC 2013 Chapter 14: Climate Phenomena and their
>
> Relevance for Future Regional Climate Change Supplementary Material. *Climate*
>
> *Change 2013: The Physical Science Basis. Contribution of Working Group I to the*
>
> *Fifth Assessment Report of the Intergovernmental Panel on Climate Change*, 62.
>
> http://doi.org/10.1017/CBO9781107415324.028

Cook, J. (2006). *Estimating Required Contingency Funds for Construction Projects*

> *Using Multiple Linear Regression*. Air Force Institute of Technology.

CRREL. (2012). Permafrost Tunnel Research Facility. Retrieved January 1, 2017, from

> http://permafrosttunnel.crrel.usace.army.mil/permafrost/general_facts.html

Curry, J., & Webster, P. (1999). *Thermodynamics of Atmospheres & Oceans*. (J. Holton,

> Ed.)*International Geophyics Series* (1st ed.). San Diego, California: Acadademic
>
> Press.

Davis, N. (2001). *Permafrost: A Guide to Frozen Ground In Transition*. Fairbanks,

Alaska: University of Alaska Press.

Dhananjay, M., & Abhilash, K. (2014). Study of Thermal Gradient in Concrete Slabs Through Experimental Approach. *Global Journal of Researches in Engineering: Civil Structural Engineering*, *14*(5).

DoD. (2014). *2014 Climate Change Adaptation Roadmap*. Retrieved from http://thediplomat.com/2015/08/why-climate-change-could-be-chinas-biggest-security-threat/%5Cnpapers3://publication/uuid/A75FCCBA-7B40-4B88-B8FF-E16B3644FC10

Duffy, K. C. (2015). Land Use Control Management Plan (LUCMP) Update – Coastal Erosion Study for Barter Island LRRS , Oliktok LRRS , and Cape Lisburne LRRS , Alaska.

Esch, D., & Osterkam, T. (1990). Climatic Warming Concerns for Alaska. *Cold Regions Engineering*, *4*(1), 6–14.

Fallis, A. . (2013). Alaska Population Overview: 2013 Estimates. *Alaska Department of Labor and Workforce Development*. http://doi.org/10.1017/CBO9781107415324.004

Foreman, G., Rajek, J., & Bliss, D. (2016). *F-35A Flight Simulator (EIE365A)*. Anchorage, AK.

GAO. (2013). Climate Change: Future Federal Adaptation Efforts Could Better Support Local Infrastructure Decision Makers, (April).

GAO. (2014). Climate Change Adaptation: DoD Can Improve Infrastructure Planning and Processes to Better Account for Potential Impacts, (May).

GAO. (2016). Climate Change: Improved Federal Coordination Could Facilitate Use of

Climate Information in Design Standards , Building Codes , and Certifications, (November).

GIPL 2.0 - Spatially Distributed Model of Permafrost Dynamics in Alaska. (2010). Retrieved October 19, 2016, from http://permafrost.gi.alaska.edu/content/modeling

Graboski, A., Bierhaus, Z., Cantu, G., & Schmidt, C. (2016). *STAT 535 Practicum 3: Basketball Predictions*. Wright-Patterson AFB, Ohio.

Green, M. C. (2016). 65% Design Submittal Specifications. Fairbanks, Alaska.

Hamilton, L. C. (2011). Education, politics and opinions about climate change evidence for interaction effects. *Climatic Change*, *104*(2), 231–242. http://doi.org/10.1007/s10584-010-9957-8

Hinzman, L., Kane, D., Gieck, R., & Everett, K. (1991). Alaskan Arctic. *Cold Regions Engineering*, (19), 95–110.

Inc, G. A. (2016a). *EIE 376, F-35A Hangar/Propulsion/Mx/Dispatch*. Anchorage, AK.

Inc, G. A. (2016b). *Soil Reports*.

Instanes, A., & Anisimov, O. a. (2008). Climate Change and Arctic Infrastructure. *Ninth International Conference on Permafrost*, (1), 779–784.

Instanes, B., & Instanes, A. (2006). Foundation Design Using a Heat Pump Cooling System Conventional Foundation Design in Svalbard Climatic Conditions in Svalbard, 785–788.

IPCC. (1990a). *Climate Change 1990: The IPCC Impacts Assessment. Contribution of Working Group II to the First Assessment Report of the Intergovernmental Panel on Climate Change*. (& G. D. C. Tegart, W. J., McG. Sheldon G. W., Ed.)*Climate change*. Canberra: Australian Government Publishing Service. Retrieved from

https://www.ipcc.ch/ipccreports/far/wg_II/ipcc_far_wg_II_full_report.pdf

IPCC. (1990b). *Climate Change: The IPCC Scientific Assessment*. (J. Houghton, G. Jenkins, & J. Ephraums, Eds.)*Intergovernmental Panel on Climate Change*. New York, NY: Cambridge University Press. http://doi.org/10.1097/MOP.0b013e3283444c89

IPCC. (2007). *Climate Change 2007: Working Group I: The Physical Science Basis*.

IPCC. (2013). Summary for Policymakers. *Climate Change 2013: The Physical Science Basis. Contribution of Working Group I to the Fifth Assessment Report of the Intergovernmental Panel on Climate Change*, 33. http://doi.org/10.1017/CBO9781107415324

Jorgenson, M., & Osterkamp, T. (2005). Response of boreal ecosystems to varying modes of permafrost degradation. *Canadian Journal of Forest Research*, *35*, 2100–2111. http://doi.org/10.1139/x05-153

Jorgenson, M. T., Racine, C. H., Walters, J. C., & Osterkamp, T. E. (2001). Permafrost degradation and ecological changes associated with a warming climate in central Alaska. *Climatic Change*, *48*(4), 551–579. http://doi.org/10.1023/A:1005667424292

Jumikis, A. (1966). *Thermal Soil Mechanics* (1st ed.). New Brunswick, NJ: Rutgers University Press.

Kudryavtsev, V., Garagulya, L., Kondrat yeva, K., & Melamed, V. (1977). *Fundamentals of Frost Forecasting in Geological Engineering Investigations (Osnovy Merzlotnogo Prognoza pri Inzhenerno-Geologicheskikh Issledovaniyakh),*. Hanover, NH.

Leiserowitz, A. A. (2005). American risk perceptions: Is climate change dangerous? *Risk Analysis*, *25*(6), 1433–1442. http://doi.org/10.1111/j.1540-6261.2005.00690.x

Lemke, P., Ren, J., Alley, R. B., Allison, I., Carrasco, J., Flato, G., … Zhang, T. (2007). IPCC: Observations: Changes in snow, ice and frozen ground. *Climate Change 2007: The Physical Science Basis. Contribution of Working Group I to the Fourth Assessment Report of the Intergovernmental Panel on Climate Change*, 337–383. http://doi.org/10.1016/j.jmb.2004.10.032

Lundardini, V. (1996). Climate Warming and the Degradation of Warm Permafrost. *Permafrost and Perigalcial Processes*, (7), 311–320.

Marchenko, S., Romanovsky, V., & Tipenko, G. (2008). Numerical Modeling of Spatial Permafrost Dynamics in Alaska. *Proceedings of the Ninth International Conference on Permafrost*, 0–5. Retrieved from http://www.lter.uaf.edu/pdf/1308_Marchenko_Romanovsky_2008.pdf

McClave, J., Benson, P., & Sincich, T. (2014). *Statistics for Business and Economics* (12th ed.). London, U.K.: Pearson Education Limited.

Nelson, F., & Outcalt, S. (1987). A Computational Method for Prediction and Regionalization of Permafrost. *Arctic and Alpine Research*, *19*(3), 279–288.

Nicolsky, D. J., Romanovsky, V. E., & Tipenko, G. S. (2007). Using in-situ temperature measurements to estimate saturated soil thermal properties by solving a sequence of optimization problems. *Cryosphere*, *1*(1), 41–58. http://doi.org/10.5194/tc-1-41-2007

Osterkamp, T. (1983). *Response of Alaskan Permafrost to Climate. Final Proceedings, Fourth International Conference on Permafrost.* Washington D.C.

Osterkamp, T. E. (2005). The recent warming of permafrost in Alaska. *Global and Planetary Change*, *49*(3-4), 187–202.

http://doi.org/10.1016/j.gloplacha.2005.09.001

Osterkamp, T., & Jorgenson, M. (2009). Permafrost conditions and processes. *Young, R. and Thompson, H.(eds), National Park Service Geological Monitoring Manual, Geological Society of America: Boulder, Co*, *10*(9), 205–227. http://doi.org/10.1130/2009.monitoring(09).

Panda, S. (2011). *Permafrost Distribution Mapping and Temperature Modeling Along Permafrost Distribution Mapping and Temperature Modeling Along the Alaska Highway Corridor , Interior Alaska*. University of Alaska Fairbanks.

Panda, S., Marchenko, S., & Romanovsky, V. (2014). High-Resolution Permafrost Modeling in Denali National Park and Preserve, (January). Retrieved from http://permafrost.gi.alaska.edu/sites/default/files/High-resolution permafrost modeling in DENA.pdf

Pastick, N. J., Jorgenson, M. T., Wylie, B. K., Nield, S. J., Johnson, K. D., & Finley, A. O. (2015). Distribution of near-surface permafrost in Alaska: Estimates of present and future conditions. *Remote Sensing of Environment*, *168*, 301–315. http://doi.org/10.1016/j.rse.2015.07.019

Riseborough, D., Shiklomanov, N., Etzelmuller, B., Gruber, S., & Marchenko, S. (2008). Recent Advances in Permafrost Modeling. *Permafrost and Periglacial Processes*, *19*, 137–156. http://doi.org/10.1002/ppp

Romanovsky, V. E., & Marchenko, S. (2009). The GIPL Permafrost Dynamics Model, (907), 7pp. Retrieved from http://permafrost.gi.alaska.edu/content/modeling

Rupp, S. (2007). Scenarios Network for Alaska + Arctic Planning. Retrieved October 19, 2016, from https://www.snap.uaf.edu/

Shadish, W., Cook, T., & Campbell, D. (2002). *Experimental and Quasi-Experimental Designs for Generalized Causal Inference* (2nd ed.). Belmont, Ca: Wadsworth Cengage Learning.

Shankel, K. (1985). *Design of foundations in permafrost . Institutional Archive of the Naval Postgraduate School*.

SNAP Data Sources. (n.d.). Retrieved from https://www.snap.uaf.edu/methods/data

Solomon, S., Qin, M., Manning, Z., Chen, M., Marquis, K. B., Averyt, M. T., … Miller. (2007). Summary for Policymakers. In: Climate Change 2007: The Physical Science Basis. Contribution of Working Group I to the Fourth Assessment Report of the Intergovernmental Panel on Climate Change. *New York Cambridge University Press*, 996. http://doi.org/10.1038/446727a

Stendel, M., & Christensen, J. H. (2002). Impact of global warming on permafrost conditions in a coupled GCM, *29*(13), 5–8.

Stephani, E., Fortier, D., Shur, Y., Fortier, R., & Doré, G. (2014). A geosystems approach to permafrost investigations for engineering applications, an example from a road stabilization experiment, Beaver Creek, Yukon, Canada. *Cold Regions Science and Technology*, *100*, 20–35. http://doi.org/10.1016/j.coldregions.2013.12.006

Survey, U. S. G. (2015). Large loss of Alaska permafrost projected by 2100. *Science Daily*. Retrieved from https://www.sciencedaily.com/releases/2015/11/151130163426.htm

Thawing Permafrost Threatens Alaska's Ecosystem, University of Alaska Fairbanks Researcher Says. (n.d.). Retrieved April 11, 2016, from http://www.huffingtonpost.com/alaskadispatchcom/thawing-permafrost-

threat_b_6901490.html

Treat, C. C., Wisser, D., Marchenko, S., & Frolking, S. (2013). Modeling the effects of climate change and disturbance on permafrost stability in northern organic soils. *Mires and Peat*, *12*(Zoltai 1993), 1–17.

UFC. (2005). UfC 3-220-10N: Soil Mechanics.

Wagner, A. (n.d.). Permafrost Experiment Station. Retrieved from http://www.erdc.usace.army.mil/Media/Fact-Sheets/Fact-Sheet-Article-View/Article/476647/permafrost-experiment-station/

Washburn, A. L. (1979). Permafrost Features as Evidence of Climatic Change*. *Earth-Science Reviews*, *15*, 327–402.

Wei, M., Guodong, C., & Qingbai, W. (2009). Construction on permafrost foundations: Lessons learned from the Qinghai-Tibet railroad. *Cold Regions Science and Technology*. http://doi.org/10.1016/j.coldregions.2009.07.007

Witt, G. (2013). Using Data from Climate Science to Teach Introductory Statistics. *Journal of Statistics Education*, *21*(1), 1–24.

Zhi, W., Yu, S., Wei, M., Jilin, Q., & Wu, J. (2005). Analysis on effect of permafrost protection by two-phase closed thermosyphon and insulation jointly in permafrost regions. *Cold Regions Science and Technology*, *43*, 150–163. http://doi.org/10.1016/j.coldregions.2005.04.001

Designator Number | AFIT-ENV-MS-17-M-189

Title | **THE IMPACTS OF CLIMATE CHANGE AND ANTHROPOGENIC PROCESSES ON PERMAFROST SOILS AND USAF INFRASTRUCTURE WITHIN NORTHERN TIER BASES**

Student's Name and Rank | Capt Alexander Graboski

Approved:

Committee Chair Signature | BARTLETT.KEVIN.S.1034010796 Digitally signed by BARTLETT.KEVIN.S.1034010796 DN: c=US, o=U.S. Government, ou=DoD, ou=PKI, ou=USAF, cn=BARTLETT.KEVIN.S.1034010796 Date: 2017.02.24 11:30:35 -05'00' | Date | Feb 24, 2017

Committee Member Signature | VALENCIA.VHANCE.V.1167651948 Digitally signed by VALENCIA.VHANCE.V.1167651948 Date: 2017.02.24 11:46:34 -05'00' | Date | Feb 24, 2017

Committee Member Signature | PRIGGE.DIEDRICH.NMN.1523149110 Digitally signed by PRIGGE.DIEDRICH.NMN.1523149110 Date: 2017.02.27 10:25:19 -05'00' | Date | Feb 27, 2017

Committee Member Signature | | Date |

For Dissertations Only

Dean's Acceptance | | Date |

ADEDEJI B. BADIRU, Ph.D.
Dean, Graduate School of Engineering and Management

REPORT DOCUMENTATION PAGE

1. REPORT DATE (DD-MM-YYYY) 24 Mar 2017	2. REPORT TYPE Master's Thesis	3. DATES COVERED (From – To) 27 Aug 2015 – 24 Mar 2017

4. TITLE AND SUBTITLE The Impacts of Climate Change and Anthropogenic Processes on Permafrost Soils and USAF Infrastructure within Northern Tier Bases	5a. CONTRACT NUMBER
	5b. GRANT NUMBER
	5c. PROGRAM ELEMENT NUMBER

6. AUTHOR(S) Graboski, Alexander J., Captain, USAF	5d. PROJECT NUMBER N/A
	5e. TASK NUMBER
	5f. WORK UNIT NUMBER

7. PERFORMING ORGANIZATION NAMES(S) AND ADDRESS(S) Air Force Institute of Technology Graduate School of Engineering and Management (AFIT/ENV) 2950 Hobson Way, Building 640 WPAFB OH 45433-8865	8. PERFORMING ORGANIZATION REPORT NUMBER AFIT-ENV-MS-17-M-189

9. SPONSORING/MONITORING AGENCY NAME(S) AND ADDRESS(ES) Sponsor Agency Name, if none, type "Intentionally Left Blank" Intentionally Left Blank	10. SPONSOR/MONITOR'S ACRONYM(S) N/A
	11. SPONSOR/MONITOR'S REPORT NUMBER(S)

12. DISTRIBUTION/AVAILABILITY STATEMENT

DISTRIBUTION STATEMENT A. APPROVED FOR PUBLIC RELEASE; DISTRIBUTION UNLIMITED

13. SUPPLEMENTARY NOTES

14. ABSTRACT

The Department of Defense is planning over \$552M in military construction on Eielson Air Force Base within the next three fiscal years. Although many studies have been conducted on permafrost and climate change, the future of our climate as well as any impacts on permafrost soils, remains unclear. This research focused on future climate predictions to determine likely scenarios for the United States Air Force's Strategic Planners to consider. The most recent 2013 International Panel on Climate Change report predicts a 2.2ºC to 7.8ºC temperature rise in Arctic regions by the end of the 21st Century in the Representative Concentration Pathways, (RCP4.5) emissions scenario. This study provides an explanation as to the impacts of this temperature rise on permafrost soils and Arctic infrastructure. This study developed regression models to analyze historical data related to degree-days, temperature, and seasonal lengths. Initial analysis using regression/forecast techniques show a 1.17ºC temperature increase in the Arctic by the end of the 21stCentury. Additionally, UAF's GIPL 2.1 model was used to calculate active layer thicknesses and permafrost thickness changes from 1947 to 2100. Results show that the active layer is thinning with some permafrost degradation. This research focused on Central Alaska while further research is recommended on the Alaskan North Slope and Greenland to determine additional impacts on Department of Defense infrastructure.

15. SUBJECT TERMS
   Permafrost, Climate Change, Infrastructure, Global Warming, Environmental, Climate

16. SECURITY CLASSIFICATION OF:			17. LIMITATION OF ABSTRACT	18. NUMBER OF PAGES	19a. NAME OF RESPONSIBLE PERSON Bartlett, Kevin S., Lt Col, PhD, USAF
a. REPORT U	b. ABSTRACT U	c. THIS PAGE U	UU	151	19b. TELEPHONE NUMBER (Include area code) (937) 255-2208 (Kevin.Bartlett.1@us.af.mil)